NTNU
Norwegian University of
Science and Technology

Dimensioning Loads for a Tidal Turbine

Marie Lunde Sæterstad

Norges teknisk-
naturvitenskapelige universitet
NTNU

Fakultet for Ingeniørvitenskap og Teknologi
Institutt for energi- og prosessteknikk

◻ NTNU

EPT-M-2011-43

MASTEROPPGAVE

for
Stud.techn.

Marie Lunde Sæterstad
Våren 2011

Dimensjonerende laster på en tidevannsturbin
Dimensioning load for a tidal turbine

Bakgrunn

Utviklingen av tidevannsturbiner har akselerert i de siste år. Det finnes ikke kommersielt til-
gjengelige turbiner ennå, men det er flere selskap som jobber med prototyper. Disse er installert
offshore på bunnfaste installasjoner. Flere selskap som utvikler tidevannsturbiner har hatt prob-
lemer med at turbinbladene har brukket. Dette skyldes sannsynligvis at bladene ikke er dimen-
sjonert riktig og at de dimensjonerende kreftene som er definert ikke er riktig. De dynamiske
kreftene som virker på en slik turbin er formidabel og det er derfor viktig å kunne beregne disse
og deretter definere de dimensjonerende kreftene.

Det jobbes med å utvikle en referanseturbin på 1 MW som skal benyttes i forskningssammen-
heng på tidevannsturbiner. Denne prosjektoppgaven blir et ledd i utviklingen av denne referanse-
turbinen.

Mål

Beregne dynamiske krefter på NTNU's referanse tidevannsturbin

Oppgaven bearbeides ut fra følgende punkter:

1. Litteratursøk
   a. Finne relevante publikasjoner der de dynamiske kreftene til tidevannsturbiner er bereg-
      net eller testet.

2. Beregne de dynamiske krefter til en 1 MW tidevannsturbin fra følgende fenomener:
   a. Tidevannsbølgen
   b. Bølge-strøm interaksjon
   c. Vertikal hastighetsprofil
   d. Turbulens
   e. Wake fra substruktur

3. Sammenligne beregninger fra bølge-strøm interaksjon med målinger på modellturbin fra Ma-
   rintek sammen med PhD-student Celine Faudot.

4. Alle resultatene skal legges tilgjengelig på NTNUs hjemmeside som omhandler fornybar
   energikilder

5. Dersom det er tid skal studenten gjennomføre en CFD-analyse av en eller flere av de dyna-
   miske kreftene som påvirker tidevannsturbinen.

Senest 14 dager etter utlevering av oppgaven skal kandidaten levere/sende instituttet en detaljert fremdrift- og eventuelt forsøksplan for oppgaven til evaluering og eventuelt diskusjon med faglig ansvarlig/veiledere. Detaljer ved eventuell utførelse av dataprogrammer skal avtales nærmere i samråd med faglig ansvarlig.

Besvarelsen redigeres mest mulig som en forskningsrapport med et sammendrag både på norsk og engelsk, konklusjon, litteraturliste, innholdsfortegnelse etc. Ved utarbeidelsen av teksten skal kandidaten legge vekt på å gjøre teksten oversiktlig og velskrevet. Med henblikk på lesning av besvarelsen er det viktig at de nødvendige henvisninger for korresponderende steder i tekst, tabeller og figurer anføres på begge steder. Ved bedømmelsen legges det stor vekt på at resultatene er grundig bearbeidet, at de oppstilles tabellarisk og/eller grafisk på en oversiktlig måte, og at de er diskutert utførlig.

Alle benyttede kilder, også muntlige opplysninger, skal oppgis på fullstendig måte. For tidsskrifter og bøker oppgis forfatter, tittel, årgang, sidetall og eventuelt figurnummer.

Det forutsettes at kandidaten tar initiativ til og holder nødvendig kontakt med faglærer og veileder(e). Kandidaten skal rette seg etter de reglementer og retningslinjer som gjelder ved alle (andre) fagmiljøer som kandidaten har kontakt med gjennom sin utførelse av oppgaven, samt etter eventuelle pålegg fra Institutt for energi- og prosessteknikk.

I henhold til "Utfyllende regler til studieforskriften for teknologistudiet/sivilingeniørstudiet" ved NTNU § 20, forbeholder instituttet seg retten til å benytte alle resultater og data til undervisnings- og forskningsformål, samt til fremtidige publikasjoner.

Ett -1 komplett eksemplar av originalbesvarelsen av oppgaven skal innleveres til samme adressat som den ble utlevert fra. Det skal medfølge et konsentrert sammendrag på maksimalt én maskinskrevet side med dobbel linjeavstand med forfatternavn og oppgavetittel for evt. referering i tidsskrifter).

Til Instituttet innleveres to - 2 komplette kopier av besvarelsen. Ytterligere kopier til eventuelle medveiledere/oppgavegivere skal avtales med, og eventuelt leveres direkte til de respektive. Til instituttet innleveres også en komplett kopi (inkl. konsentrerte sammendrag) på CD-ROM i Word-format eller tilsvarende.

NTNU, Institutt for energi- og prosessteknikk

Dato: 3/1 - 2011

Olav Bolland
Instituttleder

Ole Gunnar Dahlhaug
Faglig ansvarlig/veileder

Medveileder: Celine Faudot

Preface

This work is a part of the project of developing a 1 MW reference tidal turbine at the Norwegian University of Science and Technology. Dimensioning loads on the tidal turbine are calculated with use of Matlab. This work is written at the Water Power Laboratory, as the final year Master thesis and is a part of the study program, Energi og Miljø, Department of Energy and Process Engineering. The master thesis is a continuation of the project thesis from the fall semester 2010.

I would like to thank my co-supervisor Céline Faudot for her guidance and Florian for good teamwork and interesting discussions. I would also like to thank my supervisor Ole Gunnar Dahlhaug.

Trondheim 10.06.2011

Marie Lunde Sæterstad

Abstract

The main dynamic loads on a tidal turbine are due to the tidal current variation, turbulence, wave-current interaction and wake from the tower and upstream turbines. The design of the turbine is highly dependent on the dynamic loads acting on the turbine's blades and its structure. Cyclic loading and unloading of any material over a period of time will lead to fatigue and structural damage.

In this work dimensioning loads for NTNU's 1 MW reference tidal turbine are calculated due to the vertical no-slip current velocity profile, wave-current interaction, the horizontal and vertical velocity component due to the waves, turbulence and the tidal wave. Based on mathematical models the dimensioning loads for the turbine are calculated with a Matlab code written for this work. The influence of each of the components causing a dynamic load on the tidal turbine blades is evaluated and analyzed with the rainflow counting algorithm, which can be used for fatigue analysis.

Results from Matlab calculations are compared to experimental results in order to validate the Matlab code. In the comparison the trends are the same for calculation and experimental results, oscillating curves with the same period. It is noticed that in large waves the Matlab code predicts very well the dynamic loads in terms of mean and peak-to-peak values.

For the thrust force and the shaft torque the horizontal component of the velocity due to the waves has the largest influence on the peak-to-peak values and the turbulence induces a high number of cycles. For the pitch moment as well the horizontal component due to the waves has the largest influence on the peak-to-peak values, but also the vertical component has a certain influence. For the pitch moment the consistently main oscillations inducing cyclic loading are due to the vertical no-slip current velocity profile. This is also the case for the yaw moment, but here the vertical wave component has the largest influence on the peak-to-peak values. For calculation with the tidal wave it is noticed that higher velocities gives higher maximum values.

The Matlab code is a reliable and fast tool. Despite the simplifications done in the calculations, it calculates the dimensioning loads for a tidal turbine with a good accuracy.

Sammendrag

De dimensjonerende krefter på en tidevannsturbin er gitt av tidevannsbølgen, turbulens, bølge-strøminteraksjon og vake fra substruktur og oppstrøms turbiner. Designet av turbinen er svært avhengig av de dynamiske krefter som virker. Vekslende krefter på et materiale over en tidsperiode kan føre til utmatting og strukturelle skader.

I denne oppgaven er de dimensjonerende laster på NTNUs 1 MW tidevannsturbin beregnet med utgangspunkt i det vertikale hastighetsprofilet, bølge-strøminteraksjon, den horisontale og vertikale bølgekomponenten, turbulens og tidevannbølgen. Basert på matematiske modeller er dimensjonerende krefter beregnet ved hjelp av en Matlabkode skrevet for denne oppgaven. Innflytelsen fra hver enkelt av komponentene som forårsaker en dynamisk belastning på turbinen er analysert ved hjelp av en algoritme, rainflow counting algorithm, som kan brukes til analyse av utmatting av materialer.

Resultater fra Matlabberegninger er sammenlignet med eksperimentelle resultater for å validere Matlabkoden. I sammenligningene er trendene de samme, oscillerende kurver med samme periode, for både Matlabberegninger og testresultater. Ved store bølger er Matlabkoden en god tilnærming til eksperimenter med tanke på gjennomsnitt- og maksimalverdier.

For skyvekraften og dreiemomentet har den horisontale bølgekomponenten størst påvirkning på maksimalverdier og turbulens er den komponenten som bidrar til et høyt antall sykluser. Også for vridningsmomentet har den horisontale bølgekomponenten størst påvirkning på maksimalverdier, men i tillegg har den vertikale komponenten en innflytelse. Her skyldes den gjennomgående viktigste komponenten for oscillasjon det vertikale hastighetsprofilet. Dette er også tilfelle for bøyningsmomentet, men den vertikale bølgekomponenten har størst innflytelse på maksimalverdier. For beregninger med tidevannsbølgen vil høyere hastigheter gir høyere maksimalverdier for alle krefter som virker.

Denne oppgaven er et ledd i utviklingen av NTNUs 1 MW referanseturbin som skal benyttes i forskningssammenheng på tidevannsturbiner.

Contents

x

List of Figures

List of Tables

List of symbols

α	Angle of attack	$[rad]$
a	Axial induction factor	$[-]$
a'	Rotational induction factor	$[-]$
A	Area	$[m^2]$
c	Propagation speed of the wave	$[\frac{m}{s}]$
C_a	Axial force coefficient	$[-]$
C_D	Drag coefficient	$[-]$
C_L	Lift coefficient	$[-]$
C_p	Power coefficient	$[-]$
C_r	Rotational force coefficient	$[-]$
C_T	Thrust coefficient	$[-]$
D_t	Turbine diameter	$[m]$
ϵ	Turbulence energy dissipation rate	$[\frac{m^2}{s^3}]$
η	Sea surface elevation	$[m]$
η_{DT}	Drive train efficiency	$[-]$
η_G	Generator Speed	$[-]$
F	Prandtl's tip loss factor	$[-]$
F_g	Gravitational force	$[N]$
F_D	Drag force	$[N]$
F_L	Lift force	$[N]$
Fr	Froude number	$[-]$
γ	Angle between the blade and horizontal axis	$[rad]$
g	Gravitational acceleration	$[\frac{m}{s^2}]$
G	Universal gravitational constant	$[\frac{m^3}{kg \cdot s^2}]$
h	Mean water depth	$[m]$
H	Water depth due to the tides	$[m]$
H_{wave}	Wave height	$[m]$
k	Wave number	$[\frac{rad}{m}]$
λ	Wave length	$[m]$

l_k	Kolmogorov length scale	$[m]$
L_c	Cord length	$[m]$
μ	Dynamic viscosity	$[\frac{kg}{s \cdot m}]$
m	Mass	$[kg]$
$\dot{m}$	Mass flow rate	$[\frac{kg}{s}]$
M_x	Turbine main shaft torque	$[Nm]$
M_y	Turbine pitch moment	$[Nm]$
M_z	Turbine yaw moment	$[Nm]$
N	Blade elements	$[-]$
N_{blade}	Number of blades	$[-]$
N_i	Distance from blade tip in lower position to the seabed	$[m]$
Ω	Angular velocity of the flow	$[\frac{rad}{s}]$
ω_t	Turbine speed	$[\frac{rad}{s}]$
ω_{tide}	Angular velocity of the tide	$[\frac{deg}{h}]$
ω_w	Wave frequency	$[\frac{rad}{s}]$
φ	Flow angle	$[rad]$
Φ	Velocity potential	$[\frac{m^2}{s}]$
p	Pressure	$[Pa]$
p_i	Phase tidal component	$[deg]$
P_G	Generator power output	$[W]$
ρ	Density	$[\frac{kg}{m^3}]$
r	Radius	$[m]$
Re	Reynolds number	$[-]$
σ	Standard deviation	$[-]$
s	Wave steepness	$[-]$
S_f	Turbine scale	$[-]$
θ	Twist angle	$[rad]$
τ	Macro time scale	$[s]$
τ_k	Kolmogorov time scale	$[s]$
t	Time	$[s]$
T	Thrust force	$[N]$
TI	Turbulence intensity	$[-]$
TSR	Tip speed ratio	$[-]$
T_{tide}	Period of the tide	$[s]$
T_{wave}	Wave period	$[s]$
υ	Kinematic viscosity	$[\frac{m^2}{s}]$
u	Rotational speed of the flow	$[\frac{m}{s}]$
u_k	Kolmogorov velocity scale	$[\frac{m}{s}]$
U	Rotational speed of the turbine	$[\frac{m}{s}]$
U_{tip}	Rotational speed at blade tip	$[\frac{m}{s}]$
vvc	Vertical wave velocity component	$[\frac{m}{s}]$
V	Undisturbed flow	$[\frac{m}{s}]$

V_{design}	Current velocity (water particle velocity) at design point	$\left[\frac{m}{s}\right]$
V_{max}	Maximum water particle velocity	$\left[\frac{m}{s}\right]$
V_{tiplp}	Water particle velocity at blade tip in lower position	$\left[\frac{m}{s}\right]$
V_{tipup}	Water particle velocity at blade tip in upper position	$\left[\frac{m}{s}\right]$
V_{wave}	Water particle velocity at the surface	$\left[\frac{m}{s}\right]$
W	Relative flow	$\left[\frac{m}{s}\right]$
WD	Water depth	$[m]$
WD_{up}	Depth of turbine blade tip in upper position	$[m]$
z	Distance below water surface	$[m]$

Chapter 1

Introduction

The concept of extracting kinetic energy from the tidal currents is today not very well developed, but under intense research and development. The technology is still immature and on the pilot stage. NTNU and STATKRAFT are designing and building a model tidal turbine, which is tested at Marintek, Norwegian Marine Technology Research Institute, in Trondheim. This turbine will be the small scale model of a 1 MW reference tidal turbine. This work is a part of the project of designing the reference turbine, which is to be used in research and development of tidal turbines.

The purpose of this work is to define the dimensioning loads for the tidal turbine due to the vertical no-slip current velocity profile, wave-current interaction, the horizontal and vertical velocity component due to the waves, turbulence and the tidal wave. This work is a continuation of the project thesis, where the wave-current interaction on the tidal turbine blades was evaluated.

The dynamic loads on the tidal turbine will be calculated with a Matlab code written for this work. The code is based on linear wave theory, harmonic analysis of the tides, hydrofoil geometry, blade element momentum theory, turbulence theory with Reynolds decomposition and the rainflow counting method. The time varying forces calculated are the thrust force, T, the main shaft torque, M_x, and the thrust induced pitch moment, M_y, and yaw moment, M_z.

To validate the Matlab code comparisons with experiments are done. Calculations are done for a turbine operating under the same conditions as the model turbine tested at Marintek and compared to the test results.

Chapter 2

Background

2.1 Tidal Energy

Every day the sea level rises and falls in a cyclic pattern. These periodic changes of the sea level are called the tides. They are caused by gravitational forces exerted by the moon and the sun on the rotating earth and its oceans. The motion of sea water, periodic oscillations in water level and associated tidal currents in coastal areas are the phenomena for generating energy due to the tides. Tidal energy is renewable and has the advantage of being highly predictable compared to other renewable energy sources.

Figure 2.1: Bay of Fundy, Canada, at high and low tides [2].

2.2 State of Art

The tides cause two effects from which energy can be extracted. The tidal range leads to a difference of the sea level. This potential energy can be exploited. The variation of the gravitational field causes mass flow throughout the oceans. This water moves at certain velocities. Therefore, also kinetic energy from the tidal currents can be extracted. For both ways of extracting energy the prediction of tides is precise and reliable. Tidal energy has a large potential worldwide. The industry is still immature, with technology on the pilot stage [37], but in recent years the tidal stream turbine industry has witnessed considerable development.

Tidal power is not widely used for electric power generation. Four large-scale power plants do currently exist [25] [27]. The first tidal power plant is the La Rance Tidal Power Station in France, opened in 1966. La Rance is, in terms of installed capacity, the largest tidal power station in the world. It has a capacity of 240 MW using the barrage method, which is a method of extracting the potential energy from the tides, where a barrage is build across a bay or a river and turbines are installed in the barrage. As the water flows in and out the turbines are generating power. Annapolis Royal Generating Station, Canada, with a capacity of 17.8 MW, Jiangxia Tidal Power Station, with a capacity of 3.2 MW, and Kislaya Guba, Russia, with a capacity of 0.4 MW, are the largest tidal power stations operating today.

The concept of extracting kinetic energy from tidal currents is of intense research and development. The tidal energy industry faces many challenges. The main challenge of tidal turbines is linked to their field of application. The ocean poses certain properties. The salty seawater is a corrosive environment that has to be taken into account. The tidal current turbine is extracting energy from the movement of the water, under the condition that the density of water is almost thousand times larger than the density of air. Therefore the loads the turbine and its structure have to withstand are enormous and affect the lifetime of the turbine.

Today there are many manufacturers developing tidal energy convertors using different types of devices. Marine Current Turbines Ltd. is with a 1.2 MW prototype tidal turbine, SeaGen, operating in Strangford Lough, Northern Ireland, one of the world's leading tidal system developer [11]. Since 2003 the company has been operating a 300 kW prototype, SeaFlow, near Lynmount in North Devon Coast, England. This was the world's first tidal turbine. A 10.5 MW tidal energy farm is by Marine Current Turbines planned for 2013/2014 at the coast of the Welsh island of Anglesey, using several SeaGen devices, and they are also targeting to install Scotland's first tidal energy farm by 2013 [5].

Tidal Generation Ltd. is in front of design, development and manufacturing of tidal turbines. A 500 kW unit is currently operating at EMEC, European Marine Energy Centre [12]. TGL is also developing a 1 MW tidal stream turbine with the Energy Technologies Institute, ETI, to collect and publish data for the development

of the tidal energy industry.

Open Hydro became in 2006 the first company that has installed a tidal turbine at the EMEC facility. The test installation is located close to the Orkney island of Eday in Scotland. Open Hydro is working with Alderney Renewable Energy to install an array of turbines in the water's of Alderney, and with Nova Scotia Power to create a tidal demonstration project in the Bay of Fundy in Canada [9].

Voith Hydro is today a leading company within hydropower equipment and services [14]. They are working on a tidal turbine park in South Korea. A 1 MW tidal turbine will be installed off the Scottish coast and a two year trial operation period is due to start at EMEC in the Orkney Island waters in 2011 [15]. Another company, Atlantis Resources Corporation, installed a 1 MW tidal turbine at EMEC in August 2010 [1].

Figure 2.2: Hammerfest Strøm, HS1000 [4].

The first tidal power system utilizing the tidal phenomenon, converting kinetic energy into electricity delivered to the electric grid, was installed in 2003. This was a 300 kW prototype tidal turbine located in Kvalsundet, Norway, manufactured by Hammerfest Strøm. The company has designed HS1000, shown in figure 2.2, a 1000 kW tidal turbine based on the 300 kW prototype, which is expected to be in operation in 2011 [4], installed by the EMEC.

According to EMEC [3], there are four main devices for tidal energy conversion due to stream generators. The devices can be found in figure 2.3.

- *a: Horizontal axis turbine:* As the wind turbines extract energy from the moving air, the tidal horizontal axis turbines extract in the same way energy from the motion of the water.

- *b: Vertical axis turbine:* The turbine is mounted on a vertical axis. The turbine extracts, just as the horizontal axis turbine, energy from the moving water.

- *c: Oscillating Hydrofoil:* Oscillating devices do not have a rotating component. A hydrofoil is attached to an oscillating arm. The tidal current is flowing on each side of the wing. This produces a lift force and motion of the wing. This arm is connected to a hydraulic system, which can convert the motion into electricity.

- *d: Venturi effect:* The Venturi effect means that a fluid flow is constricted into a section of a pipe. This results in reduction in fluid pressure. The turbine is housed in a duct. The fluid flow with increased velocity is concentrated trough the duct and drives the turbine.
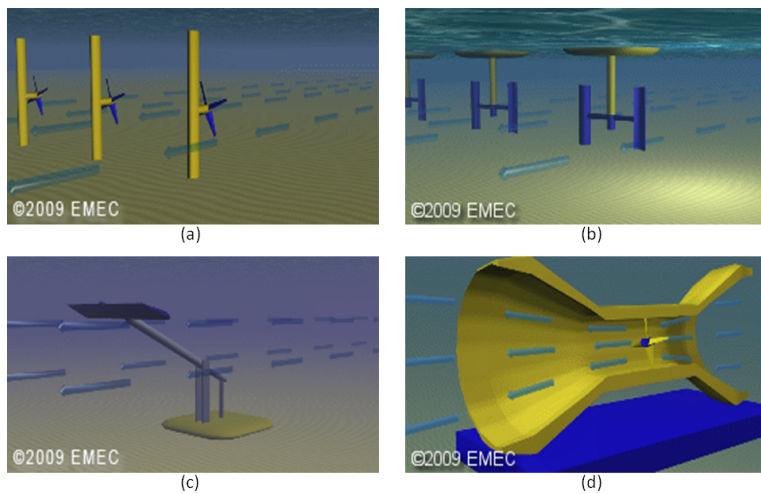
Figure 2.3: (a) Horizontal axis turbine, (b) vertical axis turbine, (c) oscillating hydrofoil and (d) the Venturi effect [3].

2.3 Literature Review

The tidal industry is a developing industry and literature on dimensional loading for a tidal turbine is still limited. Barltrop et al. at Universities of Glasgow and Strathclyde, UK, did a study on wave-current interaction on marine current turbines. G. McCann et al, Garrad Hassan Group Limited, UK, highlighted the site specific conditions and I.A Milne et al. at University of Auckland, New Zealand, did three publications on tidal turbine blade loading.

2.3.1 Barltrop et al.

N. Barltrop, K.S. Varyani, A. Grant, D. Clelland, Xuan Pham [17] showed in 2006, using both numerical models and experimental testing, that increasing the wave period leads to greater root bending moments. Simulation results, based on mathematical models; linear wave theory and blade element momentum theory, are validated with experiments.

The dynamic property of bending moments acting about the roots of the tidal stream rotor is specifically considered. The bending moments fluctuates with significant amplitudes. The fluctuations are as much as 50 % of the mean value for out-of-plane bending moment and 100% for in-plane bending moment. Figure 2.4 is showing in-plane, M_x, and out-of-plane, M_y, bending moments about roots of rotor blades in long waves. Sim_Mx and Sim_My refer to simulation results and Exp_Mx and Exp_My to the corresponding experimental results. In long waves the dynamic response of both bending moments can be well predicted with blade element-momentum theory and linear wave theory, but in steep waves, the linear wave theory underestimates, probably due to high non-linearities, these responses. A general observation on dynamic characteristics of bending moments is the main oscillation at the encountered wave frequency. Also the effect of the vertical component of wave particle velocity is of interest and affects mainly the flow incidence angle onto the airfoil. This parameter shows a small effect at the main peaks of the wave loads. Figure 2.5 is showing the out-of-plane bending moment with and without the vertical wave velocity component.
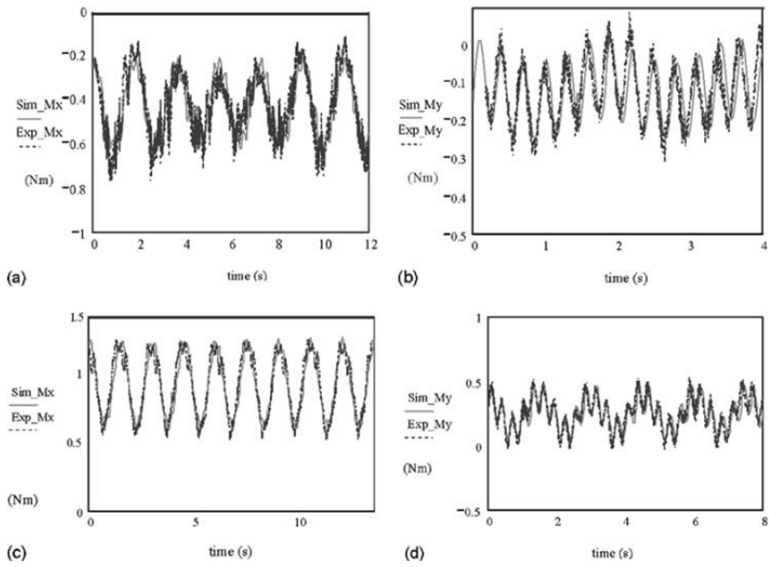
Figure 2.4: Barltrop et al.: Turbine at model scale, long waves of 150 mm height and frequency of 0.5 Hz. (a) Out-of-plane bending moment and (b) in-plane bending moment for current speed of 0.3 m/s. (c) Out-of-plane bending moment and (d) in-plane bending moment for current speed of 1.0 m/s.
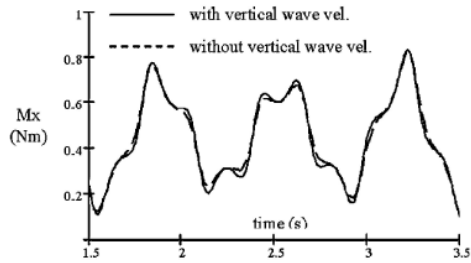
Figure 2.5: Barltrop et al.: M_x with and without vertical wave velocity.

2.3.2 McCann et al.

In 2008, G. McCann, M. Thomson and S. Hitchcock [33] highlighted the importance of understanding the specific environmental conditions at the installation site. Investigation of the site specific conditions on the prediction of loading and power on a tidal stream device is done in this work. Data are collected from EMEC's tidal test site to analyse and evaluate tidal flow characteristics due to annual mean flow distribution, flow probability distribution, vertical velocity profiles and flow direction. The impact of waves and turbulence coherence structure and intensities on structural loading is also analysed. These are all critical parameters for design consideration.

2.3.3 I.A. Milne et al.

In 2010, I.A. Milne, R. N. Sharma, R. G. J. Flay and S. Bickerton in Department of Mechanical Engineering at University of Auckland, New Zealand, published three articles about tidal turbine blade loading.

A preliminary parametric analysis suggest that the horizontal mean flow speed, longitudinal turbulence intensity, wave state and depth of hub relative to channel hub are the most dominant parameters for the blade loads, which are modelled in both fatigue and extreme load analysis [35]. In terms of fatigue loads, these parameters produce the greatest increase in magnitude of the loads in the high load, low cycle loading of the loading distribution. The mean velocity distribution has a relatively minor influence on the blade load lifetime damage.

Figure 2.6 shows the results of comparison of blade root M_y (a) fatigue loads and (b) maximum loads for various onset parameters. The analysis is performed by varying one parameter at a time while the other parameters are held constant at the values stated in the figure. The analysis is done at two different mean hub-height velocities. The effect of the vertical shear profile is analyzed by changing the shear exponent, α. The tidal stream may differ in direction and with the yaw angle the tidal turbine can realign the rotor plane with the mean flow. The longitudinal turbulence intensity, TI_u, is held constant as the effect of the lateral and vertical turbulence intensities, TI_v and TI_w, are analysed. The wave induced loads will vary with the depth through the water column and different hub heights above seabed are considered. The fatigue loads are analyzed by using damage equivalent loads (DEL's), which equates the damage expected from a variable loading time history to a load inflicted by a single amplitude sinusoidal load applied at a given frequency. m is the slope of the S-N curve. The trends are similar for fatigue and maximum loads and the analysis is showing that the vertical shear, yaw angle, lateral and vertical turbulence intensity and turbulence length scale is of secondary influence for both load analyses.
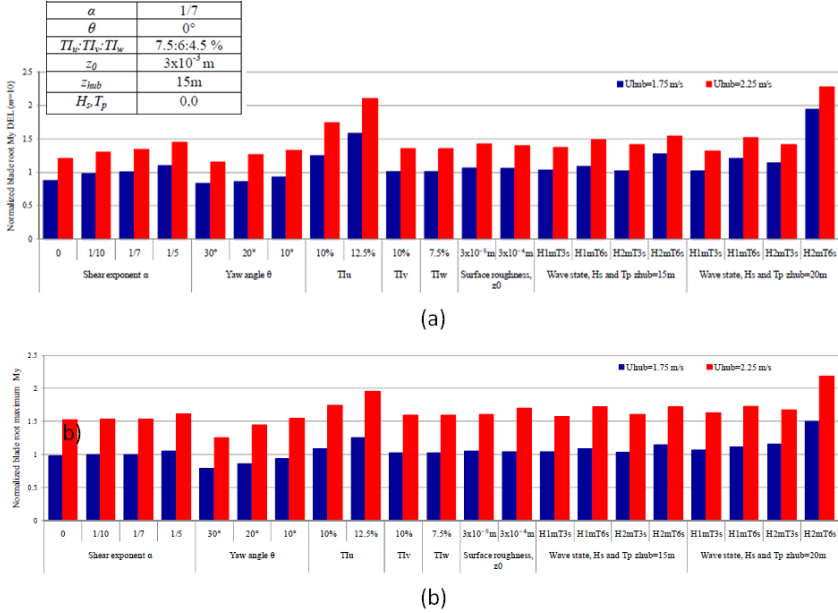
Figure 2.6: I.A. Milne et al.: Comparison of blade root M_y (a) fatigue loads and (b) maximum loads for various onset parameters.

Surface waves have a significant contribution to unsteady loading on tidal turbines. In another paper, [36] the role of waves on tidal turbine unsteady blade loading is analysed. The paper demonstrates, using a combination of theory and simulations for both regular and irregular waves, that the wave height, period, direction and hub height relative to the surface are dominant parameters affecting the loads. Also the channel depth affects the loading induced by long period waves. Linear wave theory is used to model the wave particle kinematics and expresses the wave induced perturbation components as u, horizontal, v, lateral, and w, vertical. Although the w component fluctuates at the same order of magnitude as the u component, the latter induces the greatest variations in angle of attack and thrust. What Barltrop stated in 2006 is also showed in this paper. The u component will be the primarily driver of the fluctuating out-of-plane bending moment.

The third paper is about the role of onset turbulence on tidal turbine blade loads [34]. A simulation-based approach is used to investigate the sensitivity of the blade loads for a tidal turbine to the structure of the turbulent onset flow. The unsteady hydrodynamic loads dominate over the gravitational and inertia forces. The longitudal turbulence intensity is the dominant parameter. The analysis investigates the sensitivity of the root out-of-plane bending moment, M_y, due to the turbulence intensity and the integral length scale. The blade extreme and fatigue root bending moments are likely to be similar for the integral length scales of in-

terest, which are a measure of the average sizes of turbulent eddies. The number of large, fatigue inducing cycles increases with reduction in length scale. The extreme and fatigue loads are similar for the von Karman and Kaimal spectral models.

Chapter 3

Theory

3.1 The Tidal Phenomenon

3.1.1 Tides and Tidal Currents

Tides are variation in level of the surface of the sea caused by gravitational interaction between the earth, the moon and the sun. Tides are periodic motion of the sea water, they are highly predictable and have an endlessly repeating cycle. The tidal range is the difference in the height of the water at low and high tides. It varies between a few centimeters to many meters depending on the position on the globe, costal configuration and bathymetry, which is underwater topology. Tidal currents are horizontal movement of sea water as a result of rise and fall of sea level due to the tides. They vary in time and place and switch direction with the transitions of the tides between high and low. In most coastal areas the regular fall and rise of the sea level occurs two times a day, two rises and two falls [18].

3.1.2 Tide Generating Forces

The forces causing the tides are called tide generating forces. Newton established the theory that the gravitational force between two masses depends on the product of the two masses, m_1 and m_2, and the square of their separation, R [26]:

$$F_g = \frac{G \cdot m_1 \cdot m_2}{R^2} \qquad [N] \qquad (3.1)$$

where G is the universal gravitational constant, $G = 6.67300 \cdot 10^{-11} \frac{m^3}{kg \cdot s^2}$

The moon is the main tide generating body. The moon and the earth have a common centre of mass. Because the earth is larger and more massive than the moon this centre is located inside the earth. If both planets had equal size and mass the centre of mass would be on a point halfway between them. The earth-moon system rotates around their common centre. The tide generating force is the difference between local gravitational attraction and the centrifugal force due to the rotation of the earth-moon system about their common centre of mass. Because of the great distance, the effect from the sun is smaller than the effect from the moon. The horizontal components of the tide generating forces are called tractive forces [7].

3.1.3 Tidal Cycles
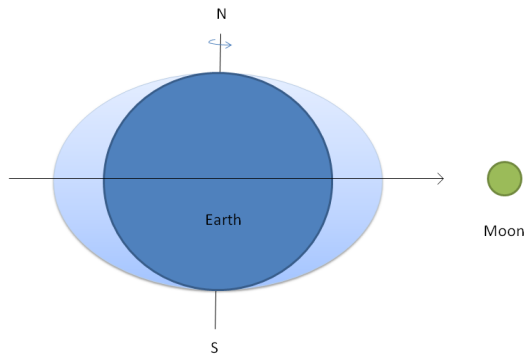
Figure 3.1: Tide producing forces.

There will be a tide generating force in vertical direction upward towards the moon two places on the earth, the side of the earth closest to the moon and on the opposite side of the earth, which is furthest away from the moon. According to the equilibrium theory of Newton the gravitational force of the moon on the water on earth would acquire a shape of an ellipsoid if the earth were covered by a continuous water layer [18]. This is shown in figure 3.1. The larger axis of the ellipsoid will always point towards the moon. The gravitational force due to the moon varies over the surface of the earth. On the larger ellipsoid axis there will be flood on the place that is located closest to the moon and on the side which is furthest away from the moon. On the side of the moon the gravitational forces are stronger and the water will be attracted towards the moon. On the opposite side of the earth the centrifugal forces will be larger than the gravitational forces and therefore this side of the earth will have flood as well.

The earth is not fully covered with water and does not acquire the perfect shape of an ellipsoid, but the water is attracted to the places closest and furthest away from the moon. The moon is revolving around the earth of a period of 27.32 days. Therefore the lunar day has 24.84 hours and exceeds the solar day, which has 24 hours. This means that it takes 24 hours and 50 minutes for the moon to return on the same location of the sky relative to the earth. An observer on a fixed location on the earth will therefore observe the moon every 24 hours and 50 minutes. This is shown in figure 3.2. Because of the equilibrium theory of Newton the tide generating forces goes through two identical cycles within one lunar day and the observer will therefore see two periods of high and low tides during this time. The tidal period is 12 hours and 25 minutes, 12.42 hours, and is called the principal semidiurnal lunar tide, M_2. The symbol M has the subscript 2, which means two cycles per day. This is characteristic for *semidiurnal tides*, which have a period of about 12 hours.
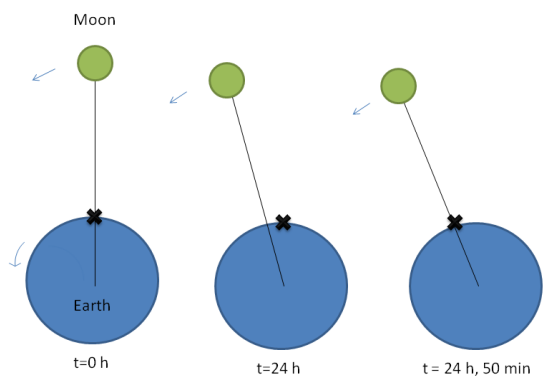
Figure 3.2: Lunar procession. Due to the earth's rotation and the moon's revolving around the earth, the moon returns to the same location on the sky relative to the earth every 24 hours and 50 minutes.

The tide caused by the sun follows the same principle as the lunar tide. Analogous to the gravitational force of the moon also the sun exerts a gravitational force on the earth. This force causes the water to shape like an ellipsoid around the earth with flood on the larger axis towards the sun and on the side farthest from the sun. The solar day has 24 hours and the period of the principal semidiurnal solar tide, S_2, is 12 hours.

Phase inequalities are characteristic for semidiurnal tides. The most notable change in tidal range is the semidiurnal range, which varies over a two weeks cycle. The mean period of phase inequality is 14.7 days. During this cycle the amplitude, the height of high or low water with respect to the mean sea level, varies from its maximum to minimum and again to its maximum. The position of the moon, sun and earth relative to each other causes variations of the tidal range. *Spring tide* is when the tide has its maximum. This occurs when the sun, moon and earth are

in a line. The *neap tide*, which is when the tide has its minimum, occurs when the moon and the sun are perpendicular to each other, relative to the earth [8].

The principal semidiurnal lunar and solar tides components, M_2 and S_2, are the main tidal components Hardisty [26] explains. There is also one large elliptic lunar semidiurnal component, N_2, which modulates the moons elliptical orbit and has a period of 12.66 hours. A lunisolar semidiurnal component K_2, which has a period of 11.97 hours, modulates the declination effects of the sun and the moon.

One high and one low tide occurring with a period close to 24 hours are called *diurnal tides*. There are solar and lunar diurnal tides components. There is one larger solar diurnal period, P_1, of 24.07 hours, and one larger lunar diurnal period, O_1, of 25.82 hours. The lunisolar declination, K_1, which has a period of 23.93 hours, expresses the lunar and solar declination. The larger lunar elliptic diurnal component, Q_1, has a period of 26.87 hours. The total tidal effect is a summation of all the components. All the components are given in table 3.1.

Component	Period
M_2	12.42
S_2	12.00
N_2	12.66
K_2	11.97
P_1	24.70
O_1	25.82
K_1	23.93
Q_1	26.87

Table 3.1: Components of the tide and their period.

3.1.4 Harmonic Analysis of the Tides

The tides are sinusoidal oscillations containing the effect of all the tidal components. The principle of tidal analysis is that the oscillations can be broken down into a collection of simple sinusoids, each representing a tidal constituent. Each constituent is defined by its period in solar hours, T_{tide}, or the angular velocity, $\omega_{tide} = \frac{360°}{T_{tide}}$ [13]. The amplitude and the phase of each component have to be determined. The partial tides, each corresponding to a single tidal constituent, is summarized and represented by the following equations [19]:

$$H = \sum H_i \cdot cos(\omega_{tide,i} \cdot t + p_i) \qquad [m] \qquad (3.2)$$

$$U = \sum U_i \cdot cos(\omega_{tide,i} \cdot t + p_i) \qquad [\frac{m}{s}] \qquad\qquad (3.3)$$

The constituent amplitude is the water level, H_i, and the water velocity, U_i. The angular velocity, $\omega_{tide,i}$, has the unit $\frac{deg}{h}$, t is the time in hours and p_i is the phase offset of each tidal component in degrees. To predict the tides at a certain site the effect of all constituents has to be evaluated and summarized. Figure 3.3 is showing the sinusoidal oscillation of the tides. The water level and the velocity have a phase offset of 90 degrees, which means that the velocity is zero at the transition between high and low tides. The figure is showing the semidiurnal range, which varies over a two weeks cycle.
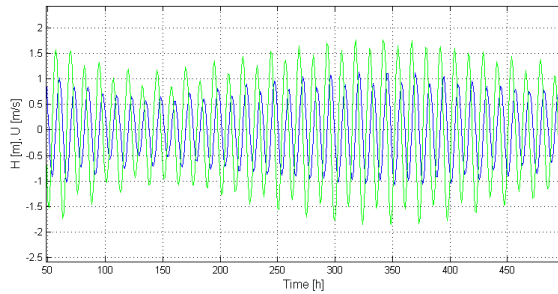
Figure 3.3: The sinusoidal oscillation of the tide. Water level is shown in blue, the velocity in green.

3.2   Linear Wave Theory

The sea surface waves are inherently nonlinear. The wave height and length are not constant and will vary in time and place. With linear wave theory we can describe the core theory of ocean surface waves. It describes the propagation of regular gravity waves on a fluid surface, in this case the ocean surface. It has to be assumed that the flow is two dimensional and the waves are travelling in x-direction, perpendicular to the rotor plane.

3.2.1   Basic Wave Motion
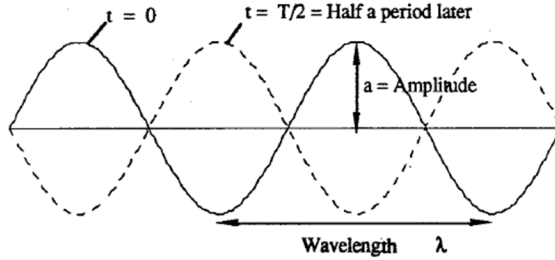
Figure 3.4: The sine wave [31].

The sine function defines a regular wave and is given in figure 3.4. According to Linear Wave Theory, Krogstad and Arntsen [31], the sea surface elevation, η, of a wave travelling in x-direction is:

$$\eta(x,t) = a \cdot sin(\frac{2\pi}{\lambda} \cdot x - \frac{2\pi}{T_{wave}} \cdot t) \qquad [m] \qquad (3.4)$$

Note that a is here the amplitude of the wave, defined in meters, and is half of the wave height, $a = \frac{H_{wave}}{2}$. λ is the wave length in meters and T_{wave} its period in seconds. The wave number, k, is defined:

$$k = \frac{2\pi}{\lambda} \qquad [\frac{rad}{m}] \qquad (3.5)$$

The angular frequency of the wave ω_{wave} is defined:

$$\omega_{wave} = \frac{2\pi}{T_{wave}} \qquad [\frac{rad}{s}] \qquad (3.6)$$

18

Note that f is the frequency, $f = \frac{1}{T_{wave}}$, and the unit is Hertz ($Hz = \frac{1}{s}$). These parameters give the simplified equation of the wave profile or the shape of the sea water surface:

$$\eta(x,t) = a \cdot sin(k \cdot x - \omega_{wave} \cdot t) \qquad [m] \qquad (3.7)$$

Wave heights are always smaller than the lengths [29]. The wave steepness, s, is the ratio of the wave height to the wave length:

$$s = \frac{H_{wave}}{\lambda} \qquad [-] \qquad (3.8)$$

The waves become unstable and have a tendency to fall apart if the height is too large. The upper limit of the wave steepness is $\frac{H_{wave}}{\lambda} = \frac{1}{7}$. The wave form moves one wavelength during one period. Its propagation speed along the water surface, c, is the phase velocity. The wave particles do not move with this velocity, only the wave form.

$$c = \frac{\lambda}{T_{wave}} = \frac{\omega_{wave}}{k} \qquad [\frac{m}{s}] \qquad (3.9)$$

3.2.2 Potential Theory

A velocity potential, $\Phi(x,z,t)$, is a function with time and space variables, which is valid in the whole fluid domain. The waves on the surface set the rest of the water into motion. At each point (x, z) the fluid has a velocity: $\mathbf{v}(x,z,t)=u(x,z,t)\mathbf{i} + w(x,z,t)\mathbf{k}$. u is the velocity in x-direction and w in the z-direction. z is the position in vertical direction from the water surface. In a two-dimensional incompressible fluid the velocity $\mathbf{v}$ will in each point satisfy the equation of continuity [40]:

$$\frac{\partial u}{\partial x} + \frac{\partial w}{\partial z} = 0 \qquad (3.10)$$

The potential function is defined that way that in any point of the fluid the derivative of the function in a certain direction is the velocity component of a fluid particle in this direction. If the fluid is irrotational the velocity potential can be expressed:

$$u = \frac{\partial \Phi}{\partial x} \qquad w = \frac{\partial \Phi}{\partial z} \qquad [\frac{m}{s}] \qquad (3.11)$$

In a uniform stream with a velocity, U, in the x-direction, the velocity potential is [40]:

$$\Phi = U \cdot x \qquad [\frac{m^2}{s}] \tag{3.12}$$

In the uniform stream the velocity of a fluid particle in x-direction is:

$$u = \frac{d\Phi}{dx} = U \qquad [\frac{m}{s}] \tag{3.13}$$

The velocity potential of a harmonic oscillating fluid in the x-direction is [29]:

$$\Phi = U \cdot x \cdot cos(\omega \cdot t) \qquad [\frac{m^2}{s}] \tag{3.14}$$

The velocity component is then:

$$u = \frac{d\Phi}{dx} = U \cdot cos(\omega \cdot t) \qquad [\frac{m}{s}] \tag{3.15}$$

It has to be assumed that the water surface slope is very small in order to use linear wave theory. The profile of a wave has the form of a sine or a cosine function and the motion of a water particle depends on the distance below the water surface, z. h is the mean water depth. The velocity potential of the harmonic wave is [29]:

$$\Phi = \frac{a \cdot g}{\omega_{wave}} \cdot \frac{cosh(k(h+z))}{cosh(k \cdot h)} \cdot sin(k \cot x - \omega_{wave} \cdot t) \qquad [\frac{m^2}{s}] \tag{3.16}$$

The wave number, k, and angular frequency, ω_{wave}, is connected. The relation is given by the dispersion relation. The dispersion relation states that the waves at a given frequency must have a certain wave length.

$$\omega_{wave}^2 = k \cdot g \cdot tanh(kh) \qquad [(\frac{rad}{s})^2] \tag{3.17}$$

For *shallow water* $kh << 1$ and $tanh(kh) = kh$ gives an angular frequency of:

$$\omega_{wave} = \pm(g \cdot h)^{1/2} \cdot k \qquad [\frac{rad}{s}] \tag{3.18}$$

For *deep water*, $h \to \infty$ and $tanh(kh) = 1$, the dispersion relation is:

$$\omega^2_{wave} = k \cdot g \qquad [(\frac{rad}{s})^2] \tag{3.19}$$

Therefore the velocity potential in deep water waves, which in this work will be considered, reduces to:

$$\Phi = \frac{a \cdot g}{\omega_{wave}} \cdot e^{kz} \cdot sin(kx - \omega_{wave}t) \qquad [\frac{m^2}{s}] \tag{3.20}$$

The latter dispersion relation, for $h \to \infty$, provides other relations between the phase velocity, c, wave length, λ, frequency, ω_{wave} and period, T_{wave} in deep water waves:

$$c = \frac{\omega_{wave}}{k} = \sqrt{\frac{g}{k}} \qquad [\frac{m}{s}] \tag{3.21}$$

$$\lambda = \frac{2\pi \cdot g}{\omega^2_{wave}} = \frac{g \cdot T^2_{wave}}{2\pi} \approx 1.56 \cdot T^2_{wave} \qquad [m] \tag{3.22}$$

3.2.3 Water Particle Kinematics

The fluid particles are moving in orbits shown in figure 3.5. The orbits are closed curves. They are elliptical in shallow water and circular in deep water. While the wave propagates the fluid particle just oscillate around its average position. Beneath the crest of a wave the water movement is with the wave and beneath the trough it is against the wave.

The wave particle velocity at the surface is the maximum velocity:

$$V_{wave} = a \cdot \omega_{wave} = \frac{H_{wave} \cdot \pi}{T} \qquad [\frac{m}{s}] \tag{3.23}$$

The velocity component in x-direction is with equation 3.11 and 3.20 expressed:

$$u = \frac{d\Phi}{dx} = a \cdot \omega_{wave} \cdot e^{kz} \cdot cos(kx - \omega_{wave}t) \qquad [\frac{m}{s}] \tag{3.24}$$

and in z-direction:
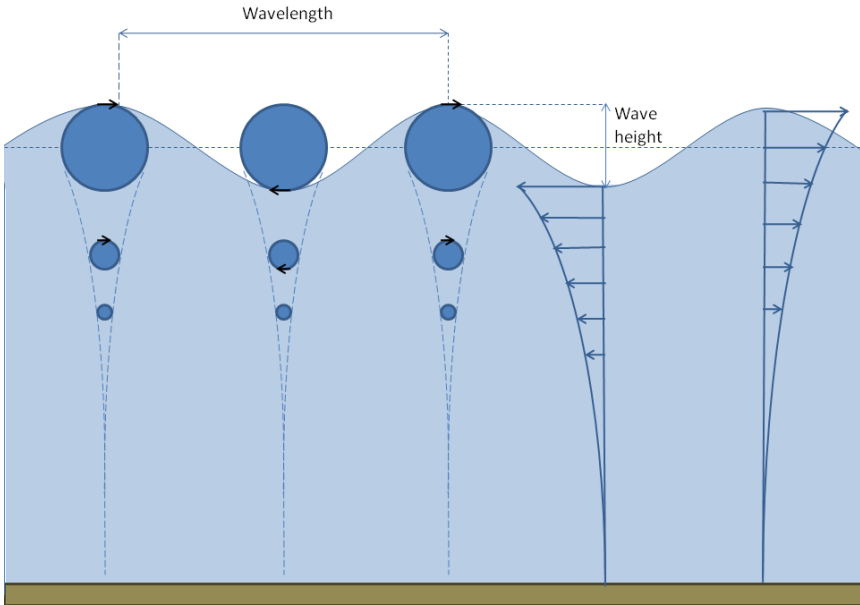
Figure 3.5: Trajectory of water particles in deep water waves.

$$w = \frac{d\Phi}{dz} = a \cdot \omega_{wave} \cdot e^{kz} \cdot sin(kx - \omega_{wave}t) \qquad [\frac{m}{s}] \qquad (3.25)$$

The circular outline velocity of a water particle at a distance z below the sea surface follows the two equations 3.24 and 3.25:

$$V_o = \sqrt{u^2 + w^2} = a \cdot \omega_{wave} \cdot e^{kz} \qquad [\frac{m}{s}] \qquad (3.26)$$

3.3 Hydrofoil Theory

The theory is based on Wind Energy Explained [32] and Analysis and Design of Wind Turbine Blades [23].

3.3.1 Hydrofoil Terminology

The cross-section of a turbine blade is shaped like a hydrofoil. The flow meets the leading edge of the hydrofoil. The angle of attack, α, is the angle between the relative flow, W, and the chord line. The cord line is the straight line connecting the leading and the trailing edge of the airfoil and has a length, L_c. The mean camber line is located halfway between the upper and lower surfaces of the airfoil. The thickness is the distance between the upper and lower surfaces, perpendicular to the chord line. A hydrofoil with its geometry is shown in figure 3.6.
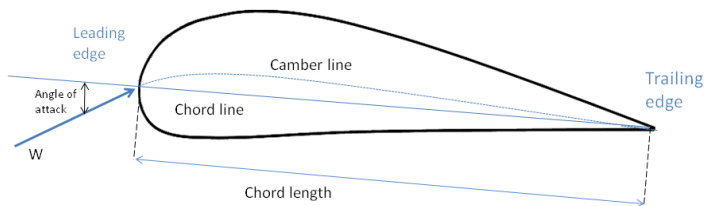
Figure 3.6: Hydrofoil terminology.

3.3.2 Forces and Non-dimensional Parameters

U is the rotational speed of the turbine blade, denoted $U = \omega_t \cdot r$, where ω_t is the angular turbine velocity and r is the position along the blade. V is the undisturbed flow and W is the relative flow. The flow is split into two separate streams over the hydrofoil. The flow velocity increases over the convex side of the airfoil resulting in a lower pressure compared to the concave side. The upper side of the hydrofoil is the suction side and the lower side is the pressure side. The pressure difference between suction and pressure side of the airfoil generates a lift force, F_L, perpendicular to the relative flow. Friction between the flow and the airfoil surface is the main reason for the drag force, F_D, a force which is parallel to the flow. The size of the lift and drag forces varies with the angle of attack, α. The torque of the blade element, M', will act along the cord line at a distance of $\frac{L_c}{4}$ from the leading edge, parallel to the rotational speed of the blade. The thrust force, T', is perpendicular to the rotational speed. The forces acting on a blade element are shown in figure 3.7.

The most important parameter to characterize the fluid flow condition is the
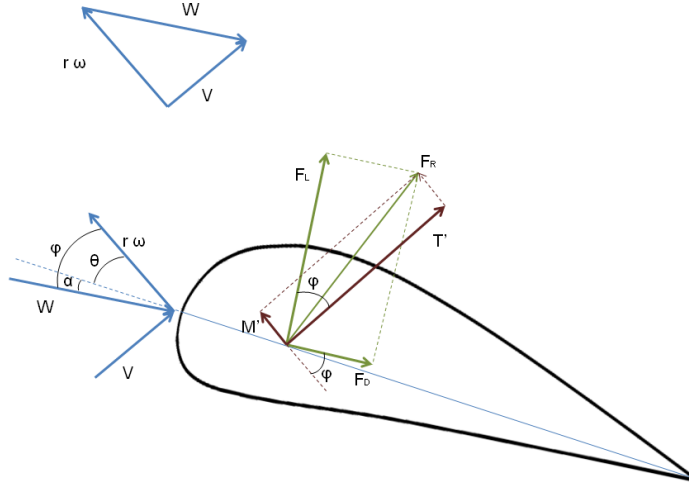
Figure 3.7: Velocities and forces on one blade element

Reynolds number. There are significant differences in hydrofoil behaviour at different Reynolds numbers. The Reynolds number is defined:

$$Re = \frac{L_c \cdot W}{\upsilon} \qquad [-] \qquad (3.27)$$

where W is the relative flow, L_c the chord length and the kinematic viscosity is $\upsilon = \frac{\mu}{\rho}[\frac{m^2}{s}]$. μ is the dynamic viscosity and ρ the density. The non dimensional lift force coefficient is defined:

$$C_L = \frac{F_L}{\frac{1}{2} \cdot \rho \cdot W^2 \cdot L_c \cdot dr} \qquad [-] \qquad (3.28)$$

where dr is the depth of the airfoil and F_L is the lift force. Similarly the drag coefficient is defined:

$$C_D = \frac{F_D}{\frac{1}{2} \cdot \rho \cdot W^2 \cdot L_c \cdot dr} \qquad [-] \qquad (3.29)$$

where F_D is the drag force. The force coefficients are functions of the Reynolds number. Drag increases with decreasing Reynolds number and lift increases with increasing Reynolds number. Thick hydrofoils normally have more drag than thin hydrofoils, but when the thickness is symmetric about the camber line it has a very little effect on the lift since it affects the pressure distribution symmetrically [24].

3.3.3   Stall

The lift force is usually much higher than the drag force. The lift coefficient is increasing linearly with increasing angle of attack, but in actual cases a large angle of attack will result in a separation of the flow from the hydrofoil surface. This effect is called stalling. The stall starts from the trailing edge. In stall regions the stream lines will no longer follow the airfoil. This will cause turbulence, backflow, reduced velocity, higher pressure and the lift of the hydrofoil is reduced. The phenomenon is shown in figure 3.8 (a).
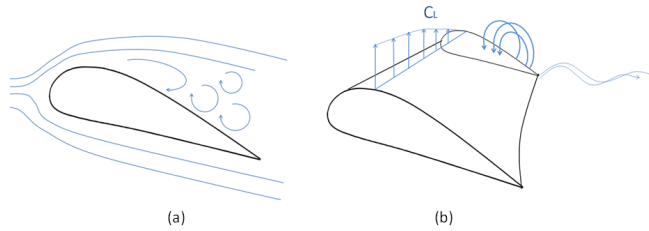
Figure 3.8: A blade element with (a) stall and (b) tip losses.

3.3.4   Tip Loss

The generation of lift on blades relies to generating a pressure difference between the upper and the lower surfaces. At the tip of the wing the flow will leak from the high to the low pressure area around the blade. This creates two effects. The lift is reduced and goes to zero at the tip and rotational flow that requires energy will create tip vortices which is a loss for the torque [24]. This is shown in figure 3.8 (b).

Among methods that have been created for including the effect of tip loss in calculations is the method created by Prandtl the most straightforward. The correction factor, F, is a function of number of blades, angle of relative wind and the position on the blade. This factor will affect the torque and the thrust on the turbine. F, given in equation 3.30, is always between 0 and 1 and characterizes the reduction of the forces along the radius [32].

$$F = \frac{2}{\pi} \cdot cos^{-1}(exp(-(\frac{(B/2) \cdot (1 - (r/R))}{(r/R) \cdot sin\varphi}))) \qquad [-] \qquad (3.30)$$

Here B is the number of blades, φ is the angle of relative wind, R is the radius of the turbine and r is the position along the blade.

3.4 The Blade Element Momentum Theory

The theory is based on Wind Energy Explained [32] and Analysis and Design of Wind Turbine Blades [23].

The blade element momentum method can be used to design turbine blades and to calculate the forces acting on a horizontal axis turbine rotor. The theory consists of momentum theory and blade element theory. Momentum theory refers to a control volume analysis of the forces acting on the turbine based on conservation of momentum. The control volume analysis provides information about how much energy that can be extracted from the flow, but does not say how this is done. Blade element theory refers to analysis of forces between the fluid and the rotor blades due to the pressure difference over the hydrofoil. The blade element momentum theory is based on the assumption of a steady state situation, uniform wind, no flow in radial direction of the blade, each bade is independent from the others and the blades are straight and do not bend or flex.

The method is a simplified approach and these assumptions are not true for a real turbine, but it can be helpful to predict and get a good impression of the performance of the turbine. This method is basically to be used for wind turbines, but is also applicable on tidal turbines. The energy in the wind is in the motion of the air. For tidal turbines as well the velocity is the important factor, but it has to be connected to other parameters, like interaction with the waves, the tidal cycle, turbulence and wake from tower and upstream turbines. In this work the dynamic forces acting on a tidal turbine blades is calculated using theory from the blade element momentum method.

3.4.1 Actuator Disk Theory

The kinetic energy in the wind is transformed to mechanical energy in the device. The momentum theory assumes a control volume where the boundaries are the surface of a stream tube and two cross sections. The turbine is at first represented by a uniform actuator disk, shown in figure 3.9.
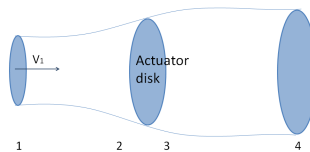
Figure 3.9: The control volume with the actuator disk.

By using the actuator disk theory it will be possible to find the absolute highest efficiency the turbine can have. Four different regions are considered. The first

region, 1, is far upstream of the turbine, 2 is just before the actuator disk and 3 is just after. 4 is the region far downstream from the turbine. The velocity of the flow will be reduced by the turbine. Because of continuity the velocity has to be the same just before and just after the swept area. The pressure far upstream, p_1, and the pressure far downstream, p_4, are equal. Because of the differential pressure over the rotor, there is a force acting on the swept area of the turbine, $F = \Delta p \cdot A_2$ [N].

The Bernoulli's equation is valid from region 1 to 2, and from 3 to 4. The pressure difference over the turbine, Δp, can be found by using the expressions for the two streamlines:

$$\Delta p = p_2 - p_3 = \frac{1}{2} \cdot \rho \cdot (V_1^2 - V_4^2) \qquad [Pa] \tag{3.31}$$

By using Newton's second law, the force, caused by the pressure difference over the area, has to balance the change in momentum over the control volume surface:

$$F = \Delta p \cdot A_2 = (V_1 - V_4) \cdot (\rho \cdot V_2 \cdot A_2) \qquad [N] \tag{3.32}$$

By equating the two expressions for the pressure, from Bernoulli, equation 3.31, and from change in momentum, equation 3.32, the velocities, V_1 and V_4 can be related. The axial induction factor, a, which is an expression for the speed reduction in front of the disk is defined:

$$a = \frac{V_1 - V_2}{V_1} \qquad [-] \tag{3.33}$$

and the velocity in region 4 can be expressed by the known free stream velocity and the axial induction factor:

$$V_4 = V_1 \cdot (1 - 2 \cdot a) \qquad [\frac{m}{s}] \tag{3.34}$$

The power output can be found by inserting the expression for the velocity, V_4, in equation 3.31 for the difference in pressure and then multiply by the area and the velocity:

$$P = \Delta p \cdot A_2 \cdot V_2 = 2 \cdot \rho \cdot A_2 \cdot V_1^3 \cdot a \cdot (1 - a)^2 \qquad [W] \tag{3.35}$$

The turbine rotor performance is characterized by the power coefficient, C_p, which is the rotor power due to the power in the wind:

27

$$C_p = \frac{P_{rotor}}{\frac{1}{2} \cdot \rho \cdot V_1^3 \cdot A_2} = 4 \cdot a \cdot (1-a)^2 \qquad [-] \qquad\qquad (3.36)$$

By deriving this coefficient with respect to a, the result will give an optimal value of $a = \frac{1}{3}$, where $C_p(a = \frac{1}{3}) = \frac{16}{27}$. This is the maximum theoretical efficiency the turbine can have and is called *Betz limit.*

The thrust force is the force in the axial direction acting on the turbine and is expressed:

$$F_T = \frac{1}{2} \cdot \rho \cdot A_2 \cdot V_1^2 \cdot (4 \cdot a \cdot (1-a)) \qquad [N] \qquad\qquad (3.37)$$

and the thrust coefficient:

$$C_T = \frac{\Delta p \cdot A_2}{\frac{1}{2} \cdot \rho \cdot A_2 \cdot V_1^2} = 4 \cdot a \cdot (1-a) \qquad [-] \qquad\qquad (3.38)$$

The relation between the axial induction factor and the power and the thrust is known. This is an idealized model and is only valid for small values of axial induction factors.

3.4.2 Rotary Disk Theory

In actuator disk theory it was assumed that no rotation was imparted to the flow. Actuator disk theory is extended to the rotary disk theory. In this analysis the rotating rotor generates angular momentum and the wake will rotate. The rotation is in the opposite direction to the rotor. The rotating turbine is treated as a rotating disk and the blades will not be treated individually. The rotational induction is a source of energy loss and the energy extraction by the rotor is less than by a wake without rotation. The rotational speed of the flow is induced by the blades. A rotational induction factor has to be defined:

$$a' = \frac{\Omega}{2 \cdot \omega} \qquad [-] \qquad\qquad (3.39)$$

where Ω is the angular velocity imported to the flow stream and ω is the angular velocity of the turbine rotor. The rotational induction factor is similar to the axial induction factor, but here the speed is increasing across the turbine and we must add the induced velocity as we have acceleration. The rotational speed of the blade

will be denoted U and of the flow u. The tangential velocity is not constant along the blade and can be expressed at a radius r as $U = \omega \cdot r$ $[\frac{m}{s}]$. The velocity of the flow just before the blades is $u_2 = 0$ $[\frac{m}{s}]$. The velocity right after the blades is defined $u_3 = 2 \cdot a' \cdot U$ $[\frac{m}{s}]$. The average velocity of u_2 and u_3, u, is:

$$u = \frac{1}{2} \cdot (u_2 + u_3) = a' \cdot (\omega \cdot r) \qquad [\frac{m}{s}] \qquad (3.40)$$

The total rotational velocity the blades experiences at a given radius, r, is:

$$U_2 = U + u = (1 + a') \cdot (\omega \cdot r) \qquad [\frac{m}{s}] \qquad (3.41)$$

Now we have a complete model for the flow around the turbine, a wake model, describing the flow up- and downstream of the turbine, where V is the velocity of undisturbed flow and U is the rotational velocity. This is shown in figure 3.10.
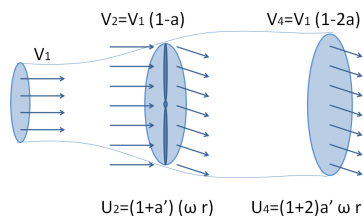
Figure 3.10: Flow model around the turbine.

3.4.3 Blade Element Theory

For this method the following assumptions has to be made: there is no interaction between the elements and the forces are determined by the lift and drag characteristics. The theory is described for an infinitely long wing with blade elements of a length dr. The blades are divided into N sections and the velocities on one blade element expressed with respect to a, a' and V_1. The lift and drag force can be combined in a resultant force, F_R. The lift and drag forces are derived from equation 3.28 and 3.29:

$$F_L = \frac{1}{2} \cdot \rho \cdot W^2 \cdot C_L \cdot L_c \cdot dr \qquad [N] \qquad (3.42)$$

$$F_D = \frac{1}{2} \cdot \rho \cdot W^2 \cdot C_D \cdot L_c \cdot dr \qquad [N] \qquad (3.43)$$

29

φ is the flow angle, the angle between the relative flow velocity and the plane the blade is rotating in, $\varphi = \theta + \alpha$, where θ is the twist angle and α is the angle of attack. Blade geometry, shown in figure 3.7, gives the following expressions for thrust and torque on one blade element.

$$T' = F_L \cdot cos\varphi + F_D \cdot sin\varphi \qquad [N] \tag{3.44}$$

$$M' = F_L \cdot sin\varphi - F_D \cdot cos\varphi \qquad [Nm] \tag{3.45}$$
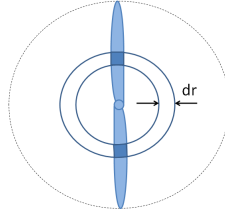
Figure 3.11: Blade element of length dr.

The forces on the rotor of a thickness dr, figure 3.11, with Z numbers of blades are:

$$dT = C_a \cdot \frac{1}{2} \cdot \rho \cdot W^2 \cdot L_c \cdot dr \cdot Z \qquad [N] \tag{3.46}$$

$$dM = C_r \cdot \frac{1}{2} \cdot \rho \cdot W^2 \cdot L_c \cdot dr \cdot Z \qquad [Nm] \tag{3.47}$$

where C_a and C_r are the axial and rotational force coefficient:

$$C_a = C_L \cdot cos\varphi + C_D \cdot sin\varphi \qquad [-] \tag{3.48}$$

$$C_r = C_L \cdot sin\varphi - C_D \cdot cos\varphi \qquad [-] \tag{3.49}$$

By expressing the relative velocity, W, with respect to a, a' and V_1 inserting this in equation 3.46 and 3.47 the new expressions for dT and dM are:

$$dT = C_a \cdot \frac{1}{2} \cdot \rho \cdot \left(\frac{V_1^2 \cdot (1-a)^2}{sin^2\varphi}\right) \cdot L_c \cdot dr \cdot Z \qquad [N] \qquad (3.50)$$

$$dM = C_r \cdot \frac{1}{2} \cdot \rho \cdot \left(\frac{V_1 \cdot (1-a)}{sin\varphi}\right) \cdot \left(\frac{r \cdot \omega \cdot (1+a')}{cos\varphi}\right) \cdot L_c \cdot dr \cdot Z \qquad [Nm] \qquad (3.51)$$

To calculate the total forces on the turbine the forces has to be summarized over the whole blade:

$$T = \int dT = \sum T_i \qquad [N] \qquad (3.52)$$

$$M = \int dM \cdot r = \sum M_i \cdot r_i \qquad [Nm] \qquad (3.53)$$

The geometry of the blade is in this project already known and with these equations the thrust and torque on the tidal turbine blade can be calculated. Also the tip loss, using Prandtl's tip loss factor, F, will be considered. In this theory a uniform velocity profile over the turbine rotor is used for calculation of the forces. This is not the case for a real turbine. The change in velocity over the turbine rotor has to be considered in the calculation of the dynamic loads.

3.5 Turbulence

3.5.1 The Properties of Turbulence

Turbulence is present in almost all natural flows and most flows of engineering interest, in the atmosphere, in the ocean, rivers, pipe flow etc. The phenomenon has no rigid definition, but can basically be characterized by chaotic, stochastic property changes of fluid flow. Turbulence is random fluctuations in time and space, three dimensional and time dependent. Turbulent flow is diffusive, irregular, random and has a spectrum of different scales [20].

A fluid flow is characterized by the Reynolds number given in equation 3.27. At a low Reynolds number the flow is laminar. Viscous effects dominate and damp out perturbations. As the Reynolds number is increasing the perturbations are no longer being damped and a transition to turbulent flow will occur.

3.5.2 Energy Cascade

Turbulence can be imagined as formation of eddies, which are of different scales [28]. The larger scales are the energy containing scales. The kinetic energy of the turbulent motion is contained in the large structures. Large scales break down to smaller vortices. In the cascade process the energy will be transported from large to smaller scales. The smaller scale is set by the viscosity and the rate which energy is supplied by the largest scales. Eventually viscous dissipation of energy takes place and the kinetic energy of the smallest scales is transformed into internal energy. The rate of energy supply must be equal to the rate of energy dissipated by viscosity. Figure 3.12 is showing the energy spectrum, with energy on the y-axis and the wave number, here κ, on the x-axis, which means that the large scale eddies are to the left and the small scale eddies to the right in the figure.
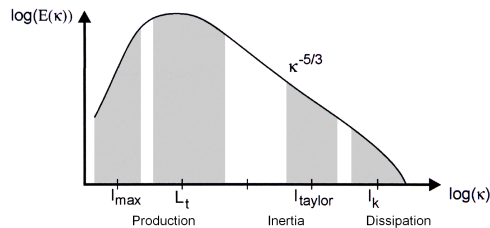
Figure 3.12: Energy spectrum [30].

3.5.3 Kolmogorov Microscale and Scale Separation

As mentioned above turbulence is a spectrum of different scales. The largest scales are related to geometric scales. The large length and velocity scales are L and U, and the timescale $\tau = \frac{L}{U}$. The smallest scale is the Kolmogorov micro scale. The Kolmogorov length, velocity and time scales are defined [28]:

$$l_k = \eta \approx (\frac{\nu^3}{\epsilon})^{1/4} \ [m], \quad u_k = u_\eta \approx \sqrt{\frac{\nu}{\epsilon}} \ [\frac{m}{s}], \quad \tau_k = \tau_\eta \approx (\nu \cdot \epsilon)^{1/4} \ [s] \qquad (3.54)$$

ϵ is the average rate of energy dissipation and has the unit $[\frac{m^2}{s^3}]$. The separation between the largest and the smallest size eddies is determined by the Reynolds number. The relation between the large scale and Kolmogorov micro scale are defined [28]:

$$\frac{L}{\eta} \approx Re^{3/4}, \qquad \frac{U}{u_\eta} \approx Re^{1/4}, \qquad \frac{\tau}{\tau_\eta} \approx Re^{1/2} \qquad (3.55)$$

3.5.4 Reynolds Decomposition

The flow velocity, u, can be split into a mean part, $\bar{u}$, and a fluctuating part, u', using Reynolds decomposition [40]. This is shown in equation 3.56 and figure 3.13.

$$u = \bar{u} + u' \qquad [\frac{m}{s}] \qquad (3.56)$$
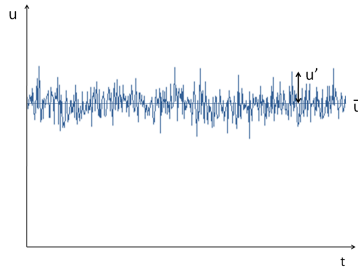
Figure 3.13: Mean and fluctuating turbulent velocity.

The time mean of the turbulent velocity is:

$$\bar{u} = \frac{1}{T} \int_0^T u \ dt \qquad [\frac{m}{s}] \qquad (3.57)$$

The turbulence intensity is the most basic measure of the turbulence. The turbulence intensity, TI, is a non-dimensional number and is defined as the ratio of the standard deviation of the velocity to the mean [32]:

$$TI = \frac{\sigma_u}{\bar{u}} \quad [-] \tag{3.58}$$

$$\sigma_u = \sqrt{\frac{1}{N_s - 1} \sum_{i=1}^{N_s} (u_i - \bar{u})^2} \quad [-] \tag{3.59}$$

σ_u is the standard deviation, given in sampled form, u_i are the observed values and $\bar{u}$ is the mean value of the observation. N_s is the number of samples.

3.6 Fatigue Loads

This chapter is based on Mechanical Behaviour of Materials [21] and theory from NDT Resource Senter [6].

3.6.1 Stress, Strain and Fatigue

The components of machines, vehicles and structures are frequently exposed to alternating loads, resulting in cyclic stresses, which can cause microscopic damage on the material. These microscopic damages can under cyclic loading develop into cracks and larger failures.

Stress is a measure of the internal forces acting at a certain cross-sectional area of a deformable body. Stress is used to express loading and is the applied force that tends to deform a body. The dimension of stress is as for pressure and has the unit $Pa = \frac{N}{m^2}$. Strain is the response of a system to an applied stress. A stress is produced when a material is loaded with a force. The stress causes deformation of the material. Strain is a description of deformation in terms of relative displacement of particles in the body. The definition of strain is the amount of deformation in the direction of the applied force divided by the initial length of the material.

Cyclic loading and unloading of any material will lead to a failure phenomenon called fatigue. Fatigue is structural damage that occurs when a material is exposed to alternating loading over a period of time. Lifetime under cyclic loading is significantly smaller than under static loads, which do not vary and are continuously present. Cyclic loading will cause microscopic cracks, which enlarge during the cycles. Once these cracks have reached a critical size they cause a sudden fracture of the structure.

3.6.2 The S-N Curve
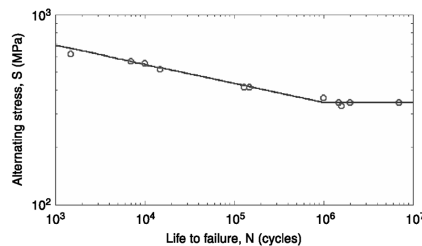
Figure 3.14: Stress versus life (S-N) curve [16].

35

Material performance is often characterized by a S-N curve. The data are obtained by cyclic tests of material, counting the number of cycles until failure. Figure 3.14 [16] is expressing the cyclic stress range, S, against the number of cycles to failure, N. The amplitude of the stresses is on the vertical axis and the cycles, normally in a logarithmic scale, on the horizontal axis. Fatigue life is the number of cycles that will cause failure at a certain stress level. The amplitude of a cyclic loading has a major effect of the fatigue performance. If the material is loaded under the fatigue limit it will not be damaged regardless of the times loaded. For a high level of stresses the number of cycles to cause failure is low. For a decreasing level of stresses the number of cycles causing failure is increasing. The greater the applied stress range is, the shorter the lifetime is.

3.6.3 Factors Affecting Fatigue Life

Fatigue depends on the material type. The behaviour during the cycles will vary for different materials. Three factors are necessary for fatigue cracks to initiate. The first is the loading pattern, which must contain maximum and minimum peaks with large variations. Secondly, the peak stress levels must be of a sufficiently high value. And third, the material must be exposed to a large number of cycles of the applied stress.

In addition to these factors also other parameters are of importance. The environment, temperature, corrosion and internal stresses in the material, residual stress, are other factors. Geometry, variation in cross section of material can lead to stress concentration and lower the fatigue strength. Also the direction of loading is of importance. Fatigue cracks initiate at the surface and therefore also a change in microstructure and surface condition will affect the fatigue life.

3.6.4 Rainflow Counting Algorithm

The rainflow counting algorithm is used to analyse fatigue data and is an essential part of estimation of fatigue life. The rainflow counting algorithm is a cycles counting algorithm and has obtained its name from an analogy of rain falling down a pagoda roof.

A load process can be characterized by a sequence of local extremes, peaks and troughs. To do the counting method the time history has to be turned 90° clockwise and the process has to be considered as a sequence of pagoda roofs with rain falling down on them. The time serie converted to a process of peaks and troughs considered as a sequence of roofs are shown in figure 3.15.

The counting algorithm [39]:

1. At each peak and trough a rainflow is started and drips down the pagoda.

2. When a rainflow path started at a trough comes to the tip of the roof, the flow stops if the opposite trough is more negative from the one the flow started from.

3. When a rainflow path started at a peak it is stopped by a flow from a peak which is more positive than the one the flow started from.

4. If the rain flowing down a roof intercepts flow from an earlier path, the present path is stopped.

5. Count the number of half-cycles if the flow reaches the end of time history or it is stopped by a flow from a greater magnitude or a flow from an earlier roof.

6. Assign a magnitude to each half-cycle by stress ranges found as the projected distances on the stress axis.

7. Pair of half cycles of identical magnitude, but of opposite sense, are counted as complete cycles.

The rainflow counting method is a widely used counting method for fatigue calculation.
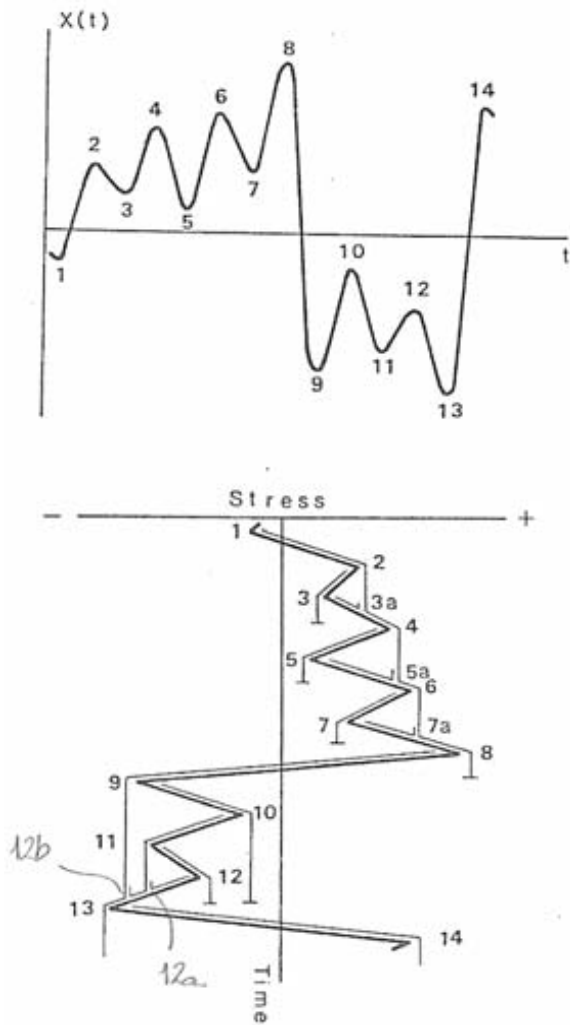
Figure 3.15: The rainflow counting algorithm [39].

Chapter 4

The 1 MW Tidal Turbine

4.1 Design of the Turbine

A model tidal turbine is designed, built and tested at Marintek. This turbine will be used for development and design of a 1 MW reference tidal turbine. The tidal turbine is designed by a PhD student, Céline Faudot, with results from the blade element momentum theory. The design of the tidal turbine has been realized and optimized with a Matlab code using blade element momentum method. The 1 MW tidal turbine and its substructure is shown in figure 4.1.
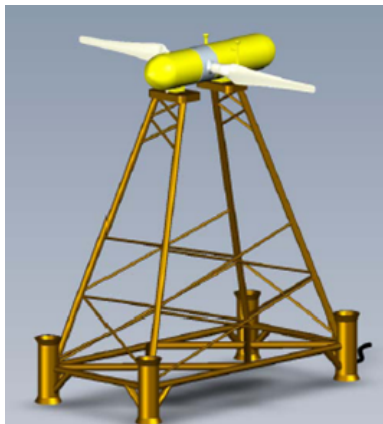
Figure 4.1: The reference 1 MW tidal turbine.

4.2 Technical Data

4.2.1 Design Parameters

The reference turbine has a power output of 1 MW. It is a horizontal axis tidal turbine (HATT) with two blades and a bottom fixed, lattice substructure, which is shown in figure 4.1. All elements for the reference turbine can be found in [22].

A reference site where the prototype can be installed is chosen. This site is Pentland Firth, between the Orkney Islands and Caithness in the north of Scotland, where the maximum current velocity has been measured up to 4 m/s. The chosen prototype turbine design parameters are listed in table 4.1.

Number of turbine blades	N_{blade}	2	-
Generator power output	P_G	1	MW
Turbine Diameter	D_t	21	m
Current velocity at design point	V_{design}	2.5	m/s
Maximum water particle velocity	V_{max}	4	m/s
Depth of turbine blade tip in the upper pos.	WD_{up}	8	m
Distance from blade tip in lower pos. to seabed	N_i	7	m
Tip Speed Ratio	TSR	7	-
Power coefficient	C_p	0.4	-
Drive train efficiency	η_{DT}	0.9	-
Generator Speed	η_G	500	-
Wave steepness	s	1/10	-
Wave period	T_{wave}	7.34	s
Density of water	ρ	1028	kg/m^3
Kinematic viscosity of water	υ	$1.31 \cdot 10^{-6}$	m^2/s

Table 4.1: Chosen prototype design parameters.

The calculated parameters for the prototype tidal turbine are listed in table 4.2. The model turbine has been tested at Marintek and is the small scaled model of the 1 MW prototype. The model turbine is designed with a turbine scale of 14, which gives a diameter, D'_t, of 1.5 meters. The chosen and calculated parameters for the model turbine are also listed in [22].

Wave length in deep water	λ	84	m
Maximum wave height	H_{wave}	8.4	m
Wave number	k	0.075	rad/m
Wave frequency	ω_w	0.856	rad/s
Water particle velocity at the surface	V_{wave}	3,6	m/s
Water particle velocity at blade tip in upper pos.	V_{tipup}	2.7	m/s
Water particle velocity at blade tip in lower pos.	V_{tiplp}	0.562	m/s
Froude number	Fr	0.174	-
Rotational speed at blade tip at design velocity	U_{tip}	17.5	m/s
Turbine speed	ω_t	1.67	rad/s
Turbine main shaft torque at design velocity	M_x	668	kNm
Thrust force at design velocity	T	779	kN
Thrust force at design velocity + wave velocity	T	1424	kN

Table 4.2: Calculated prototype parameters.

4.2.2 Blade Layout

The blade consists of 4 hydrofoil sections, S816 21%, S825 17%, S826 14%, S826 12%, with linear interpolation between the sections. Near the hub the blade is shaped like a cylinder. The hub has a length of 10% of the radius. The blade layout is described in table 4.3.

r/R	Thickness	Aerodynamic
0.10	50.00	cylinder
0.25	21.00	S816
0.75	17.00	S825
0.90	14.00	S826
0.98	12.00	S826

Table 4.3: Blade layout.

4.3 Loads on the Turbine

A significant challenge tidal stream turbines face is to survive the harsh operating environment. The tidal turbine is operating under the condition that the density of water is almost thousand times larger than the density of air. The unsteady dynamic loads on a tidal turbine are primarily driven by variation in the onset flow inducing fluctuations in the forces acting. The design of the turbine depends on the dimensional forces acting on the turbine, on its blades and its structure. The main dynamic forces acting on the tidal turbine are due to:

- tidal current variation

- turbulence

- wave-current interaction

- wake from the tower

- wake from upstream turbines

One of the most distinct features of the ocean is its waves. Any marine structure experiences the waves. Ocean waves are irregular. They travel at different speeds, with different heights and different directions of propagation causing a changing velocity profile. Beneath the crest of a wave the water movement is with the wave and beneath the trough it is against the wave. Therefore the effect of the waves will primarily be via the attenuation or reduction of the apparent velocity. The sea water level and the tidal current velocities are not constant, but vary over the tidal cycle. In the transition between low and high tides the current velocity will be zero and the water level will have its maximum or minimum. The influence of the waves depends on the water level and the depth of the hub. The variation of loads on the turbine is also caused by the vertical velocity profile, depending of viscosity of the water and seabed friction. As the turbine is rotating the blades experience a changing current velocity, depending on their position. Also turbulence intensity on the site has an influence on the loads. This changing velocity profile is a result of all the above listed components interacting, creating a dynamic load on any marine structure.

It is important to characterize the dynamic loads acting on the turbine. Cyclic loading and unloading of any material will lead to a failure phenomenon called fatigue. This is structural damage that occurs when a material is exposed to alternating loading over a period of time.

A horizontal axis tidal turbine operates perpendicular to the current and there are two main loads on the turbine, the main shaft torque and the thrust force. The thrust force is acting in the direction of the current and induces a bending moment around the y-axis, the pitch moment, and around the z-axis, the yaw moment. The torque acts around the main shaft of the turbine and is inducing rotation. Figure 4.2 is showing the thrust force and moments on the tidal turbine. Due to the concept of extracting energy from the current, the loads mentioned above are inevitable.
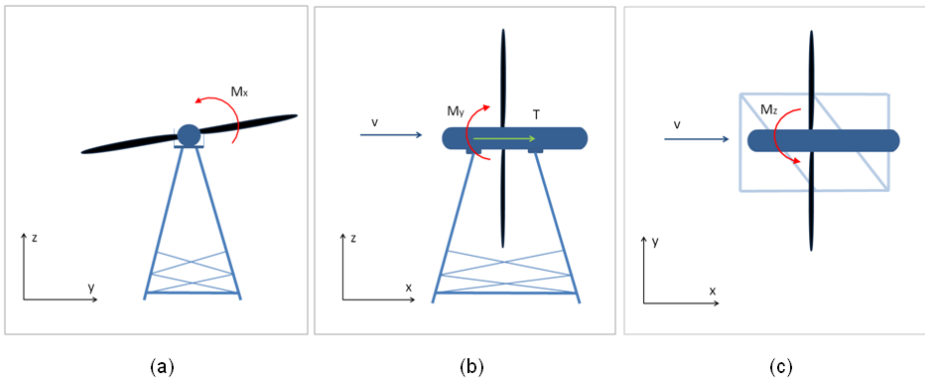
Figure 4.2: The turbine with its substructure seen from (a) front showing the main shaft torque, (b) the side showing the bending-moment around the y-axis and (c) above showing the bending moment around the z-axis.

Chapter 5

Realistic Flow Passing Through the Tidal Turbine Rotor

In the blade element momentum method the flow passing through the sweep area of the turbine is uniform. This is a simplified approach, which is not true for a real turbine. To predict the loads on the turbine it is necessary to take into account the real flow velocity distribution over the rotor area. There are several phenomena inducing a non-uniformity of the velocity. The turbine will experience a current induced vertical velocity profile, which is changing over time due to the waves and is affected by turbulence, the tidal wave and also the wake from tower and upstream turbines.

5.1   Influence of the Current

Local flow conditions are very important for the installation of a tidal turbine at a real site. The tidal current is inducing a vertical no-slip velocity profile. Because of seabed friction and water viscosity the profile will vary with the water depth. The tidal turbine and the vertical velocity profile from the current, not affected by the waves, are shown in figure 5.1.
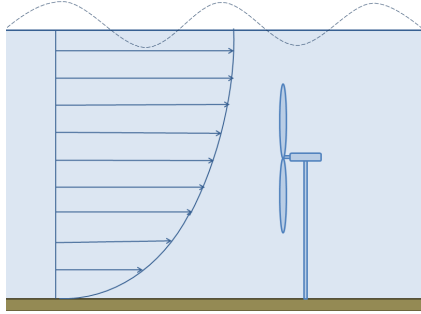
Figure 5.1: Current velocity profile with no-slip condition.

The varying velocity profile can be found with a good approximation using the power law. The equation is expressing the velocity on every position on the vertical axis [24]:

$$V(z) = V(0) \cdot (\frac{WD + z}{WD})^\alpha \qquad [\frac{m}{s}] \qquad (5.1)$$

WD is the total water depth in meters, z is the depth from the mean free sea water surface in meters, negative downwards, and α is equal to $1/7$. The waves have a large influence on the velocity profile, which will change due to the oscillating sea surface.

5.2 Influence of Waves

The waves will affect the current velocity profile. Assuming that the turbine is operating in deep water waves, the fluid particles due to the waves are moving in circular orbits, figure 3.5. The water particle velocity profile due to the waves will therefore vary between positive and negative values. Beneath the wave crest the water movement is with the wave propagation and beneath the trough it is against the wave. The waves are able to reverse, increase or cancel out the current velocity. The influence of the waves on the vertical velocity profile depends on the current velocity, the water depth, the wave length and wave height. The resulting velocity profile from the current and the waves is shown in figure 5.2.
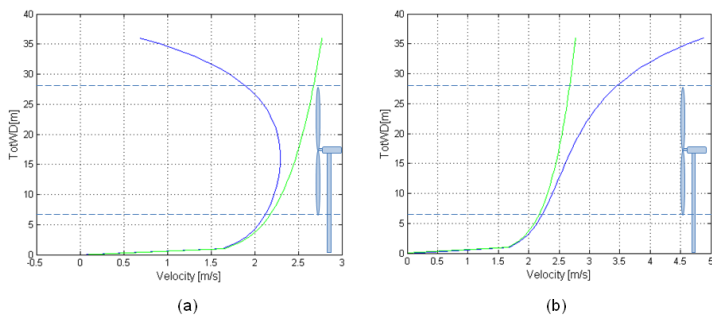
Figure 5.2: Resulting velocity profile from current and waves (blue line) when the turbine is experiencing a (a) wave trough and (b) crest. The green line is the velocity profile not affected by the waves. The horizontal dotted lines show the sweep area of the turbine. The current velocity on the axis, v, is 2.5 m/s, the wave period, T_{wave}, is 7 s and the steepness, s, is 0.05.

5.2.1 Wheeler Stretching

Because of the waves the sea surface is oscillating above a mean level. The vertical velocity profile will be stretched or compressed, so that the surface velocity component is held constant. This phenomenon is called the *Wheeler method*. A wave crest will stretch the vertical profile and the trough will compress it. The depth, z, becomes z_s, which is the stretched vertical coordinate. η is the sea surface elevation, given in equation 3.4, and WD the total water depth, both in meters. z_s is defined:

$$z_s = z \cdot (1 + \frac{\eta}{WD}) + \eta \qquad [m] \tag{5.2}$$

where $-WD < z < 0$ and $-WD < z_s < \eta$, $z_s > z$ for $\eta > 0$ and $z_s < z$ for $\eta < 0$.

5.3 Influence of Turbulence

Also the turbulence is affecting the loads on the turbine. Turbulence means an additional fluctuating velocity component added to the mean velocity. The fluctuating velocity is a dynamic load on the turbine with many cycles within a second of time. Turbulence is a spectrum of different scales. Because the turbulence is three dimensional and time dependent every point on the turbine blade is experiencing a different velocity due to the fluctuating component above the mean value of the velocity.

5.4   Influence of the Tidal Wave

Tidal currents are results of rise and fall of sea water level due to the tides. The variation in current velocity and level of the sea surface has an influence on the loads on the turbine. As the water depth is varying the vertical velocity profile will be stretched or compressed due to tidal oscillations. The turbine is placed at a fixed position at a given distance from the bottom. The position of the hub relatively to the sea surface is of importance. If the total water depth is large the waves will have a smaller influence on the current velocity profile in the sweep are of the turbine. If the distance between the turbine and the sea surface is small the turbine will experience a current velocity profile more affected by the waves. As mentioned in chapter 3.1 the current velocity has a phase offset of 90 degrees from the water height, which means that the velocity is zero at the transition between high and low tide. The blades will then be pitched, so that the turbine can operate in both directions of the flow. Figure 5.3 is showing the tidal wave at a site like Pentland Firth. The figure is showing the variation in water level and the current velocity the tidal turbine is experiencing when operating in both directions of the flow.
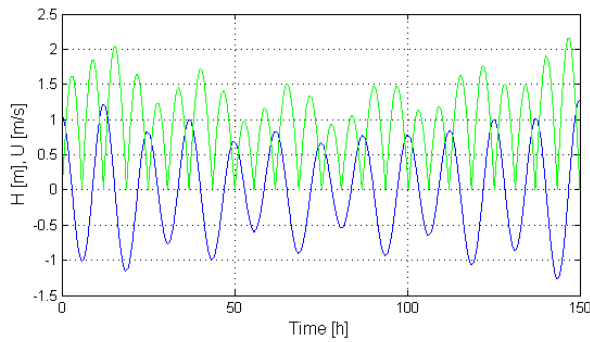
Figure 5.3: The tidal wave when the turbine is operating in both directions of the flow. Water level shown in blue and the current velocity in green.

Chapter 6

Matlab Calculations

A Matlab code is written to calculate the dynamic loads on the 1 MW reference tidal turbine. The code is based on harmonic analysis of the tides, linear wave theory, hydrofoil geometry, blade element momentum theory, turbulence theory and Reynolds decomposition. The time varying forces calculated are the thrust force, T, the main shaft torque, M_x, and the thrust induced pitch moment, M_y, and yaw moment, M_z.

6.1   Setup

In the Matlab code it is possible to do calculations with different design parameters for the turbine and with different site conditions at different waves. The input parameters in the code are listed in table 6.1. The parameters due to the design of the 1 MW reference turbine are listed in table 6.2.

The Matlab code is given in A.1 The code is iterating through all blade elements for both blades every time step in the calculations. The position of each blade has to be calculated for every time step. γ is the angle between the horizontal axis and the blade. When γ is found the position on the vertical axis, z, for each blade element is calculated. When the position of the blade element is found the resultant velocity on this position needs to be known. A function, given in A.6, which calculates the resultant velocity corresponding to the position of the element, is for each blade element called when iterating along the blade. The function is returning the resultant velocity due to the current and the waves dependent on the velocity profile and wave chosen as input parameters. This is done at every time step. At the first time step of the calculations the turbine blades are positioned horizontally and experience a wave crest. The turbine is rotating counter clockwise.

Input parameters

stream velocity at sweep area center	V	$[\frac{m}{s}]$
vertical velocity component due to the waves	vvc	on/off
turbine scale	S_f	$[-]$
number of blades	N_{blade}	$[-]$
vertical velocity profile	$V(WD, \alpha, z)$	on/off
tidal wave		on/off
turbulence intensity	TI	$[\%]$
waves		on/off
time step	Δt	$[s]$
minimum time step	t_{min}	$[s]$
maximum time step	t_{max}	$[s]$
wave steepness	s	$[-]$
wave period	T_w	$[s]$

Table 6.1: Matlab input parameters.

Design parameters

number of blade elements	N	$[-]$
turbine radius	r	$[m]$
density of water	ρ	$[\frac{kg}{m^3}]$
distance from blade tip in lower position to seabed	N_i	$[m]$
tip speed ratio	TSR	$[-]$
chord length	L_c	$[m]$
axial and rotational induction factor	$a, \ a'$	$[-]$
twist angle	θ	$[deg]$
lift and drag coefficients	$C_L, \ C_D$	$[-]$

Table 6.2: Matlab design parameters.

To implement the turbulence in the Matlab code an additional fluctuating velocity component is added to the resultant velocity due to the current and the waves. Each blade element is assigned to one fluctuating velocity signal. The signal is based on sinusoidal oscillations and is the sum of 9 components with time periods between 1 and 60 seconds and with random amplitudes and phase offsets. In order to set the turbulence intensity to the input value the turbulence signal for the whole calculation time has to be calculated right at the beginning of each calculation. In total 100 signals, one for each blade element, are calculated and than scaled due to the input value. Then the turbulence component is added as a fluctuation above the resultant velocity due to the current and the waves at the corresponding time step. With this method it is possible to implement turbulent fluctuations in space and time to the code. The turbulence function is given in A.5.

In the calculations the generated wave number and the generated angular frequency of the waves can be calculated due to the input parameters, but because of the

forward speed of the water the turbine experiences a modified wave frequency. The encountered wave frequency is calculated by considering the current velocity and the generated frequency and wave number:

$$\omega_{w,enc} = \omega_{w,gen} + k_{gen} \cdot V \quad [\frac{rad}{s}] \quad (6.1)$$

From the encounter wave frequency also the encounter wave number is found, which also has to be known to see the influence of the waves on the velocity profile. It can be chosen if both horizontal and vertical velocity component due to the waves are to be considered in the calculations or just the horizontal component.

The tidal wave is implemented in the Matlab code based on sinusoidal oscillations containing the effect of more tidal constituents. The function is given in A.3 The harmonic signal is the sum of six components with the same period, amplitude and phase as in Kvalsundet, Finnmark, because the tides are here known. The water level and the velocity is scaled up with a factor of 1.68, so that the maximum velocity is approximately 4.0 m/s, which is the maximum velocity measured at the reference site at Pentland Firth. The water depth and the current velocity in the calculations are given by the tidal wave. If the tidal wave is not considered in the calculations the current velocity on the turbine axis and the total water depth have to be given as input parameters.

L_c, a, a', and θ are parameters due to blade design and are given for each blade element. The list of a is given in A.7, the list of a' in A.8, assuming a and a' are not time dependent, and the table of L_c and θ in A.13. The lift and drag coefficients, C_L and C_D, are given for each hydrofoil section dependent on the angle of attack, α. C_L and C_D are to be found for each hydrofoil section in A.9 - A.12 and the function in A.2. The angle of attack is calculated with the known twist angle, θ, and the calculated flow angle, φ. The axial and rotational force coefficients, C_a and C_r, are calculated with blade geometry and the lift and drag coefficients, C_L and C_D, to determine the forces, thrust and torque, for each blade element, M' and T'. By integrating the forces on each blade element over the whole blade the total thrust force, T, the main shaft torque, M_x, the thrust induced pitch moment, M_y and yaw moment, M_z, are found for each time step. This is done over a period of time so that it is evident that the forces are oscillating signals causing a dynamic load on the tidal turbine blades. The tiploss is implemented by the tiploss factor, F, that goes linearly from one to zero for the last three blade elements, given in A.4.

The rainflow counting algorithm for Matlab calculations by Adam Nieslony [10] is used for rainflow analysis.

6.2   The Algorithm

The algorithm for the calculations is shown in figure 6.1. It is assumed that the prototype 1 MW tidal turbine is operating at a real site with a no-slip velocity profile and that the tidal wave and both horizontal and vertical component due to the waves are considered.
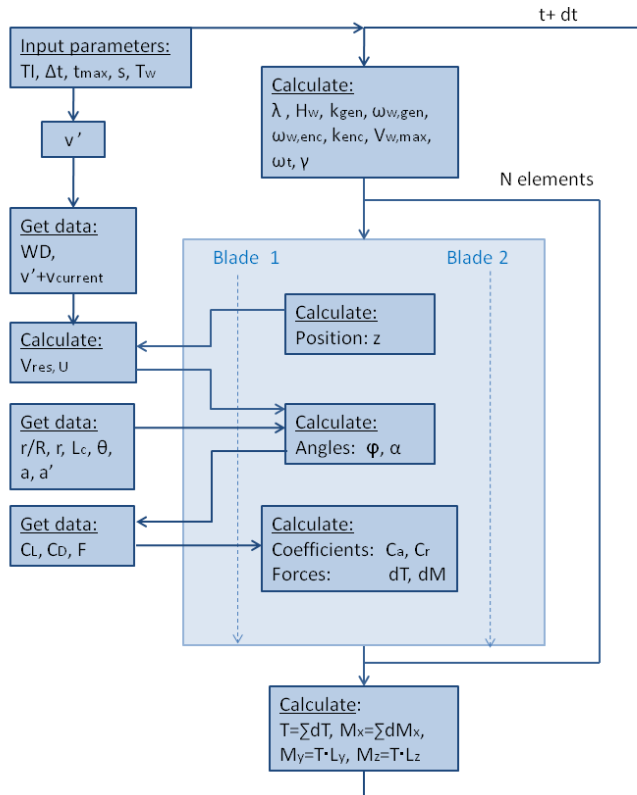
Figure 6.1: The Algorithm.

Chapter 7

Validation of the Matlab Code With Experiments

A model turbine is built and tested at Marintek in Trondheim. This is the small scaled model of the 1 MW reference tidal turbine. With an experimental setup the simulation tools can be validated, the concept proved and experience on operating the turbine in various conditions gained [22].

7.1 Setup of Experiments and Matlab Calculations

In the model tests the wave-current interaction on the turbine blades is evaluated. The tests at Marintek are done at different current velocities with different waves. For selected tests thrust and torque on one blade and the shaft torque on both blades are evaluated and compared to Matlab results for validation of the code. The model tests that are used for comparison with Matlab results are shown in table 7.1. One of the tests is in open water, which means no waves, and three of the tests are with regular waves. A current velocity of 2.5 m/s is used for comparison, which is the design velocity. The current velocity, the wave steepness and the wave period are given in the table for the tests used for comparison.

The parameters and the setup in the Matlab calculations are chosen to be as similar to the experiments as possible. The results from the experiments are given in prototype scale. The diameter of the model turbine in the tests is 1.425 meters and with a turbine scale of 14 it equals a diameter of 19.95 meters in the calculations. In the calculations the turbulence intensity is set to 3%, which is an approximation

Test	V $\left[\frac{m}{s}\right]$	s $[-]$	T $[s]$
Open water			
3040	2.5	-	-
Regular waves			
4025	2.5	0.05	5
4085	2.5	0.05	7
4145	2.5	0.05	10

Table 7.1: The model tests used for comparison.

of the turbulence intensity in the towing tank, which is not known. Both horizontal and vertical velocity component due to the waves are considered. All the Matlab calculations are done with a time step of 0.1 second and run over a time period of 1000 seconds. A parameter in the model tests that deviates from the reference turbine at a real site is the angular frequency of the turbine, ω_t, for velocities over design velocity. $\omega_t = \frac{TSR \cdot V_{design}}{R}$, where TSR is the tip speed ratio, which is fixed, V_{design} is the design velocity and R the radius of the turbine. At a real site ω_t is rated, this is not the case in the experiments and has to be considered in the Matlab code for the comparison. Tides are not considered. As the turbine is moving relatively to the current in the experiments, the vertical velocity profile is uniform. The resulting velocity profile due to the uniform current velocity profile and the varying velocity profile from the waves is shown in figure 7.1.
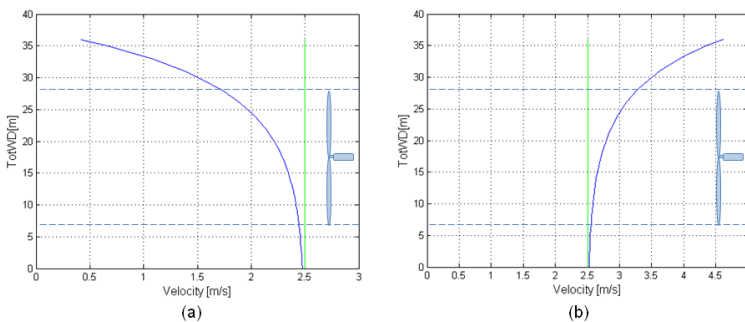
Figure 7.1: Resulting velocity profile (blue line) in experiments in prototype scale from current and waves, when the turbine is experiencing a (a) wave trough and (b) crest. The green line is the velocity profile not affected by the waves. The horizontal dotted lines show the sweep area of the turbine. The current velocity, v, is 2.5 m/s, the wave period, T_{wave}, is 7 s and the steepness, s, is 0.05.

7.2   Results and Comparison

To compare the Matlab code with the experiments the mean values for thrust and torque on one blade and shaft torque were calculated for all tests done at Marintek. Four tests at design velocity, the tests given in table 7.1, were chosen for comparison. For a current velocity of 1.0 m/s the mean values from the Matlab results deviates significantly from the experimental results. This might be caused by the effect of stall in the experiments. If stall occurs the lift force is significantly reduced, which can be the reason for the very low mean values in experiments. Therefore the tests at 1.0 m/s are not used for comparison. For tests at a velocity of 4 m/s the trends are similar to the tests at the design velocity. In table 7.2 the mean values for thrust, torque and shaft torque from both experiments and Matlab calculations are given for the four tests chosen.

	Thrust [kN]		Torque [kNm]		Shaft torque [kNm]	
Test	Exp.	Matlab	Exp.	Matlab	Exp.	Matlab
Open water						
3040	443.03	399.17	239.70	256.38	623.22	512.77
Regular waves						
4025	442.68	399.01	230.02	256.00	616.27	511.98
4085	440.21	396.01	237.29	252.77	619.09	505.45
4145	415.04	376.80	201.37	245.25	535.52	490.43

Table 7.2: Mean values from experiments and Matlab calculations.

To validate the Matlab code the deviation in per cent from the experiments is found. For thrust, torque and shaft torque from Matlab calculations the mean-, maximum- and minimum values are compared to experimental results. Also the standard deviation and the difference between maximum- and minimum values, the peak-to-peak values, are used for comparison. The deviation from experimental results was found using the formula:

$$Deviation = \frac{X_{Mat.} - X_{Exp.}}{X_{Exp.}} \qquad (7.1)$$

The deviation is shown in table 7.3 for thrust force calculated on one of the blades, table 7.4 for torque calculated on one of the blades and table 7.5 for the total shaft torque, calculation on both blades, for the tests 3040, 4025, 4085 and 4145. Mean, maximum, minimum and peak-to-peak values and standard deviation from calculations are compared to experimental results.

Thrust					
Test	Mean	Max	Min	Δ Peak	Std.dev
Open water					
3040	-9.90	-12.38	-7.24	-76.24	-70.75
Regular waves					
4025	-9.86	-13.21	-6.42	-65.42	-72.62
4085	-10.04	-13.98	-5.80	-31.70	-34.17
4145	-9.21	-25.37	16.12	-41.29	-22.19

Table 7.3: Deviation in % from experimental results for thrust on one blade.

Torque					
Test	Mean	Max	Min	Δ Peak	Std.dev
Open water					
3040	6.96	-13.63	41.98	-86.72	-93.01
Regular waves					
4025	11.29	-11.44	39.36	-70.00	-84.21
4085	6.53	-9.80	51.04	-25.20	-31.86
4145	21.79	-6.76	-67.58	-13.97	7.39

Table 7.4: Deviation in % from experimental results for torque on one blade.

Shaft torque					
Test	Mean	Max	Min	Δ Peak	Std.dev
Open water					
3040	-17.72	-19.95	-14.90	-56.34	-57.04
Regular waves					
4025	-16.92	-21.12	-12.97	-55.17	-70.72
4085	-18.36	-24.06	-5.11	-38.26	-40.28
4145	-8.42	-26.06	279.19	-30.45	-9.56

Table 7.5: Deviation in % from experimental results for shaft torque.

The tests 4025, 4085 and 4145 are done with different waves. For these tests also the signals are compared. Figure 7.2 is showing the signals for thrust and torque on one blade and figure 7.3 the signal for shaft torque for test 4145, experimental and calculation results compared. In the experiments the position of the turbine blade relative to the wave is known, but it is not known if the maximum load always is induced in the time window. The two signals, from experiments and from calculations, are plotted in the same graph, so that the maximum value of each signal are approximately at the same position on the time axis. Figure 7.4 is showing the comparison in signals between experiments and calculation for thrust, torque and shaft torque for test 4085 and test 4025.
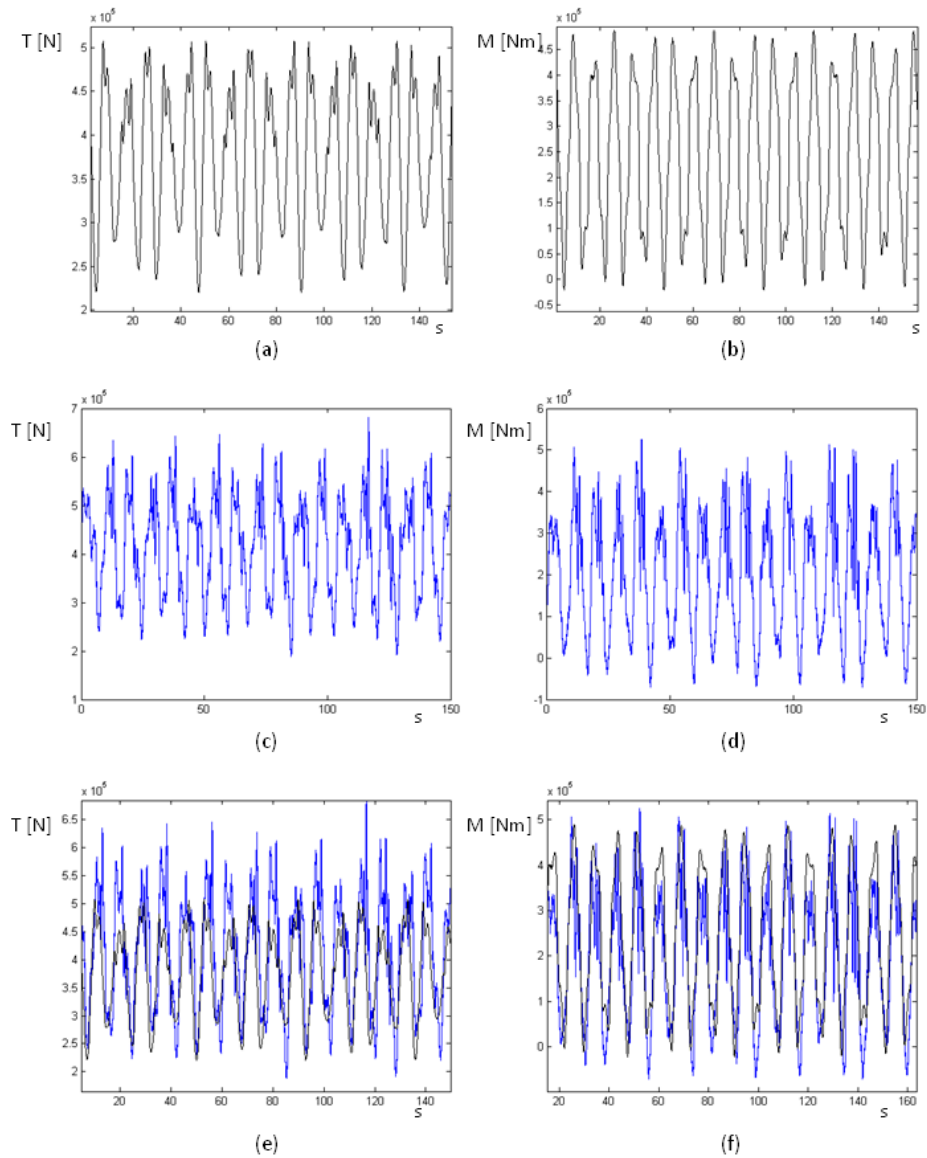
Figure 7.2: Comparison with experimental results, test 4145. (a) Thrust and (b) torque on one blade from Matlab calculations and (c) thrust and (d) torque on one blade from experiments. (e) Thrust and (f) torque from calculations (black signal) and experiments (blue signal) in the same plot.
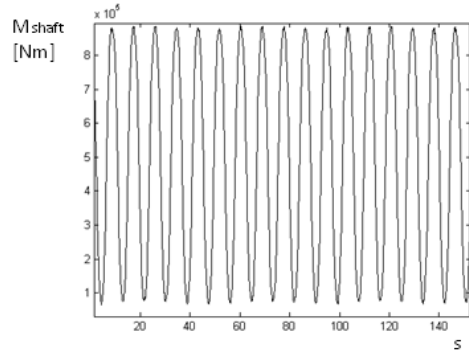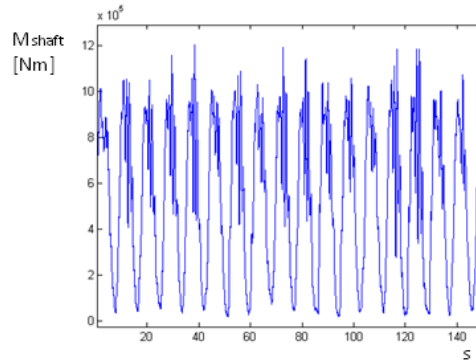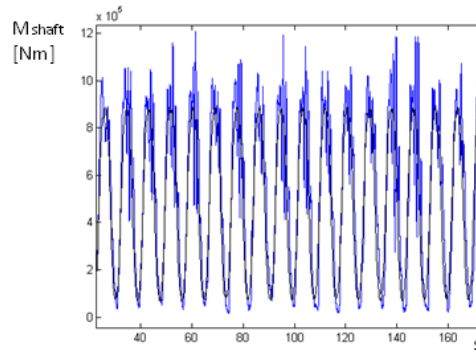
Figure 7.3: Comparison with experimental results, test 4145. Shaft torque on one blade from (a) Matlab calculations and (b) from experiments. (c) Shaft torque from calculations (black signal) and experiments (blue signal) in the same plot.
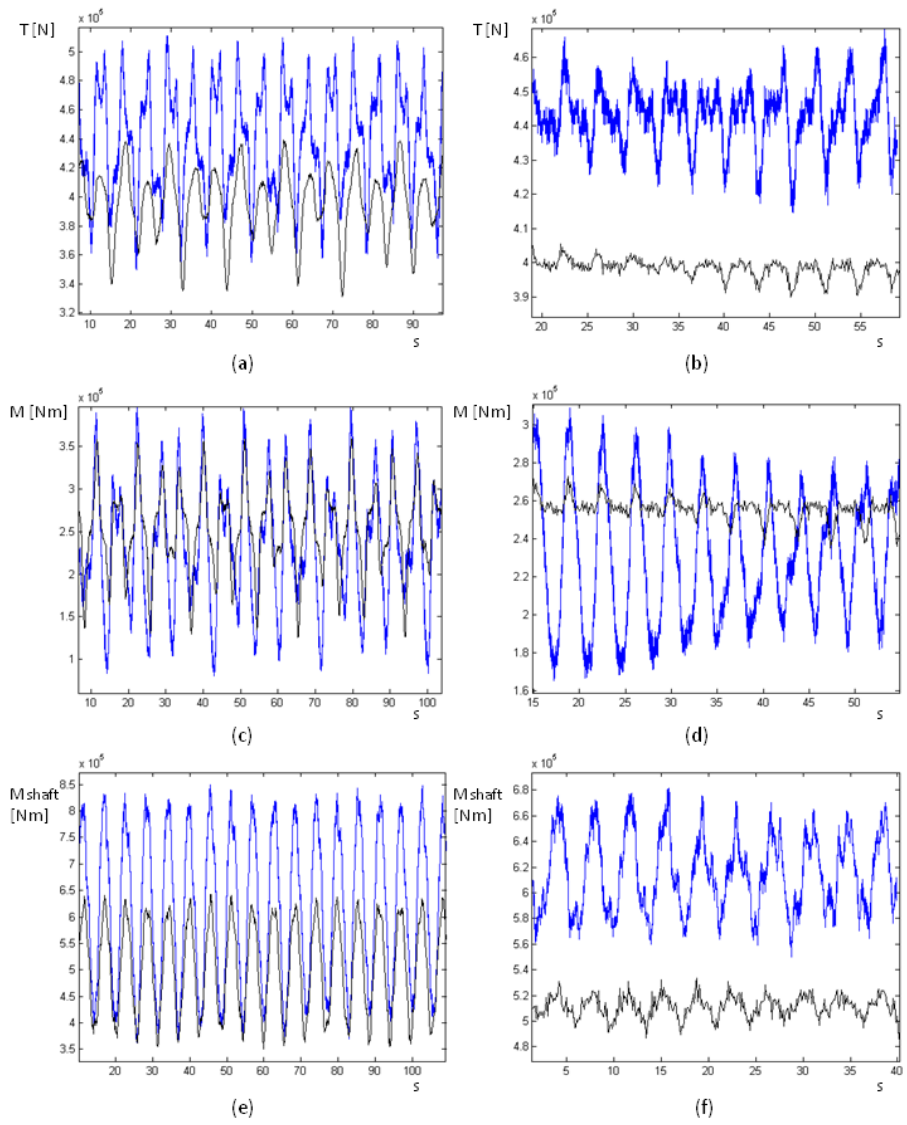
Figure 7.4: Comparison with experimental results, test 4085 to the left and test 4025 to the right. The blue signal is from experiments and the black from Matlab calculations. Comparison of thrust force signal from (a) test 4085 and (b) test 4025, torque from (c) test 4085 and (d) test 4025 and shaft torque from (e) test 4085 and (f) test 4025.

Chapter 8

Results of Matlab Calculations of Dimentional Loading and Rainflow Counting

Calculations are done for the prototype 1 MW reference tidal turbine to evaluate the influence of the vertical velocity profile, wave-current interaction, the vertical velocity component due to the waves, turbulence and the tidal wave on the loads on the turbine blades. With a rainflow analysis the lifetime of the tidal turbine can be predicted due to analysing cycles of loading over a period of time. The calculations, when the tidal wave is not considered, are done at a velocity of 2.5 m/s, which is the design velocity. Calculations done with a vertical no-slip current velocity profile 2.5 m/s is the velocity on the turbine axis. Otherwise the current velocity and the water depth is determined by the tides. The wave in these calculations has a steepness of 0.05 and a time period of 10 seconds. This wave is chosen because when comparing Matlab results to experimental results, chapter 7, this wave has the smallest deviation from experiments in peak-to-peak values. For calculations with turbulence, as an approximation to the ocean and a turbine operating at a real site, the turbulence intensity is set to 12 %.

Calculations are done of thrust force, shaft torque, pitch and yaw moment. Results are given for one of the blades, blade 1, which blade that defines γ, which is zero the first time step, and for both blades, in total. Mean, maximum, minimum and peak-to-peak values are for each of the forces evaluated. Also the amplitude and the number of cycles of loading as results of rainflow analyses are given for each of the forces acting. Each of the components causing a fatigue loading on the turbine

is analysed and one after another implemented in the calculations. To evaluate the influence of each of the components the calculations and analyses are done in the following order:

1. Calculations with uniform current velocity profile.

2. Calculations with vertical current no-slip velocity profile.

3. Calculations with no-slip velocity profile and waves, without vertical wave velocity component.

4. Calculations with no-slip velocity profile and waves, vertical velocity component due to the waves added.

5. Calculations with no-slip velocity profile, waves and turbulence added.

6. Calculations with no-slip velocity profile, waves and tidal wave added. No turbulence.

The calculations without waves, for both uniform and no-slip velocity profile, case 1 and 2, are run over a time period of 900 seconds i.e. 15 minutes, real time. When waves are added the time period of calculation is 1 hour. This is done for case 3, 4 and 5. Calculations of the tidal wave are done over a time period of 3.5 days i.e. 84 hours. In the following subchapters the results of each of the forces are presented for all six cases, when one component after another is added. The signals given in the figures are plotted for 30 seconds for calculations without waves and 100 seconds when waves are added. For calculations with the tidal wave the signals are given for a time period of 84 hours as well. The rainflow analyses are done for the time period of the calculations, which means 15 minutes for case 1 and 2, 1 hour for case 3, 4 and 5 and 84 hours for case 6.

8.1 Thrust Force

	Mean	Max	Min	Δ Peak
Thrust force on one blade				
Case 1	393.84 kN	393.84 kN	393.84 kN	0.00 kN
Case 2	392.12 kN	405.47 kN	375.14 kN	30.33 kN
Case 3	364.95 kN	448.93 kN	221.18 kN	227.75 kN
Case 4	364.54 kN	498.92 kN	221.18 kN	277.74 kN
Case 5	363.75 kN	498.60 kN	213.85 kN	284.75 kN
Case 6	269.31 kN	538.89 kN	-21.24 kN	560.13 kN
Total thrust force				
Case 1	787.68 kN	787.68 kN	787.68 kN	0.00 kN
Case 2	784.23 kN	787.68 kN	780.60 kN	7.08 kN
Case 3	729.91 kN	879.37 kN	496.60 kN	382.77 kN
Case 4	729.04 kN	887.76 kN	496.60 kN	391.16 kN
Case 5	727.46 kN	892.04 kN	484.11 kN	407.93 kN
Case 6	538.60 kN	940.04 kN	-20.01 kN	960.05 kN

Table 8.1: Results of calculations of thrust force.

In the following figures the signals of each blade are shown in black and green and the signal for the total thrust force is shown in blue. The rainflow diagram for one blade is given at the bottom of each figure and the rainflow diagram for both blades at the top. This is similar for all forces calculated.
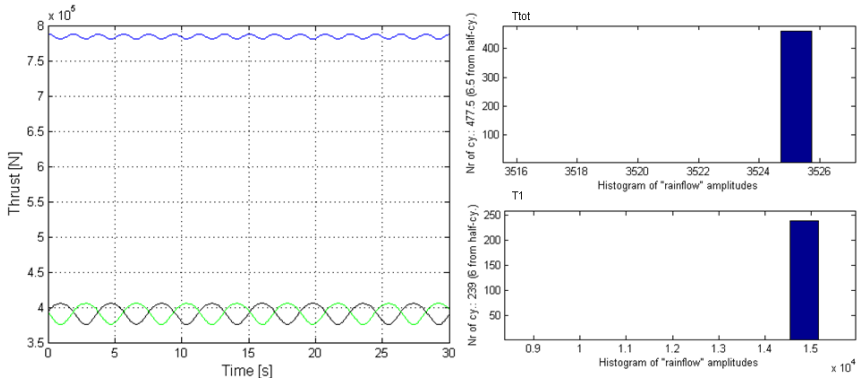
Figure 8.1: Case 2: Thrust force with no-slip profile.
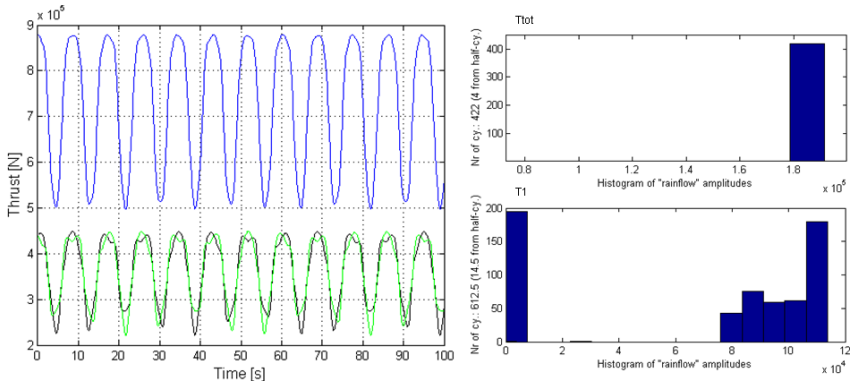
Figure 8.2: Case 3: Thrust force with waves added.
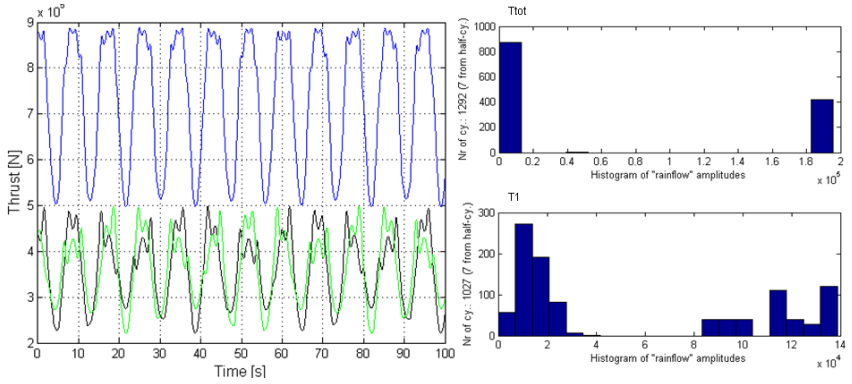
Figure 8.3: Case 4: Thrust force with vertical wave component added.
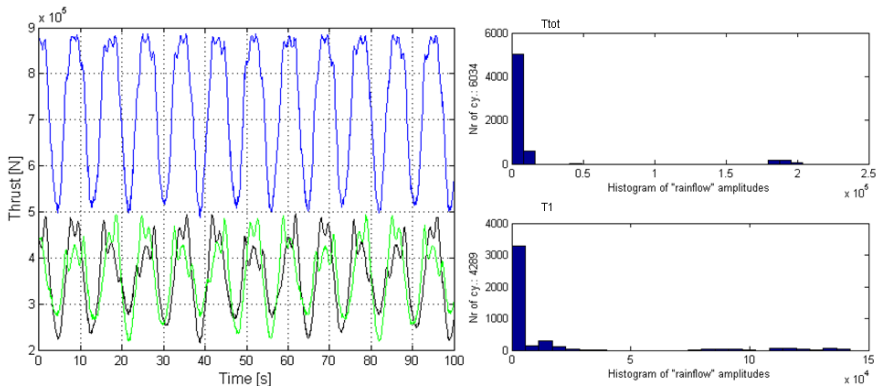
Figure 8.4: Case 5: Thrust force with turbulence added.
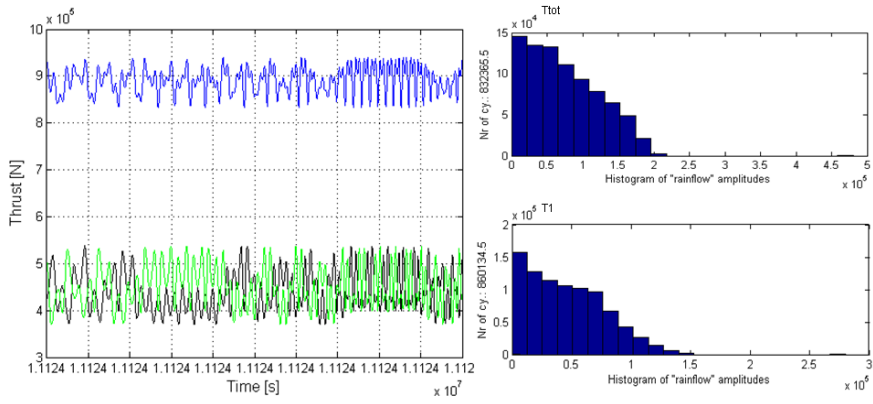
Figure 8.5: Case 6: Thrust force with tidal wave added.
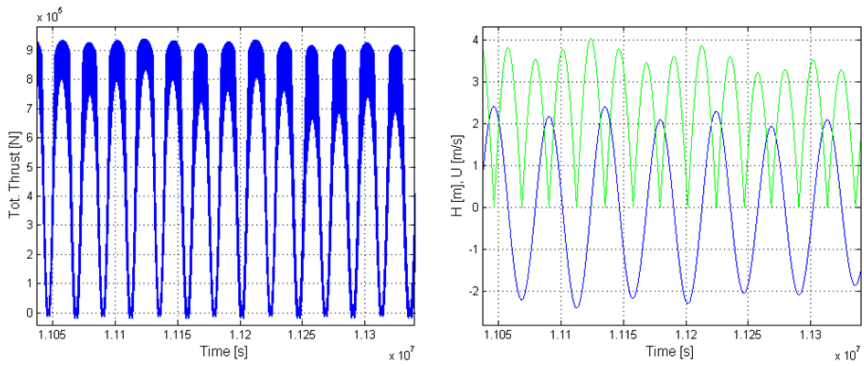
Figure 8.6: Case 6: Thrust force with tidal wave over 3.5 days.

65

8.2   Shaft Torque

	Mean	Max	Min	Δ Peak
Shaft torque on one blade				
Case 1	275.70 kNm	275.70 kNm	275.70 kNm	0.00 kNm
Case 2	272.28 kNm	306.18 kNm	231.10 kNm	75.08 kNm
Case 3	249.61 kNm	498.03 kNm	-7.94 kNm	505.97 kNm
Case 4	248.50 kNm	498.03 kNm	-7.94 kNm	505.97 kNm
Case 5	248.51 kNm	507.17 kNm	-15.09 kNm	522.26 kNm
Case 6	225.89 kNm	565.00 kNm	-39.10 kNm	604.10 kNm
Total shaft torque				
Case 1	551.41 kNm	551.41 kNm	551.41 kNm	0.00 kNm
Case 2	544.52 kNm	551.41 kNm	537.28 kNm	14.13 kNm
Case 3	499.21 kNm	870.04 kNm	64.73 kNm	805.31 kNm
Case 4	496.97 kNm	870.04 kNm	64.73 kNm	805.31 kNm
Case 5	496.98 kNm	902.02 kNm	50.03 kNm	851.99 kNm
Case 6	451.76 kNm	1,041.00 kNm	-39.10 kNm	1,080.10 kNm

Table 8.2: Results of calculations of shaft torque.
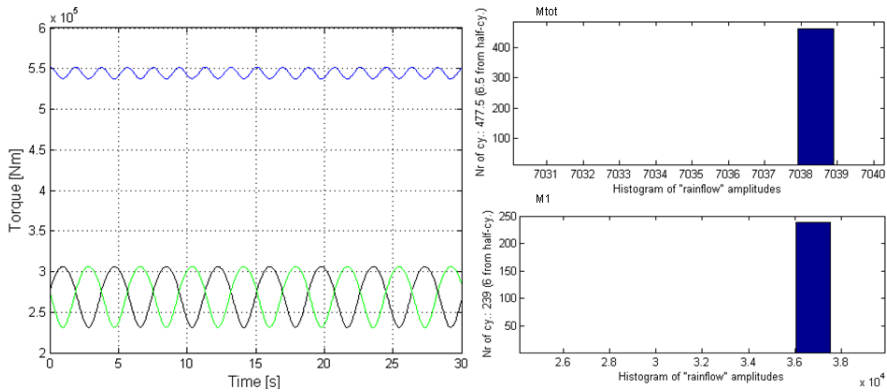
Figure 8.7: Case 2: Shaft torque with no-slip profile.
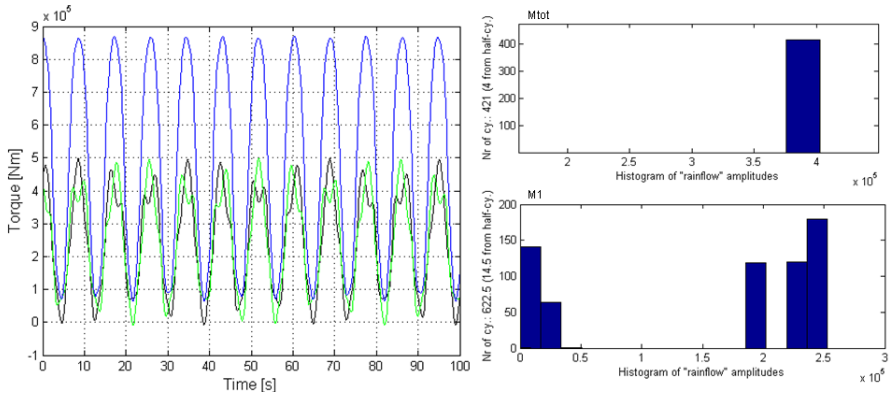
Figure 8.8: Case 3: Shaft torque with waves added.
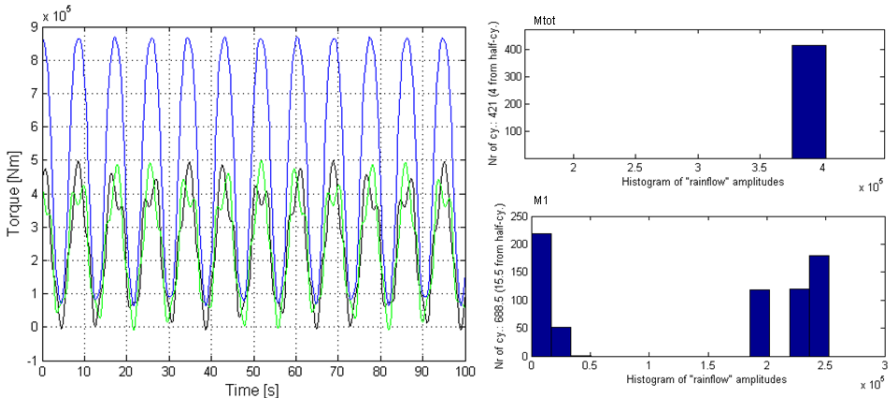
Figure 8.9: Case 4: Shaft torque with vertical wave component added.
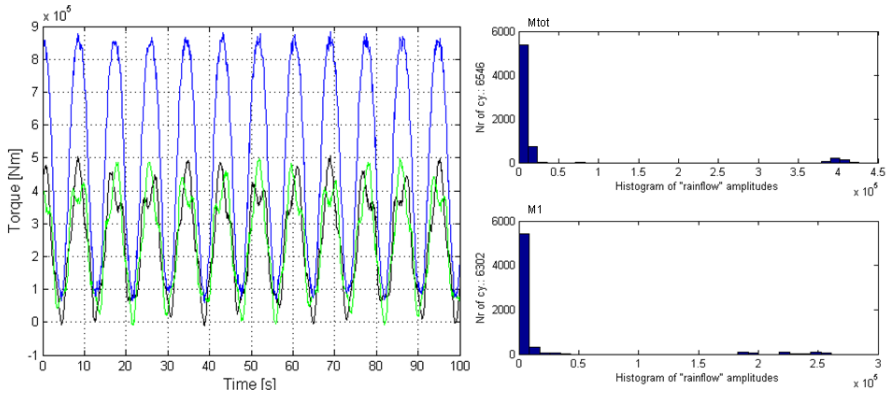
Figure 8.10: Case 5: Shaft torque with turbulence added.
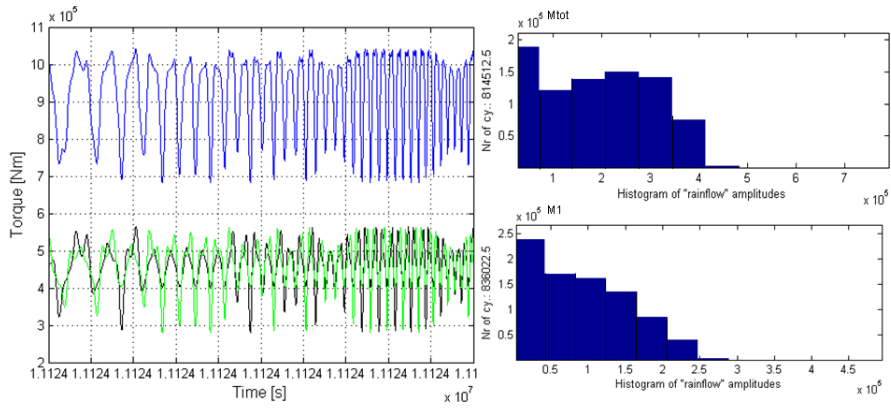
Figure 8.11: Case 6: Shaft torque with tidal wave added.
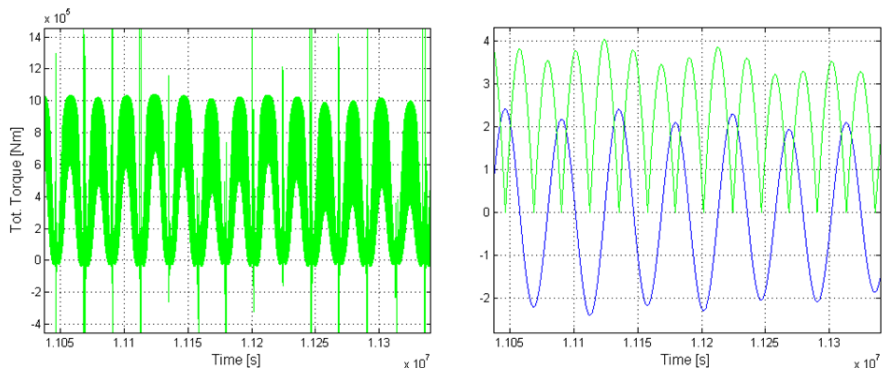
Figure 8.12: Case 6: Shaft torque with tidal wave over 3.5 days.

8.3   Pitch Moment

	Mean	Max	Min	Δ Peak
Pitch moment on one blade				
Case 1	1.93 kNm	2,822.60 kNm	-2,822.60 kNm	5,645.20 kNm
Case 2	54.54 kNm	2,904.30 kNm	-2,689.80 kNm	5,594.10 kNm
Case 3	-0.94 kNm	3,198.80 kNm	-3,041.80 kNm	6,240.60 kNm
Case 4	-0.62 kNm	3,198.80 kNm	-3,041.80 kNm	6,240.60 kNm
Case 5	0.78 kNm	3,214.60 kNm	-3,058.40 kNm	6,273.00 kNm
Case 6	-10.01 kNm	3,328.80 kNm	-3,212.80 kNm	6,541.60 kNm
Total pitch moment				
Case 1	0.00 kNm	0.00 kNm	0.00 kNm	0.00 kNm
Case 2	105.24 kNm	214.51 kNm	0.00 kNm	214.51 kNm
Case 3	-2.00 kNm	253.88 kNm	-412.59 kNm	666.47 kNm
Case 4	-1.39 kNm	550.36 kNm	-412.62 kNm	962.98 kNm
Case 5	1.42 kNm	554.30 kNm	-454.54 kNm	1,008.84 kNm
Case 6	-19.95 kNm	594.34 kNm	-597.63 kNm	1,191.97 kNm

Table 8.3: Results of calculations of pitch moment.
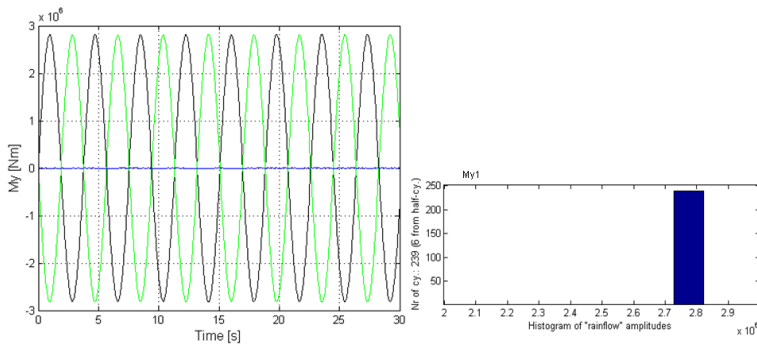
Figure 8.13: Case 1: Pitch moment with uniform velocity profile.
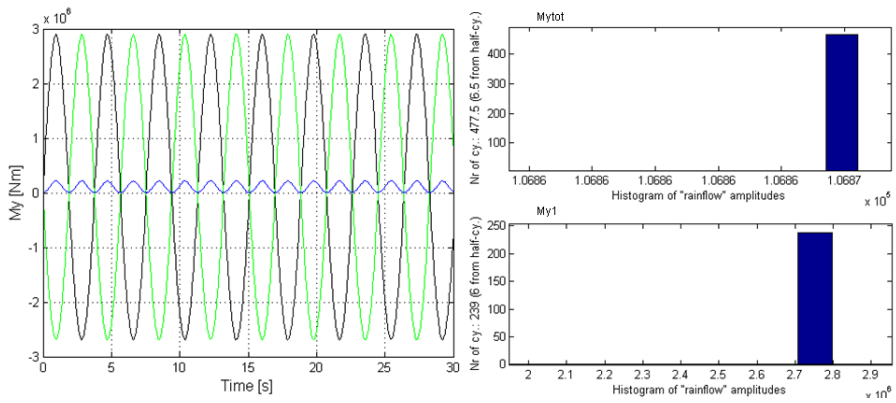
Figure 8.14: Case 2: Pitch moment with no-slip profile.
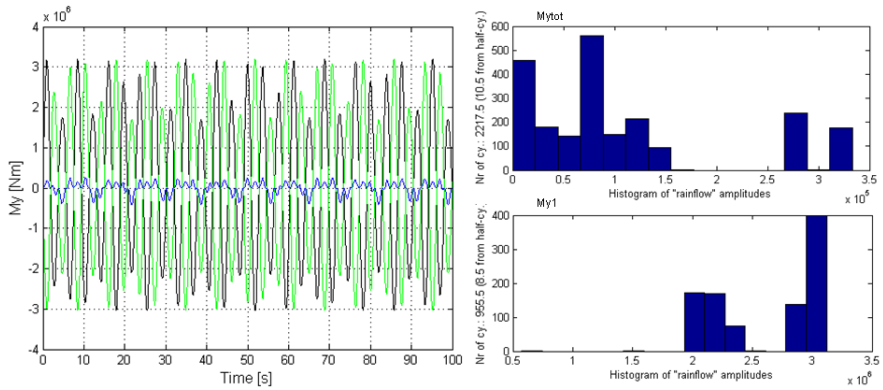
Figure 8.15: Case 3: Pitch moment with waves added.
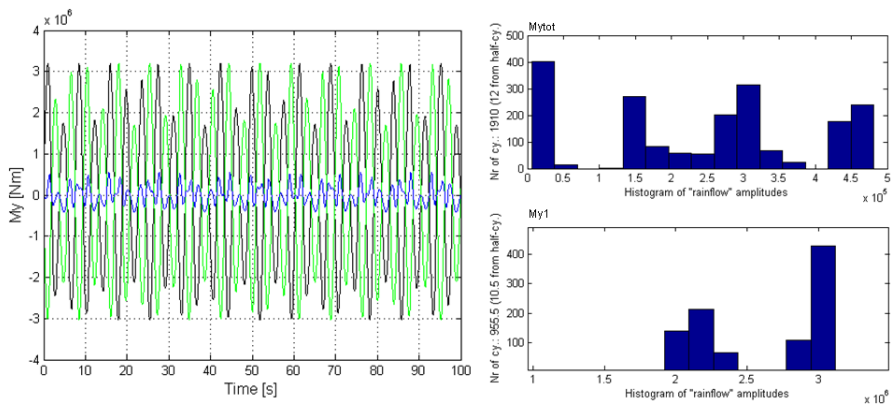
Figure 8.16: Case 4: Pitch moment with vertical wave component added.
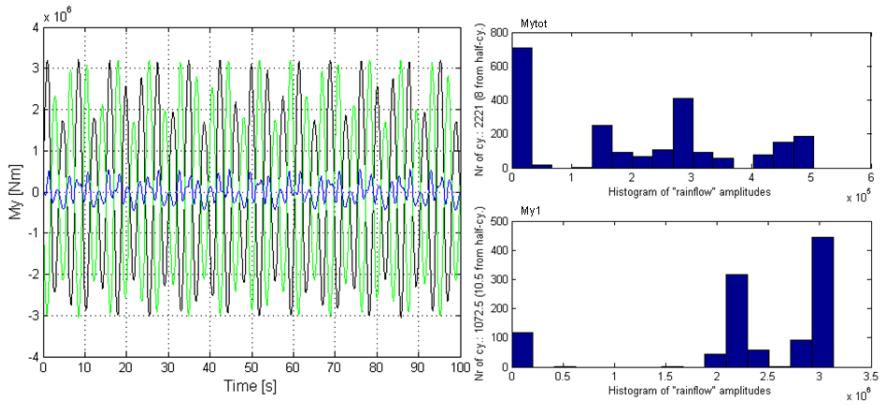
Figure 8.17: Case 5: Pitch moment with turbulence added.
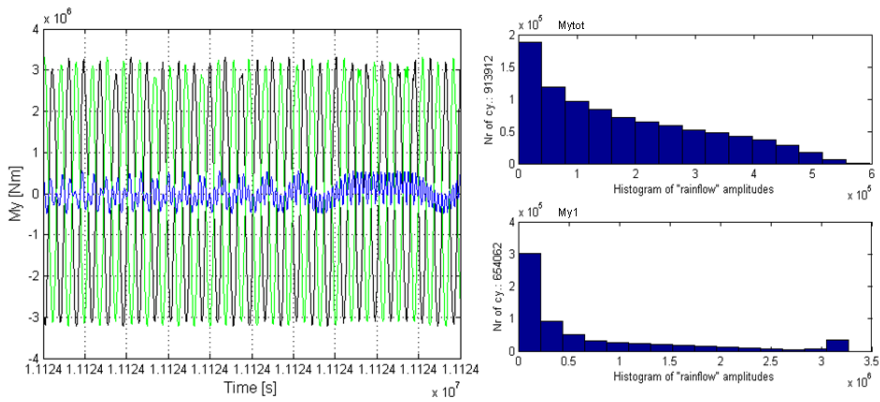
Figure 8.18: Case 6: Pitch moment with tidal wave added.
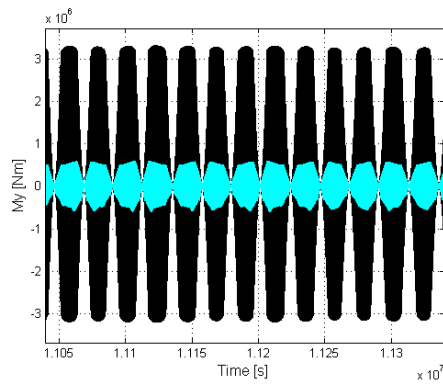
Figure 8.19: Case 6: Pitch moment with tidal wave over 3.5 days.

71

8.4 Yaw Moment

	Mean	Max	Min	Δ Peak
Case 1	-1.73 kNm	2,822.50 kNm	-2,822.60 kNm	5,645.10 kNm
Case 2	-1.69 kNm	2,824.40 kNm	-2,824.30 kNm	5,648.70 kNm
Case 3	0.02 kNm	3,137.20 kNm	-3,137.10 kNm	6,274.30 kNm
Case 4	-0.1 kNm	3,447.30 kNm	-3,446.90 kNm	6,894.20 kNm
Case 5	-0.23 kNm	3,443.60 kNm	-3,451.00 kNm	6,894.60 kNm
Case 6	-0.20 kNm	3,721.40 kNm	-3,721.40 kNm	7,442.80 kNm
Case 1	0.00 kNm	0.00 kNm	0.00 kNm	0.00 kNm
Case 2	0.07 kNm	103.35 kNm	-103.35 kNm	206.67 kNm
Case 3	0.01 kNm	201.12 kNm	-201.07 kNm	402.19 kNm
Case 4	-0.22 kNm	777.56 kNm	-777.36 kNm	1,554.92 kNm
Case 5	-0.21 kNm	788.86 kNm	-786.65 kNm	1,575.51 kNm
Case 6	-0.12 kNm	1,039.80 kNm	-1,041.20 kNm	2,081.00 kNm

The two section rows spanning the full width read: **Yaw moment on one blade** and **Total yaw moment**.

Table 8.4: Results of calculations of yaw moment.
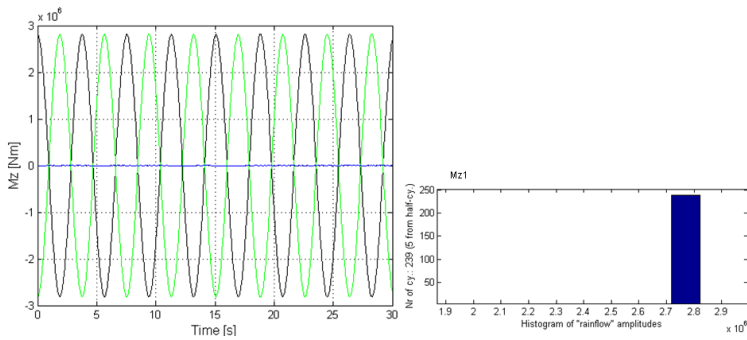
Figure 8.20: Case 1: Yaw moment with uniform velocity profile.
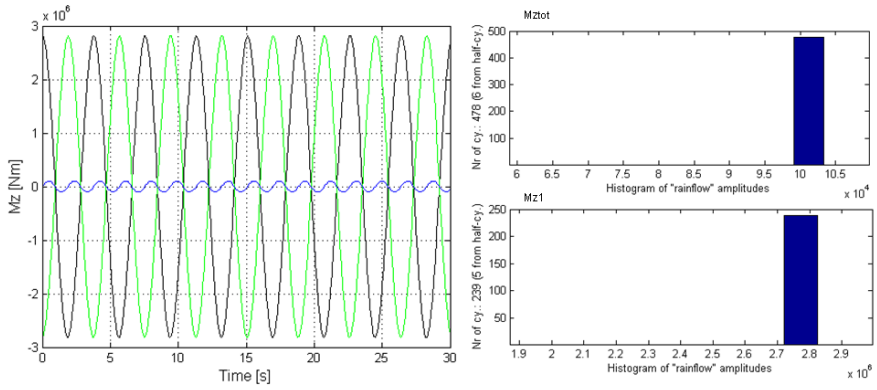
Figure 8.21: Case 2: Yaw moment with no-slip profile.
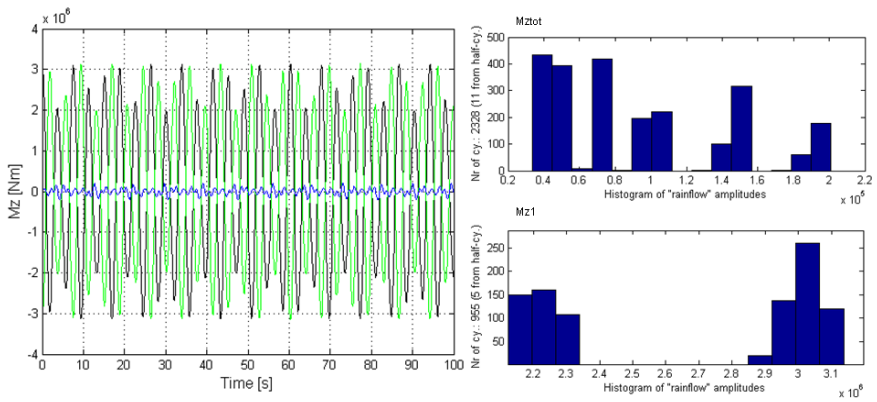
Figure 8.22: Case 3: Yaw moment with waves added.
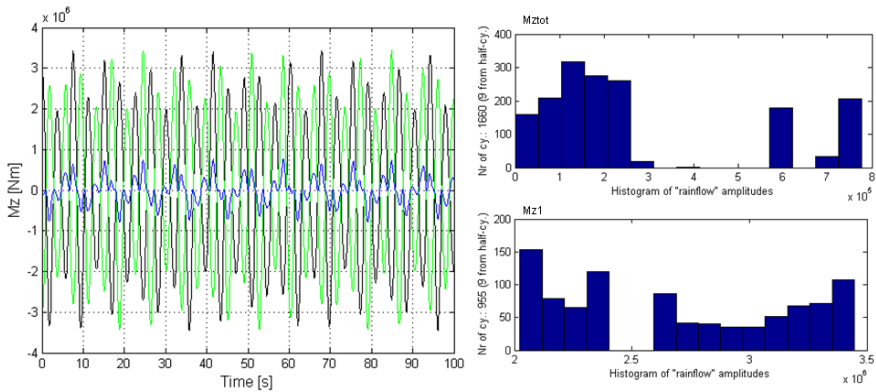
Figure 8.23: Case 4: Yaw moment with vertical wave component added.

73
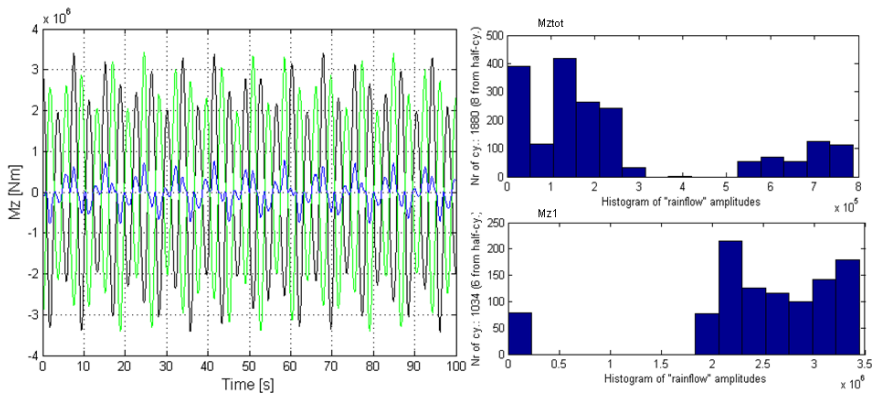
Figure 8.24: Case 5: Yaw moment with turbulence added.
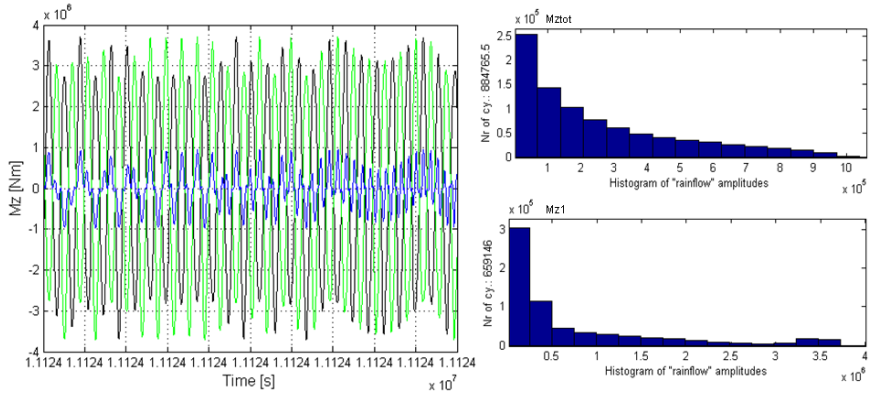
Figure 8.25: Case 6: Yaw moment with tidal wave added.
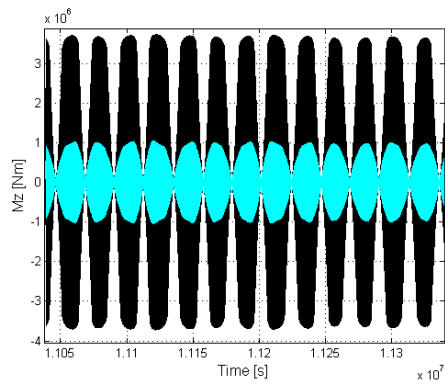
Figure 8.26: Case 6: Yaw moment with tidal wave over 3.5 days.

74

Chapter 9

Discussion

9.1   Simplifications in the Matlab Code

Simplifications in the Matlab code have to be done to be able to do the calculations. The simplifications may affect the results of the calculations and has to be considered when evaluating the results.

Linear wave theory is used to describe the waves, but sea surface waves are inherently nonlinear and irregular with varying steepness and period in time and space. The theory describes the basics of sea surface waves, but is not the reality. In deep water waves the fluid particles will move in perfect circular orbits. This is a theoretical approach and will not be the case for a turbine operating at a real site.

A turbine blade consists of four hydrofoil sections and a cylindrical shape closest to the root. In the Matlab code it is not interpolated between the hydrofoil sections, which mean that the turbine blade does not have a smooth shape.

To implement the tip loss it is said that the tip loss factor, F, is one for the first 97 blade elements. For the last 3 elements the tip loss factor is going linearly to zero, so that the last blade element has a tip loss factor of zero.

The axial and rotational induction factors, a and a', are for each blade element constant for all time steps. For each blade element each of the values are taken from a list and implemented into the program.

When calculating the encounter frequency of the waves the current velocity on the turbine axis is considered. The current velocity varies along the depth and the position of each blade element on the vertical axis should be considered to get an

exact solution.

The angular frequency of the turbine depends only on the current velocity. The waves do not have an influence on the turbine frequency, which means that when the current velocity is zero the turbine is not rotating even though the waves are inducing a velocity profile.

To implement the turbulence in the calculations each blade element is given a time varying, fluctuating signal. There is one signal per blade element, in total hundred, which means symmetry over the hub. The turbulent signal is in the calculations random fluctuations, but at a real site there will probably be a connection in gradients between two neighbouring blade elements due to vortices. This is not considered.

To calculate the effect of the tides the implementation in the code is based on the tides at Kvalsundet, where tidal data are known. The tidal components from Kvalsundet are used in the harmonic analysis and multiplied by a factor so that the maximum velocity is the same as on the reference site. This is an approximation done because tidal data at this reference site are not known.

The effect of the natural frequency of the turbine, deflection of the blades and wake from substructure are not considered in the calculations.

9.2 Comparison with Experiments

Four tests are used to compare the Matlab code with experiments. The tests that are chosen for comparison is one test without waves and three tests with waves, whereas all tests are at a current velocity of 2.5 m/s, which is the design velocity. Tests and calculations are done for thrust force on one of the blades, torque on of the blades and main shaft torque, which is calculation of both blades. The tendency seen in table 7.3, 7.4 and 7.5 for the four tests is that Matlab calculates a lower value of thrust force on one blade and shaft torque than the experiments. The calculated torque on one blade has a tendency to be higher than the experiments. This means that the Matlab code underestimates the thrust on one blade and the shaft torque and overestimates the torque on one blade.

For all tests done in open water the deviation of the mean values for all current velocities are similar to test 3040 with the trends mentioned above. In test 3040, as in most of the tests, the standard deviation is lower in the Matlab calculations. The peak-to-peak values deviates significantly from the experiments and they have all a lower value.

The tests with waves, tests 4025, 4085 and 4145, have a wave steepness of 0.05 and wave period of 5, 7 and 10 seconds. Figure 7.2, 7.3 and 7.4 show that the trends

for both experiments and calculations are the same for thrust, torque and shaft torque. For all tests the signals are oscillating curves that are experiencing a peak at every wave period of encounter.

The maximum values for all tests with waves are lower than the experiments. For test 4025 and test 4085 the minimum values for thrust and shaft torque are lower than experiments and for torque on one blade Matlab calculates a higher minimum value than experiments. For test 4145 the minimum values for thrust and shaft torque are higher than the experiments and torque on one blade lower. The peak-to-peak values also for all tests with waves are lower for Matlab calculations than experiments.

It is notable in table 7.2 that in Matlab calculations with different waves the mean value of thrust, torque and shaft torque are decreasing with increasing wave periods. This trend can also be seen in the experiments. The mean values of thrust force from experiments reduce continuously for increasing wave period. Also for torque on one blade and shaft torque the mean values are higher in open water than in waves with a large period, but the mean values do not decrease successively.

Looking in the tables 7.3-7.5 the same trend is to be seen for the standard deviation. The deviation from experiments is larger for the tests in open water than the test with a large wave period.

Looking in the figures, the maximum values from Matlab calculations are increasing for an increasing wave period for thrust, torque and shaft torque. This trend is the same for experiments. The deviation in maximum values of Matlab results from experiments are for thrust and shaft torque increasing for larger wave periods and for torque on one blade the deviation decreases.

The minimum values from Matlab calculations are decreasing with larger wave periods, and so is the trend for experiments, but here, in contrast to the maximum values, no obvious trends for deviation in Matlab calculations from experiments are notable.

The difference between maximum and minimum values, the peak-to-peak values, is for both experiments and Matlab calculations increasing with an increasing wave period. This because, as mentioned above, the maxima are increasing and the minima decreasing as the wave period is increasing. It is notable that the deviation from experiments is decreasing as the wave period and peak-to-peak values are increasing. For torque on one blade and shaft torque the deviation in peak-to-peak values are decreasing continuously. This is also the trend for the thrust force although it's not decreasing successively.

The simplifications in the Matlab code are given above, but there are also assumptions done due to reproducing the experiments. The turbulence intensity in the experiments is not known and is in the Matlab calculations as an approximation

set to 3 %.

In the Matlab calculations the water depth is constant and set to 36 meters at prototype scale. This is not the case in the towing tank, where the water depth varies. The water depth affect the influence of the waves on the turbine and this difference in water depth between experiments and calculations can affect the results.

In the Matlab code the axial and the rotational induction factor for each blade element are constant for all time steps. This will not be the case for a real turbine since the values will change in time.

The Matlab code is based on the blade element momentum method, which is a static analysis of the loads on the turbine. As the rotating turbine is operating in sea water waves the system is highly dynamic.

What is notable in results of comparison is that the deviation in peak-to-peak values is increasing as the wave period is decreasing. A large wave period means a low frequency of the wave. A small wave period means high frequency and much dynamism. A reason for the large deviation in peak-to-peak values in this case might be that the resulting velocity from the current and the waves is changing very fast due to the high frequency of the waves. This will make the angle of attack vary very fast. Matlab is able to do calculations due to fast changes, but in the experiments the turbine blades may not be capable to keep up with the very fast changes in velocity and the very maxima and minima are in the experiments getting lost.

The mean values of the thrust, torque and shaft torque are decreasing with increasing wave periods. The reason for this is unknown. The angular frequency of the wave is inverse proportional to the wave period, $\omega \propto \frac{1}{T}$, and the wave length is proportional to the square of the wave period, $\lambda \propto T^2$. This means that the maximum velocity of the wave is proportional to the wave period, $V_{w,max} \propto T$. When the wave period increases also the maximum velocity of the wave will increase. If this is connected to the decrease in mean values when the wave period increases has to be further investigated.

In experiments there will always be an uncertainty in the measurements. The results will be affected by errors due to instrumentation and so on. The exact uncertainty from the experiments is not yet known.

9.3 Matlab Calculations of Dimensional Loading and Rainflow Analysis

The influence of each of the components causing a dynamic load on the tidal turbine blades is calculated and evaluated for the thrust force and moment about x-, y- and z-axis. As the turbine is rotating it will experience an oscillating load. As a result of work done in the project thesis [38] the turbine blade has the highest load when the blade is positioned vertically, $\gamma = \frac{\pi}{2}$, experiencing a wave crest and the lowest value when the blade is positioned vertically, $\gamma = \frac{\pi}{2}$, experiencing a wave through. In the first time step the turbine is positioned horizontally experiencing a wave crest. As the turbine is rotating the position of the turbine blade relative to the wave is changing. At a current velocity of 2.5 m/s the angular frequency of the turbine is 1.67 rad/s and the turbine period is 3.77 seconds. This means that between every wave crest the turbine has rotated 14.39 radians. At a wave crest the blade has a position of 1.83 radians rotation relative to the last wave crest. The position of the turbine blade relative to the wave with an encounter period of 8.62 seconds is shown in figure 9.1.
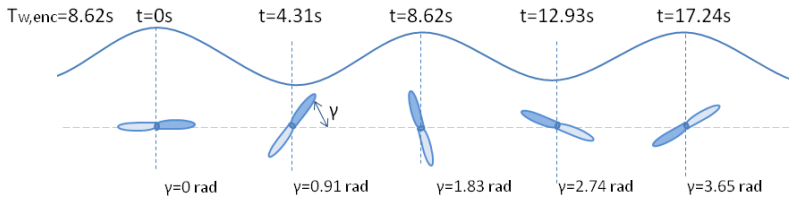
Figure 9.1: Position of the turbine blade relative to the wave.

9.3.1 Thrust Force

Analysis of signal and values

The mean, maximum, minimum and peak-to-peak values for the thrust force are presented in table 8.1 and the signals and rainflow analyses in the figures 8.1 to 8.6. In the table the values for thrust force calculated on one blade and the total thrust force is presented. This is similar in the calculation of shaft torque, pitch moment and yaw moment.

Calculations with a uniform velocity profile gives a constant value of the thrust force on one blade and the total thrust force.

When the vertical no-slip current velocity profile is added the signals are oscillating curves with constant amplitude. The signal for each blade has a peak every 3.77

seconds, which is the turbine period, and the signal for the total thrust has two peaks every turbine period. The mean values for total thrust and thrust on one blade are decreasing when the no-slip velocity profile is added. The maximum value of the total thrust is the same as the mean value for calculations with a uniform velocity profile, when the blades are horizontal. The total thrust force, both blade summarized, has a smaller peak-to-peak value than the thrust force on one blade.

For calculations with waves the signals have a peak every wave period of encounter, which is 8.62 seconds for the wave in the calculations. When waves are added it is possible to see a significantly larger difference in peak-to-peak values. The mean values are decreasing with the added wave and the maximum values are increasing, but the wave has the largest influence on the minimum values, which are decreasing rapidly.

In the fourth case the vertical component due to the waves is added. This component has almost no influence on the mean or the minimum values of the total thrust and the thrust one blade, but is increasing the maximum values, which gives larger peak-to-peak values. The influence of this component is very notable in the signal in figure 8.3, where each peak consists of many smaller peaks.

The turbulence is limitedly decreasing the mean values, but adds small oscillating cycles to the signals additional to the oscillations due to other components. The maximum value of one blade is approximately the same as the case above, but the maximum value of the total thrust force is increasing. The minimum values are decreasing for one blade and for both blades, giving a larger difference in peak values when turbulence is added compared to results without turbulence.

The tidal wave is implemented and calculations are run over 84 hours, which means that the current velocity and the water depth are oscillating between 0 m/s and 4 m/s and 33.6 meters and 38.4 meters. Here the thrust force is oscillating also due to the tidal wave. In figure 8.6 the oscillations due to the tides are very notable with a peak every time the velocity reaches its maximum, which is approximately 4 m/s. This is also the current velocity in the plot in figure 8.5. The thrust force has a peak every 12.42 hours, which is the semidiurnal tidal component. For calculations with the tidal wave the mean values and the minimum values are decreasing and the maximum values increasing. The tidal component is giving the largest difference in peak-to-peak values of all cases calculated.

Looking at table 8.1 there are notable trends of the mean, maximum, minimum and peak-to-peak values. The mean values are decreasing for each case for the thrust force on one blade and the total thrust force. When adding one component after another the maximum values are increasing and the minimum values decreasing. This gives a peak-to-peak value which is increasing for each component added.

Rainflow analysis

Rainflow analysis of the thrust force for the second case, with a no-slip velocity profile, gives the number of 239 cycles with an amplitude of 15.17 kN for calculations on one blade, and 477.5 cycles with an amplitude of 3.54 kN for calculation on both blades for a time period of 900 seconds. Because the amplitude is constant for both calculations only the number of cycles will increase for a longer time period.

When adding the waves, in case 3, the thrust force on one blade does not have constant amplitude, but cycles with varying amplitudes. There is a certain number of cycles due to the wave period to the right in the rainflow diagram, with the largest amplitude of 113.75 kN for calculation on one blade. Also the number of 195 cycles with a very small amplitude due the no-slip velocity profile, position of the blade relative to the waves, all components interacting, can be seen to the left in the rainflow diagram for one blade and as many smaller amplitudes on each peak in the signal. For both blades the variation in amplitude in the signal is not notable and the number of cycles is 422 with constant amplitude of 195.58 kN over a time period of 1 hour.

In case 4 the vertical velocity component gives an increase in number of cycles. For the total thrust force the number of 422 cycles due to the wave period can be recognized in the rainflow diagram, but also a number of 870 cycles with an amplitude smaller than 10 kN due to the vertical wave velocity component is to be seen to the left in the rainflow diagram. Also for the thrust force on one blade the number of cycles with a small amplitude, between 0 and 40 kN, has increased.

The turbulence in case 5 has a large influence on the cyclic loading on the turbine. For the thrust force on one blade the turbulence causes a number of more than 3000 cycles and for the total thrust force more than 5600 cycles over a time period of 1 hour. The number of cycles due to the wave period can be seen to the right in the rainflow diagram for the total thrust force and thrust force on one blade, with a small number of cycles compared to the number of cycles induced by the turbulence.

For case 6, calculations with the tidal wave over a time period of 84 hours, the rainflow analysis shows a large variation in amplitudes. The amplitude vary between 0 kN and 280.07 kN for one blade and 0 kN and 480.03 kN for the total thrust, with the largest number of cycles for the smallest amplitudes. The amplitudes of 280.07 kN for one blade and 480.03 kN for both blades are due to the tidal wave, which have 13 cycles over 84 hours.

9.3.2   Shaft Torque

Analysis of signal and values

For the shaft torque the trends are the same as for the thrust force for case 1 and case 2.

The waves have a very large influence on the shaft torque and give a significantly leap in the peak-to-peak values. The mean and minimum values are decreasing and the maximum values increasing. As the thrust force, the signals have a peak at every wave period of encounter. The waves give the largest contribution to the peak values of the shaft torque of all components added.

Looking at case 4, the vertical velocity component due to the waves is less significant for the shaft torque. The vertical velocity component is not notable in the figures of the signals. The mean values are decreasing very little and the maximum and minimum values are not changing.

Also the turbulence, case 5, has a very small influence on the mean values, but the oscillations of the signals due to the turbulence are notable in the figures. The maximum values are increasing and the minimum values are decreasing, causing a larger peak-to-peak value for the shaft torque, for one and both blades, when turbulence is added.

When adding the tidal wave, the mean values of the total shaft torque and the torque on blade are decreasing, the maximum values increasing and the minimum values decreasing, causing a larger difference in peak values. The oscillations of the shaft torque due to the tides are notable in figure 8.12 with a peak every time the velocity reaches its maximum, which is every 12.42 hours. Also notable in this figure is that the Matlab code not is able to calculate the shaft torque when the current velocity is 0 m/s. The very high peaks and lower points are neglected when searching for the maximum and minimum values of the signals.

The trends in table 8.2 for the shaft torque are similar to the trends in the table for thrust force.

Rainflow analysis

The rainflow diagram in case 2 for the shaft torque is similar to the diagram for the thrust force. Also in case 3, when adding the horizontal velocity component due to the waves, the trends are the same as for the thrust force.

The vertical velocity component, case 4, has a smaller influence on the shaft torque than on the thrust force. For the total shaft torque the vertical wave component has no influence on the number of cycles and the number of 421 cycles due to the wave period can be recognized in the rainflow diagram. For the torque on one blade the number of cycles with the smallest amplitude has increased with 66 cycles over a period of 1 hour.

The turbulence has a large influence on the cyclic loading on the turbine for the

shaft torque as well as the thrust force. The turbulence causes an additional number of almost 6000 cycles for both the total shaft torque and the torque on one blade over a time period of 1 hour. The cycles due to turbulence are to the left in the rainflow diagram with a low value for the amplitude. The number of cycles due to the wave period can be seen to the right in the rainflow diagram for the total shaft torque and torque on one blade.

In case 6 the amplitude varies between 0 kNm and 302.05 kNm looking at only one blade, with the largest number of cycles for the smallest amplitudes. For the total shaft torque, both blades, the amplitude varies between 0 kNm and 540.05 kNm. The very largest amplitudes in the signals are due to the tidal wave. Because of the very large range on the axis in the diagram, the small number of 13 cycles for the largest amplitude cannot be seen in the rainflow diagram.

9.3.3 Pitch Moment

Analysis of signal and values

Results of the pitch moment are useful for the design of the substructure. Calculations with an uniform velocity profile gives an oscillating pitch moment on one blade due to the varying arm of the moment with a constant amplitude and a period equal to the turbine period. Due to the second blade phase offset the resultant pitch moment for both blades is constant.

When adding the vertical no-slip velocity profile, case 2, the total pitch moment is oscillating above a mean value of 105.24 kNm with constant amplitude. The minimum value of the total pitch moment is zero, which is the value of calculations with a uniform velocity profile. The pitch moment of one blade is with a no-slip profile oscillating with constant amplitude and a period of 3.77 seconds, the turbine period. The maximum and the minimum values for one blade with a no-slip velocity profile are larger than for calculations with a uniform velocity profile, but the peak-to-peak value is for this case smaller than for case 2. The peak-to-peak value for both blades is smaller than peak-to-peak value for one blade.

When adding the waves, case 3, the signals for one blade and both blades are no longer oscillating with constant amplitude, but each blade does still have a peak every turbine period. The signal of the total pitch moment has a period equal to the wave period of encounter and is also oscillating due to the varying amplitude of each blade. The maximum value for one blade and both blades are increasing, the mean values and minimum values are decreasing, causing larger peak-to-peak values than the calculation without waves.

The vertical component due to the waves in case 4 has a limited influence on the mean value and no influence on the maximum and minimum value of pitch moment

on one blade. For the total pitch moment in contrary, the mean and the maximum values are increasing, while the minimum value is constant, increasing the difference in peak values. It is also possible to see that this component is affecting the signal of the total pitch moment in figure 8.16.

The added turbulence in case 5 is increasing the mean and the maximum values for one and both blades. The minimum values are decreasing and the peak-to-peak values are increasing. The turbulence is not very notable in the figure, but does affect the results to a certain extent in terms of increasing the peak-to-peak values.

Also the tidal wave, case 6, is increasing the maximum values and decreasing the minimum values. The mean values are lower than for the calculations in case 5 and the peak-to-peak values higher. The signal in figure 8.19 has a peak every 12.42 hours, similar to the thrust force and the shaft torque.

The table 8.3 is showing no obvious trend for the mean values when components are added. The minimum value is decreasing and the maximum and peak-to-peak value is increasing for the total pitch moment. This is also the case for the pitch moment on one blade, but the values are not decreasing and increasing successively. The deviation from continuous decrease or increase is in calculations without waves. The peak-to-peak values for one blade for all cases are much larger than for both blades.

Rainflow analysis

The number of cycles for calculation of pitch moment on one blade with a uniform velocity profile over a time period of 900 seconds is 239 due to the turbine period. For the total pitch moment the number of cycles is zero due to phase offset of the blades.

The rainflow diagram has the same trend as thrust force in case 2. When adding the waves in case 3 pitch moment does not have a constant amplitude for one blade or in total, but cycles with varying amplitudes. For calculation on one blade the major part of the cycles have an amplitude between approximately 1900 kNm and 3120.30 kNm. For calculations on both blades the amplitude varies between 0 kNm and 333.24 kNm, with the largest number of cycles for smaller amplitudes.

The vertical wave velocity component in case 4 has a smaller influence on the pitch moment than the horizontal wave component has. The component gives a decrease in total number of cycles on both blades, but now there are cycles with a larger amplitude than analyses without the vertical wave component. The number of cycles on one blade is constant and the trend in the rainflow diagram is similar to the one without the component, but it shows an increase in number of cycles with a large amplitude and a decrease in number of cycles with the smallest amplitude.

The turbulence in case 5 has a smaller influence on the pitch moment than it

has on the thrust force and the shaft torque. The turbulence gives an additional number of 117 cycles on one blade and 311 cycles on both blades. These cycles has a very small amplitude and can be seen to the left in the rainflow diagrams. For calculations on one blade, the cycles with large amplitude, cycles due to the wave period, can be recognized from the rainflow analysis above and is to be seen to the right in the rainflow diagram. For the total pitch moment it is notable in the rainflow diagram that the largest amplitude has increased with added turbulence.

Calculations with the tidal wave over a time period of 84 hours the rainflow analysis shows a large variation in amplitudes. The amplitude varies between 0 kNm and 3270.80 kNm for one blade with the largest number of cycles for the smallest amplitudes. For the total pitch moment the amplitude varies between 0 kNm and 595.99 kNm, also with the largest number of cycles for the smallest amplitude.

9.3.4 Yaw Moment

Analysis of signal and values

Also the yaw moment is important for the substructure design. For a uniform velocity profile the trend is the same as for pitch moment. This is also the case when the vertical no-slip current velocity profile is added, case 2, but the oscillations are here above zero. When adding the vertical velocity profile the maximum and the peak-to-peak values are increasing and the minimum values decreasing for one blade and both blades in total.

In case 3, when adding the waves, the trends are the same as for the pitch moment, but it is hard to recognize a connection between the wave period and the signal of the total yaw moment.

The component which has the largest influence on the total yaw moment is the vertical component due to the waves, case 4. This is notable in table 8.4 and figure 8.23. The minimum value is decreasing and the maximum and peak-to-peak values are increasing with a large value. In the signal for the total yaw moment the oscillation due to the turbine period and also the oscillation due to the wave period of encounter can be recognized. Also for calculation of one blade the peak-to-peak values are larger with the vertical velocity component added.

The turbulence in case 5 has a limited influence on the maximum, minimum and peak-to-peak values and is hardly notable in the figures. The maximum and the minimum value of one blade are decreasing, but the peak-to-peak value remains approximately constant. For the total yaw moment the minimum value is decreasing and maximum and peak-to-peak values are increasing due to the turbulence.

The trend for the tidal wave, case 6, is the same as for the pitch moment.

The mean values for all cases are approximately zero and the signals are oscillating above this mean value, which means that the maxima and minima have the same absolute values. The minimum value is decreasing and the maximum and peak-to-peak values are increasing for the total yaw moment for each component added. This is also the case for the yaw moment on one blade, but the maximum value is not increasing successively. The deviation from continuous increase is in calculations with turbulence. The peak-to-peak values for one blade for all cases are much larger than for both blades, similar to the pitch moment.

Rainflow analysis

The rainflow trend is the same as for the pitch moment in case 1 and case 2.

When adding the waves in case 3 the signals have cycles with varying amplitudes. For calculations on one blade the cycles with the smallest amplitudes are to the left in the rainflow diagram, with amplitudes between approximately 2100 kNm and 2350 kNm. To the left in the diagram the largest cycles can be seen with the largest amplitude of 3127.15. The number of cycles on one blade is 955, which is the same as for pitch moment for calculations with waves. For calculations on both blades the amplitude varies between 40 kNm and 201.10 kNm, with the largest number of cycles for smaller amplitudes.

When adding the vertical wave velocity component in case 4 the number of cycles on one blade does not change. The rainflow diagram shows that this component gives a larger variation in amplitude, with a larger maximum amplitude for both analyses. The vertical wave component has a large influence on the total yaw moment, where the maximum amplitude in the rainflow diagram increases from 201.10 kNm to 776.46 kNm, but the number of cycles decreases from 2328 to 1660 cycles. The major part of the cycles is to the left in the rainflow diagram for the total yaw moment. The number of cycles on one blade is in the rainflow diagram equal to calculation without the component.

The turbulence has a small influence on the yaw moment. The turbulence gives an additional number of 79 cycles on one blade and 220 cycles on both blades for analysis over a time period of 1 hour where the total number of cycles are 1034 and 1880 for calculation with turbulence. The additional cycles has a very small amplitude and can be seen to the left in the rainflow diagrams. The largest amplitude for one blade has a small increase with added turbulence, but this is not notable in the rainflow diagram.

Calculations with the tidal wave over a time period of 84 hours the rainflow analysis shows a large variation in amplitudes, similar to the other forces calculated. The amplitude varies between 0 kNm and 3721.40 kNm for one blade. For the total pitch moment the amplitude varies between 0 kNm and 1040.50 kNm. The smallest amplitudes have the largest number of cycles.

9.4 Further Work

In the comparison with experiments the trend that the mean values are decreasing with an increasing wave period is apparent, this for both experiments and Matlab calculations. The reason for this is not known and should be further investigated. Also the influence of the axial and rotational induction factors on the loads when varying these should be considered. The deviation in peak-to-peak values and how these depend on the wave period and dynamic effects should also be further investigated.

Another suggestion for further work is to look at the wake from the substructure and interaction with the turbine blades. The Matlab code is not able to calculate the shaft torque for current velocities of 0 m/s and needs improvement for calculations with this velocity. It would also be interesting to implement irregular waves in the Matlab code. The results of calculations of dimensional loading and the rainflow analysis can be used for a fatigue analysis of the turbine blades.

Chapter 10

Conclusion

Results from Matlab calculations are compared to experimental results in order to validate the Matlab code. Comparison is done with a current velocity of 2.5 m/s with three different waves and without waves. The tendency seen in the comparison is that the Matlab code underestimates the thrust force and the shaft torque and overestimates the torque on one blade, but the trends for all forces are the same with oscillating signals and a peak every wave period of encounter. An increasing wave period, with a constant steepness, increases the peak-to-peak values for both experiments and Matlab calculations and results in a decreasing deviation between experimental and calculation results in peak-to-peak values. The larger the wave period is the more valid and applicable is the Matlab code.

The loads on the tidal turbine blades are calculated to evaluate the influence of the vertical velocity profile, the horizontal and vertical velocity component due to the waves, the turbulence and the tidal wave on the loads on the turbine blades. The total loading is an interaction between all components acting, but calculation results show that some of the components have a larger influence on the loads than others.

For the thrust force on one blade and the total thrust force, both blade summarized, the horizontal component due to the waves gives the largest contribution in peak-to-peak values. Also the vertical velocity component due to the waves increases the maximum values inducing a further increased peak-to-peak value. Besides increasing the peak-to-peak values, the turbulence induces the largest number of cycles.

Also for the shaft torque, for one blade and in total, the horizontal component due to the waves has the largest influence on the peak-to-peak values. The vertical wave velocity component has a minor influence on the shaft torque. For the shaft

torque as well as the thrust force, the largest contribution of cycles is from the turbulence, which also increases the peak-to-peak values.

The horizontal velocity component due to the waves has the largest influence on the peak-to-peak values also for the pitch moment, but for pitch moment on one blade also the vertical component has an influence on the maximum values. The turbulence increases the peak-to-peak values further, but has a minor influence on the number of cycles induced. The consistently main oscillations inducing cyclic loading are due to the vertical no-slip current velocity profile.

For the yaw moment the vertical component due the waves has a large influence. The horizontal component due to the waves increases the peak-to-peak values as well, but the vertical component has the major influence. Also for the yaw moment the turbulence has a minor influence and the main oscillations causing a cyclic loading are due to the vertical no-slip current velocity profile.

The tidal wave gives the largest peak-to-peak values of all cases calculated for all forces. The velocity oscillates between 0 m/s and 4 m/s and the maximum values of the loads are when the turbine experiences the maximum velocity.

The results from the rainflow analysis can be used for a fatigue analysis of the turbine blades. Fatigue life is a compromise between the amplitude and the number of cycles.

The Matlab code is a reliable and fast tool. Despite the simplifications done in the calculations, it calculates the dimensioning loads for a tidal turbine with a good accuracy.

Bibliography

[1] Atlantis Resources Corporation. http://www.atlantisresourcescorporation.com/.

[2] Bay of Fundy - Wikipedia, the free encyclopedia. http://en.wikipedia.org/wiki/Bay_of_Fundy.

[3] EMEC: European Marine Energy Centre - tidal energy devices. http://www.emec.org.uk/tidal_devices.asp.

[4] Hammerfest Strøm AS - teknologi. http://www.hammerfeststrom.com/.

[5] Marine Current Turbines. http://www.marineturbines.com/.

[6] NDE/NDT Resource Center. http://www.ndt-ed.org/index_flash.htm.

[7] Notes from course physical processes in the ocean, School of Oceanography, University of Washington. *http://www.washington.edu/*.

[8] OC2910 - tides: Basic concepts and terminology. http://www.oc.nps.edu/nom/day1/partc.html#tide.

[9] OpenHydro - tidal technology. http://www.openhydro.com/home.html.

[10] Rainflow counting algorithm - file exchange - MATLAB central. http://www.mathworks.de/matlabcentral/fileexchange/3026.

[11] SeaGen · sea generation tidal turbine. http://www.seageneration.co.uk/default.asp.

[12] Tidal Generation. http://www.tidalgeneration.co.uk/.

[13] Virginia Institute of Marine Science. http://web.vims.edu/.

[14] Voith Hydro. http://www.voithhydro.com/index_en.php.

[15] Your renewable news. http://www.yourrenewablenews.com.

[16] J.A Bannantine, J.J Corner, and J.L Handrock. *Fundamentals of Metal Fatigue Analysis*. 1990.

[17] N. Barltrop, K. S. Varyani, A. Grant, D. Clelland, and Xuan Pham. Wave-current interactions in marine current turbines, June 2006.

[18] L Bernshtein and Haeyang Yon'guso (Korea). *Tidal power plants*. Korea Ocean Research and Development Institute, Seoul Korea, 1996.

[19] Ole G. Dahlhaug. Lecture notes energy from environmental flows.

[20] Carlos Alberto Dorao. Lecture notes fluids engineering, 2010.

[21] Norman Dowling. *Mechanical behavior of materials : engineering methods for deformation, fracture, and fatigue.* Pearson/Prentice Hall, Upper Saddle River N.J., 3rd ed. edition, 2007.

[22] Céline Faudot and Ole G. Dahlhaug. Memo, tidal turbine model test, August 2010.

[23] Lars Frøyd and Svein Kjetil Haugset. Analysis and design of wind turbine blades, 2010.

[24] Per Åge Krogstad. Lecture notes wind technology, January 2010.

[25] A.M. Gorlov. Tidal energy, 2001.

[26] J Hardisty. *The analysis of tidal stream power*. Wiley, Chichester UK ;;Hoboken NJ, 2009.

[27] K. Heinloth. Renewable energy. In *Numerical Data and Functional Relationships in Science and Technology*, volume 3C.

[28] Christoph Hirsch. Lecture notes Technische Verbrennung, TU München, Lehrstuhl für Thermodynamik, 2010.

[29] J.M.J Journee and Jakob Pinkster. Introduction in ship hydromechanics, April 2002.

[30] F. Kiesewetter. Modellierung des Verbrennungsinduzierten Wirbelaufplatzens in Vormischebrennern. PhD thesis, TU München, 2005.

[31] Harald E. Krogstad and Øivind A. Arntsen. Linear wave theory, 2000.

[32] J Manwell. *Wind energy explained : theory, design and application*. Wiley, Chichester ;;New York, 2002.

[33] Graeme McCann, Mat Thomson, and Stuart Hitchcock. Implications of Site-Specific condition on the prediction of loading and power performance of a tidal stream device, 2008.

[34] I. A. Milne, R. N. Sharma, R. G. J. Flay, and S. Bickerton. Onset turbulence on tidal turbine blade loads, 2010.

[35] I. A. Milne, R. N. Sharma, R. G. J. Flay, and S. Bickerton. A preliminary analysis of the effect of the onset flow structure on tidal turbine blade loads, 2010.

[36] I. A. Milne, R. N. Sharma, R. G. J. Flay, and S. Bickerton. The role of waves on tidal turbine unsteady blade loading, 2010.

[37] Statkraft. Wave- and tidal power.

[38] Marie Lunde Sæterstad. Design of a tidal turbine, December 2010.

[39] John Wægter. Stress range histories and rain flow counting, 2009.

[40] Frank White. *Fluid mechanics*. McGraw-Hill, New York, 6th ed. edition, 2008.

Appendix A

The Matlab Code

A.1 The Algortim

```matlab
1  clc
2  clear all
3  close all
4
5  %————————————————input variables————————————————
6
7  config=[1 0 1 2 1 0 0 1];
8  %config(1): vertical velocity component due to the waves:
9                                          %0:off, 1:on
10 %config(2): 0:regular waves, 1:irregular waves
11 %config(3): turbine scale, 1:prototype, 14:model
12 %config(4): number of blades
13 %config(5): vertical velocity profile 0:uniform,1:no—slip
14 %config(6): tides 0:off, 1:on
15 %config(7): turbulence intensity TI 0:off, X:X in%
16 %config(8): without waves:0, with waves: 1
17
18 fid = fopen('var.txt','r');
19 c= textscan(fid, '%f %s', 'delimiter','\t');
20 vari= c{1};
21 V_ini=vari(1);     %input velocity [m/s] —
22                           %if tides not considered
23 tmin=vari(2);      %input t start
24 Δt=vari(3);     %input Δ t [s]
25 tmax=vari(4);      %input t end
26 steepness=vari(5); %input steepness wave
27 Twave=vari(6);     %input period wave
28 fclose(fid);
29
30 hydrofoils={'S816—re123.txt', 'S825—re194.txt',...
```

I

```matlab
31          'S826_14re198.txt','S826_12re191.txt'};
32   aero_arr=cell(1, length(hydrofoils));
33                          %empty 1*4 array of matrices
34
35   for i=1:1:length(hydrofoils)
36       %fill the aero_arr with one hydrofoil for
37       %each cell:aero_arr{i}
38       aero_arr{i}=load(hydrofoils{i});
39       %loads the variables from a MAT—file into a %
40       %structure array, aero_arr
41   end
42
43   sf=config(3);        %turbine scale
44   Nblade=config(4);    %number of blades
45
46   %————————————————————————const param—————————————————————————
47
48   N=100;               %100 elementer
49   Dt=21/sf;            %turbine diameter [m],
50                        %comparison: 19.95m, otherwise: 21m.
51   R=Dt/2;              %radius [m]
52   dr=R/N;              %depth of element [m]
53   if config(3)==1      %density of water [kg/m^3]
54       rho=1028;
55   else
56       rho=1000;
57   end
58   Ni=7/sf;             %distance from blade tip in lower
59                        %position to seabed[m]
60   TSR=7;               %tip speed ratio
61   TotWD_ini=36/sf;     %total water depth,
62                        %mean water surface [m]
63   WDup_ini=(TotWD_ini—Ni—Dt);%depth of turbine blade
64                        %tip in upper position
65                        %from mean water surface [m]
66
67   %————————————————————————read file————————————————————————————
68
69   fid = fopen('TIDAL.txt','r');
70   C = textscan(fid, '%f %f %f %f %f', 'delimiter','\t');
71   rR = C{1};
72   r = C{2};
73   Lc= C{3};
74   Twist = C{4};
75   fclose(fid);
76
77   fid = fopen ('a_axial.txt', 'r');
78   d= textscan(fid, '%f %s', 'delimiter','\t');
79   a_ax= d{1};
80   fclose(fid);
81
82   fid = fopen ('a_rotational.txt', 'r');
83   e= textscan(fid, '%f %s', 'delimiter','\t');
84   a_rot= e{1};
85   fclose(fid);
86
87   %————————————————————————matrices—————————————————————————————
```

```
88
89   t=tmin:Δt:tmax;                    %time array
90   gamma=zeros(1,Nblade);             %array, angle between horizontal
91                                      %axis and each blade
92   z=zeros(1,Nblade);                 %array, distance betweeen blade
93                                      %element and mean water level
94   u=zeros(1,Nblade);                 %rotational speed
95   v=zeros(1,Nblade);                 %flow velocity
96   phi=zeros(1,Nblade);               %flow angle
97   alpha=zeros(1,Nblade);             %angle of attack
98   ca=zeros(1,Nblade);                %axial induction coefficient
99   cr=zeros(1,Nblade);                %rotational induction coefficient
100  Cl=zeros(1,Nblade);                %lift coefficient
101  Cd=zeros(1,Nblade);                %drag coefficient
102  dT=zeros(1,Nblade);                %thrust on one blade element for
103                                     %each blade
104  dM=zeros(1,Nblade);                %torque on one blade element for
105                                     %each blade
106  T=zeros(Nblade,length(t));         %thrust force each blade, sum
107                                     %all blade elements due to time
108  Mx=zeros(Nblade,length(t));        %torque each blade, sum all
109                                     %blade elements due to time
110  Ttot=zeros(1,length(t));           %thrust all blades due to time
111  Mtot=zeros(1,length(t));           %torque all blades due to time
112  H=zeros(1,length(t));              %water level due to the tides
113  WaterDepth=zeros(1,length(t));     %total water depth [m]
114  U=zeros(1,length(t));              %water velocity due to the tides
115  Vel=zeros(1, length(t));           %current velocity [m/s]
116  u_fluct_ini=zeros(N,length(t));    %intial u fluctuations
117                                     %matrix,[N—elements,t—time]
118  u_fluct=zeros(N,length(t));        %scaled u fluctuations
119                                     %matrix,[N—elements,t—time]
120  Tm=zeros(Nblade, length(t));       %thrust*arm
121  r_Tm=zeros(Nblade, length(t));     %position where the total
122                                     %thrust force is acting
123  length_Mz=zeros(Nblade,length(t)); %arm—moment around z—axis
124  length_My=zeros(Nblade,length(t)); %arm—moment around x—axis
125  My=zeros(Nblade, length(t));       %My,pitch moment expressed,
126                                     %at the hub for each
127                                     %blade due to time
128  Mz=zeros(Nblade, length(t));       %Mz, yaw moment expressed
129                                     %at the hub, for each blade
130                                     %due to time
131  Mytot=zeros(1,length(t));          %My all blades due to time
132  Mztot=zeros(1,length(t));          %Mz all blades due to time
133  surface_wave=zeros(1, length(t));  %water surface due to
134                                     %the waves
135  position_blade=zeros(1, length(t));%position of blade over
136                                     %time
137
138  %plot vertical velocity profile
139  % WD=TotWD_ini:—1:0;               %array total water depth,
140  %                                  %one cell for one meter
141  % vert=zeros(1, length(WD));       %vertical velocity profile
142  %                                  %at each position of WD,
143  %                                  %uniform current+waves
144  % vertw=zeros(1, length(WD));      %vertical velocity profile
```

III

```
145  %                           %at each position of WD,
146  %                           %no-slip current+waves
147  % vertical=cell(1, length(t));    %creates an empty cell
148  %                           %array of matrices
149  %                           %vert-matrix
150  %                           %in each cell, over time
151  % verticalw=cell(1, length(t));   %creates an empty cell
152  %                           %array of matrices
153  %                           %vertw-matix
154  %                           %in each cell, over time
155
156  %------------------------turbulence------------------------
157
158  if config(7)>0
159      for l=1:N
160          for k=1:length(t)
161              u_fluct_ini(l, k)=turbulence (t(k)); %fluctuations
162                                        %above mean[m/s]
163          end
164      end
165  end
166
167  %**********************************************************
168  %**********************************************************
169
170  %------------------ITERATION T TIMESTEPS ------------------
171
172  for j=1:length(t)              %iterating through time array, t
173
174  %---------------------------tides---------------------------
175
176  if config(6)==1                %if tides considered
177    [H(j),U(j)]=Tides(t(j));
178    TotWD=TotWD_ini+H(j);        %total water depth due to
179                                 %the tides[m]
180    WDup=TotWD-Ni-Dt;            %depth of turbine blade
181                                 %tip in upper position
182                                 %due to the tides[m]
183    Vin=abs(U(j));               %absolute value-magnitude [m/s]
184  else                          %else: tides not considered
185    WDup=WDup_ini;              %depth of turbine blade tip
186                                 %in upper position
187    TotWD=TotWD_ini;             %total water depth [m]
188    Vin=V_ini;                   %current velocity [m/s]
189  end
190
191  Vel(j)=Vin;
192  WaterDepth(j)=TotWD;
193
194  axisPos=WDup+(Dt/2);           %position of the axis [m]
195                                 %reference mean water surface
196
197  % %------------------turbulence fluctuations----------------
198
199  TI=config(7)/100;              %turbulence intensity
200  u_f=TI*Vin;                    %fluctuations above mean [m/s]
201
```

```matlab
202   %──────────────────────turbine control─────────────
203   %for model test: no turbine control
204
205   if Vin < 2.5
206       omegat=TSR*Vin/R;          %angular frequency turbine [rad/s]
207        % Tturbine=2*pi/omegat; %period turbine [s]
208    else
209       omegat=TSR*2.5/R;          %angular frequency turbine [rad/s]
210        %Tturbine=2*pi/omegat; %period turbine [s]
211   end
212
213   %─────────────────────────waves───────────────────
214
215   lambdaw=(9.81/(2*pi))*Twave^2;%wave length [m]
216   Hwave=lambdaw*steepness;       %wave height max[m]
217
218   k_gen=2*pi/lambdaw;            %wave number generated [rad/m]
219   omegaw_gen=2*pi/Twave;         %wave frequency generated [rad/s]
220
221   omegaw=omegaw_gen+k_gen*Vin; %frequency of encounter [rad/s]
222   k=(omegaw^2)/9.81;            %wave number of encounter [rad/m]
223   Twave_encounter=2*pi/omegaw; %wave period of encounter [s]
224
225   Vwmax=(Hwave/2)*omegaw;        %water particle velocity at
226                                  %the surface [m/s]
227
228   surface_wave(j)=Hwave/2*cos(-(omegaw*t(j)));%surface wave form
229                                  %──> plot
230
231   %─────────────────plot vertical velocity profile──────────
232
233   % [vertw vert]=profile(TotWD_ini, axisPos, k, Vwmax, omegaw,...
234   %t(j),Vin, Hwave, config(5), WD);
235   % verticalw{j}=vertw;
236   % vertical{j}=vert;
237   %
238   %──────────────────────────gamma─────────────────
239
240       gamma_ini=omegat*t(j);     %angle between blade and
241                                  %horisontal axis,
242                                  %reference horisontal axis
243                                  %z=Dt/2+WDup=18.5
244                                  %meters below sea level
245                                  %positiv direction left
246
247       position_blade(j)=sin(gamma_ini);%position blade ──> plot
248
249   %───────────────ITERATION N ELEMENTS─────────────────
250
251       for i=1:1:N                 %iterating through N elements
252
253   %────────────────────────tiploss─────────────────
254
255           F=tiploss(i);
256
257   %───────────────ITERATION Nblade BLADES───────────────
258
```

```
259          for index_blade=1:Nblade    %iterating through n blades
260
261 %————————————————position blade———————————————
262
263              gamma(index_blade)=gamma_ini+(2*pi)/...
264                  Nblade*(index_blade—1 ;
265                            %angle to horizontal axis
266
267              z(index_blade)=Dt/2+WDup—r(i)*...
268                  sin(gamma(index_blade));
269                          %blade element position on vertical
270                          %axis from sea surface, y(surface)=0
271
272 %————————————————velocities blade———————————————
273
274              [v(index_blade) u(index_blade)]= vel(z...
275                  (index_blade), TotWD, axisPos, k, Vwmax,...
276                  omegaw, t(j), Vin, Hwave, config(5),...
277                  config(1), r(i), omegat, gamma(index_blade),...
278                  config(8));
279
280 %————————————————————turbulence———————————————
281
282          if config(7)>0              %if turbulence considered
283                  a=(u_f/std(u_fluct_ini(i, :)));
284                              %scaling factor u_fluct_ini
285                  u_fluct(i, j)=a.*u_fluct_ini(i, j);
286                              %scaling initial u'
287                  v(index_blade)=v(index_blade)+u_fluct(i, j);
288                              %current velocity=u_mean+u'
289          end
290
291 %————————————————angles blade———————————
292 %angles in degrees from list
293
294              phi(index_blade)=atand((1—a_ax(i))*...
295                  v(index_blade)/((1+a_rot(i))*u...
296                  (index_blade)));
297
298              theta=Twist(i);                 %twist angle
299              alpha(index_blade)=phi(index_blade)—theta;
300                              %angle of attack
301
302 %————————————————force coefficients blade————————
303
304              [Cl(index_blade) Cd(index_blade)]=LiftDragCoeff...
305                  (alpha (index_blade), rR(i), aero_arr);
306
307              ca(index_blade)=Cl(index_blade)*cosd(phi...
308                  (index_blade))+Cd(index_blade)*sind...
309                  (phi(index_blade));         %axial coeff.
310              cr(index_blade)=Cl(index_blade)*sind(phi...
311                  (index_blade))—Cd(index_blade)*cosd(phi...
312                  (index_blade));             %rotational coeff.
313
314 %————————————————forces blade —————————————
315
```

```matlab
316             dT(index_blade)=ca(index_blade)*0.5*rho*Lc(i)...
317                 *dr*v(index_blade)*abs(v(index_blade))*...
318                 (1-a_ax(i))^2/(sind(phi(index_blade))*abs...
319                 (sind(phi(index_blade))))*F;
320                     %Thrust force one element on one blade
321             dM(index_blade)=cr(index_blade)*0.5*rho*Lc(i)...
322                 *dr*v(index_blade)*(1-a_ax(i))/(sind(phi...
323                 (index_blade)))*omegat*r(i)*(1+a_rot(i))/...
324                 (cosd(phi(index_blade)))*F;
325                     %Moment one element on one blade
326
327             T(index_blade, j)=T(index_blade, j)+...
328                 dT(index_blade);
329                 %Thrust force each blade, all blade elements
330             Mx(index_blade, j)=Mx(index_blade, j)+...
331                 dM(index_blade)*r(i);
332                 %Torque each blade, all blade elements
333             Tm(index_blade, j)=Tm(index_blade, j)+dT...
334                 (index_blade)*r(i);
335                 %Sum: Thrust each blade element*radius
336
337         end %end blades
338
339     end %end blade elements
340 %----------------------------------------------------------------
341
342     for index_blade=1:Nblade
343         r_Tm(index_blade,j)=Tm(index_blade,j)/...
344             T(index_blade, j);
345             %Radius, where, on the blade, the thrust force
346             %is acting
347         length_Mz(index_blade,j)=cos(gamma_ini+(2*pi)...
348             /Nblade*(index_blade-1))*r_Tm(index_blade,j);
349             %distance where the force is acting from the z-axis
350         length_My(index_blade,j)=sin(gamma_ini+(2*pi)/...
351             Nblade*(index_blade-1))*r_Tm(index_blade,j);
352             %distance where the force is acting from the y-axis
353         Mz(index_blade,j)=T(index_blade,j)*length_Mz...
354             (index_blade,j);
355             %moment around z-axis
356         My(index_blade,j)=T(index_blade,j)*length_My...
357             (index_blade,j);
358             %moment around x-axis
359     end
360
361     Ttot(j)=sum(T(:,j));    %total thrust force as a function
362                             %of time
363     Mtot(j)=sum(Mx(:,j));  %total torque as a function of time
364
365     Mytot(j)=sum(My(:,j));
366     Mztot(j)=sum(Mz(:,j));
367
368 end %end timestep
369
370 T1=T(1,:);
371 T2=T(2,:);
372
```

```
373  Mx1=Mx(1,:);
374  Mx2=Mx(2,:);
375
376  My1=My(1,:);
377  My2=My(2,:);
378
379  Mz1=Mz(1,:);
380  Mz2=Mz(2,:);
```

A.2   Lift and Drag Coefficients Function

```
1   function [cl,cd]=LiftDragCoeff(alpha, rR, aero_arr)
2
3   R=[0.1 0.25 0.75 0.90 0.98 1.0];
4
5   for i=1:1:length(R−1)
6
7       if rR≥R(i) && rR<R(i+1)        %cylinder
8           if i==1
9               cd=0.5;
10              cl=0;
11          else
12              Alpha=aero_arr{i−1}(:,1);
13                        %cell {i−1}, (:,1) all columns, first row
14              CL=aero_arr{i−1}(:,2);
15              CD=aero_arr{i−1}(:,3);
16              cl=interp1(Alpha,CL,alpha);
17              cd=interp1(Alpha,CD,alpha);
18          end
19      end
20  end
21
22  return
```

A.3   Tidal Function

```matlab
1  function [H,U]=Tides(time)
2
3  %t=time;              %timer input
4  t=time/3600;          %time[s]--->[h]
5  h_sum=0;
6  H=0;
7  u_sum=0;
8  U=0;
9
10 periode=[12.42, 12.00, 12.66, 23.93, 26.87, 24.07]; %[h]
11 omega=(2*pi)./periode;                              %[rad/h]
12 h= 1.68.*[0.913, 0.283, 0.202, 0.079, 0.013, 0.026];%[m]
13 u= 1.68.*[1.51, 0.47, 0.33, 0.13, 0.02, 0.04 ];     %[m/s]
14 phase=[50.1, 89.6, 22.5, 236.2, 23.8, 236.2];       %[rad]
15
16 for i=1:1:length(omega)
17     h_sum=h_sum+h(i)*cos(omega(i)*t+phase(i));        %[m]
18     u_sum=u_sum+u(i)*cos(omega(i)*t+phase(i)+(pi/2)); %[m/s]
19 end
20
21 H=h_sum;
22 U=u_sum;
23 return
```

A.4 Tiploss Function

```
1  function F=tiploss(N)
2    if N≤97
3      F=1;
4    elseif N==98
5      F=2/3;
6    elseif N==99
7      F=1/3;
8    elseif N==100
9      F=0;
10   end
11   return
```

A.5 Turbulence Function

```
1  function u_fluct=turbulence(time)
2
3  t=time;              %[s]
4  u_sum=0;
5  u_fluct=0;
6
7  periode=[1, 3, 5, 10, 20, 30, 40, 50, 60];    %[s]
8  omega=(2*pi)./periode;                         %[rad/s]
9  u=[rand(1)-0.5, rand(1)-0.5, rand(1)-0.5, ...
10     rand(1)-0.5, rand(1)-0.5, rand(1)-0.5,...
11     rand(1)-0.5, rand(1)-0.5, rand(1)-0.5 ]; %[m/s],
12                    %random numbers between 0 and 1
13 phase=(pi/2).*rand(1,9);                       %[rad]
14
15 for i=1:length(omega)
16    u_sum=u_sum+u(i)*cos(omega(i)*t+phase(i)); %[m/s]
17 end
18
19 u_fluct=u_sum;
20
21 return
```

A.6 Velocity Function

```
1  function [v u]=vel(z, TotWD, axisPos, k, Vwmax, ...
2      omegaw, t, V, Hwave, config5, config1, r,...
3      omegat, gamma, config8)
4
5  if config8==0      %config(8)=0: waves not consideres
6
7      u=omegat*r;
8
9      if config5==0;          %current — uniform profile
10         v=V;
11     else                    %current — no—slip profile
12         Vcurrentmax=V*(TotWD/(TotWD—axisPos))^(1/7);
13         v=Vcurrentmax*((TotWD—z)/TotWD)^(1/7);
14     end
15
16 else                %config(8)=1: waves considerd
17
18 %————————————————————Wheeler streching——————————
19
20     ny=Hwave/2*cos(—omegaw*t);
21     zs=z*(1—ny/TotWD)+ny;
22
23 %————————————————————Velocity wave——————————————
24
25      Vhwave=Vwmax*exp(—k*zs)*cos(—omegaw*t);
26                         % horizontal component
27      Vvwave=Vwmax*exp(—k*zs)*sin(—omegaw*t);
28                         % vertical component
29
30 %————————————————————Velocity current———————————
31
32     if config5==0;          %current — uniform profile
33         Vcurrent=V;
34     else                    %current — no—slip profile
35         Vcurrentmax=V*(TotWD/(TotWD—axisPos))^(1/7);
36         Vcurrent=Vcurrentmax*((TotWD—zs)/TotWD)^(1/7);
37     end
38
39 %————————————————————Resultant velocity—————————
40
41     v=Vhwave+Vcurrent;
42
43     if config1==0      %vertical velocity component
44                        %due to the waves not considered
45         u=omegat*r;
46     else               %vvc due to the waves considered
47         u=omegat*r+Vvwave*cos(gamma);
48     end
49 end
50  return
```

A.7 Axial Induction Factor List

1	0.3087
2	0.0464
3	0.0438
4	0.0418
5	0.0404
6	0.0402
7	0.0416
8	0.0437
9	0.0468
10	0.0511
11	0.0557
12	0.0608
13	0.1119
14	0.1642
15	0.2085
16	0.2384
17	0.2552
18	0.2624
19	0.2675
20	0.2721
21	0.2760
22	0.2518
23	0.2565
24	0.2608
25	0.2645
26	0.2902
27	0.2923
28	0.2941
29	0.2958
30	0.2975
31	0.2992
32	0.3010
33	0.3028
34	0.3044
35	0.3059
36	0.3073
37	0.3085
38	0.3097
39	0.3107
40	0.3117
41	0.3126
42	0.3135
43	0.3144
44	0.3153
45	0.3162
46	0.3174
47	0.3186
48	0.3196
49	0.3206
50	0.3216
51	0.3225
52	0.3233
53	0.3242

54	0.3250
55	0.3259
56	0.3269
57	0.3279
58	0.3290
59	0.3302
60	0.3314
61	0.3327
62	0.3340
63	0.3353
64	0.3367
65	0.3382
66	0.3397
67	0.3413
68	0.3429
69	0.3447
70	0.3466
71	0.3486
72	0.3508
73	0.3531
74	0.3540
75	0.3549
76	0.3560
77	0.3573
78	0.3587
79	0.3603
80	0.3621
81	0.3642
82	0.3665
83	0.3693
84	0.3725
85	0.3762
86	0.3803
87	0.3849
88	0.3900
89	0.3955
90	0.4016
91	0.4067
92	0.4123
93	0.4187
94	0.4263
95	0.4350
96	0.4452
97	0.4586
98	0.4784
99	0.5121
100	0.5875

A.8   Rotational Induction Factor List

1	0.3223
2	−0.0430
3	−0.0363
4	−0.0283
5	−0.0204
6	−0.0153
7	−0.0134
8	−0.0123
9	−0.0115
10	−0.0100
11	−0.0078
12	−0.0055
13	0.0063
14	0.0191
15	0.0304
16	0.0379
17	0.0409
18	0.0404
19	0.0390
20	0.0376
21	0.0362
22	0.0355
23	0.0341
24	0.0326
25	0.0313
26	0.0295
27	0.0283
28	0.0271
29	0.0260
30	0.0250
31	0.0240
32	0.0231
33	0.0222
34	0.0214
35	0.0206
36	0.0199
37	0.0192
38	0.0185
39	0.0178
40	0.0172
41	0.0166
42	0.0160
43	0.0155
44	0.0150
45	0.0145
46	0.0142
47	0.0138
48	0.0134
49	0.0131
50	0.0127
51	0.0124
52	0.0121
53	0.0118

54	0.0115
55	0.0112
56	0.0110
57	0.0107
58	0.0105
59	0.0103
60	0.0101
61	0.0099
62	0.0097
63	0.0095
64	0.0094
65	0.0092
66	0.0091
67	0.0090
68	0.0089
69	0.0088
70	0.0087
71	0.0086
72	0.0085
73	0.0085
74	0.0083
75	0.0082
76	0.0080
77	0.0079
78	0.0078
79	0.0077
80	0.0076
81	0.0075
82	0.0074
83	0.0074
84	0.0074
85	0.0074
86	0.0074
87	0.0074
88	0.0075
89	0.0075
90	0.0077
91	0.0076
92	0.0077
93	0.0077
94	0.0078
95	0.0079
96	0.0082
97	0.0086
98	0.0094
99	0.0112
100	0.0174

A.9   S816 re123

```
 1  Alpha       C_L        C_D
 2  −180.000000  0.000000   0.010000
 3  −170.000000  0.144917   0.033587
 4  −160.000000  0.289835   0.149546
 5  −150.000000  0.434752   0.327236
 6  −140.000000  0.579670   0.545270
 7  −130.000000  0.530353   0.777409
 8  −120.000000  0.441879   0.995729
 9  −110.000000  0.316122   1.173983
10  −100.000000  0.163503   1.290766
11  −90.000000  −0.000000   1.332094
12  −80.000000  −0.163503   1.290766
13  −70.000000  −0.316122   1.173983
14  −60.000000  −0.441879   0.995729
15  −50.000000  −0.530353   0.777409
16  −40.000000  −0.579670   0.545270
17  −30.000000  −0.375783   0.335677
18  −25.000     −0.3912    0.23088
19  −24.000     −0.3809    0.22445
20  −23.000     −0.3683    0.21629
21  −22.000     −0.3245    0.19613
22  −21.000     −0.2997    0.18571
23  −20.000     −0.2786    0.17572
24  −19.000     −0.2739    0.16848
25  −18.000     −0.4142    0.19140
26  −17.000     −0.4110    0.17845
27  −16.000     −0.3830    0.16185
28  −15.000     −0.3655    0.14858
29  −14.000     −0.3898    0.12854
30  −13.000     −0.4786    0.10859
31  −12.000     −0.5748    0.09641
32  −11.000     −0.5786    0.07275
33  −10.000     −0.5545    0.05857
34   −9.000     −0.4311    0.04064
35   −8.000     −0.1830    0.03656
36   −7.000     −0.0932    0.03853
37   −6.000     −0.1452    0.02912
38   −5.000     −0.2426    0.02107
39   −4.000      0.2637    0.05063
40   −3.000      0.2533    0.04609
41   −2.000      0.1335    0.03589
42   −1.000      0.1579    0.03063
43    0.000      0.2244    0.02950
44    1.000      0.2700    0.03150
45    2.000      0.2954    0.03473
46    3.000      0.3422    0.03801
47    5.000      0.3903    0.04838
48    6.000      0.4638    0.05131
49    7.000      0.5590    0.05305
50    8.000      0.6803    0.05253
51    9.000      0.8192    0.04609
52   11.000      0.9618    0.04019
53   12.000      0.9330    0.05098
```

54	13.000	0.9571	0.05820
55	14.000	0.9994	0.06350
56	15.000	1.0547	0.07068
57	16.000	1.0687	0.08433
58	17.000	1.0255	0.10486
59	18.000	0.9135	0.14150
60	19.000	0.8111	0.19576
61	20.000	0.5957	0.20183
62	21.000	0.5962	0.21831
63	22.000	0.6345	0.23707
64	23.000	0.6405	0.25184
65	24.000	0.6778	0.27249
66	25.000	0.6801	0.28677
67	26.000	0.6966	0.30362
68	27.000	0.7170	0.32018
69	28.000	0.7433	0.34319
70	29.000	0.7473	0.35723
71	30.000	0.7601	0.37463
72	31.000	0.7733	0.39210
73	32.000	0.7859	0.40931
74	34.000	0.8083	0.44917
75	35.000	0.8128	0.46534
76	36.000	0.8171	0.48111
77	37.000	0.8221	0.49790
78	38.000	0.8254	0.51418
79	39.000	0.8274	0.53009
80	40.000	0.8281	0.54527
81	50.000000	0.757647	0.777409
82	60.000000	0.631255	0.995729
83	70.000000	0.451604	1.173983
84	80.000000	0.233576	1.290766
85	90.000000	0.000000	1.332094
86	100.000000	−0.163503	1.290766
87	110.000000	−0.316122	1.173983
88	120.000000	−0.441879	0.995729
89	130.000000	−0.530353	0.777409
90	140.000000	−0.579670	0.545270
91	150.000000	−0.434752	0.327236
92	160.000000	−0.289835	0.149546
93	170.000000	−0.144917	0.033587
94	180.000000	0.000000	0.010000

A.10   S825 re194

```
 1  Alpha        C_L        C_D
 2  −180.000000  0.000000   0.010000
 3  −170.000000  0.268143   0.010000
 4  −160.000000  0.536286   0.045836
 5  −150.000000  0.804430   0.231657
 6  −140.000000  1.072573   0.460725
 7  −130.000000  0.838074   0.706468
 8  −120.000000  0.606576   0.940546
 9  −110.000000  0.387145   1.136236
10  −100.000000  0.180972   1.271601
11  −90.000000  −0.000000   1.332094
12  −80.000000  −0.180972   1.271601
13  −70.000000  −0.387145   1.136236
14  −60.000000  −0.606576   0.940546
15  −50.000000  −0.838074   0.706468
16  −49.500000  −0.850179   0.694223
17  −47.500000  −0.899377   0.645020
18  −47.000000  −0.911895   0.632681
19  −46.500000  −0.924511   0.620334
20  −46.000000  −0.937230   0.607983
21  −45.500000  −0.950059   0.595631
22  −45.000000  −0.963005   0.583281
23  −44.500000  −0.976073   0.570938
24  −44.000000  −0.989271   0.558605
25  −43.500000  −1.002606   0.546285
26  −43.000000  −1.016087   0.533982
27  −42.500000  −1.029721   0.521700
28  −40.500000  −1.085980   0.472850
29  −40.000000  −0.587300   0.397120
30  −39.500  −0.5833   0.39163
31  −39.000  −0.5789   0.38604
32  −38.500  −0.5743   0.38034
33  −38.000  −0.5694   0.37455
34  −37.500  −0.5643   0.36872
35  −37.000  −0.5588   0.36276
36  −36.500  −0.5530   0.35684
37  −36.000  −0.5472   0.35092
38  −35.500  −0.5416   0.34518
39  −34.500  −0.5289   0.33295
40  −34.000  −0.5217   0.32713
41  −33.500  −0.5146   0.32154
42  −33.000  −0.5075   0.31600
43  −32.500  −0.5001   0.31041
44  −32.000  −0.4926   0.30484
45  −31.500  −0.4850   0.29929
46  −31.000  −0.4774   0.29375
47  −30.500  −0.4698   0.28828
48  −30.000  −0.4632   0.28321
49  −29.500  −0.4571   0.27843
50  −29.000  −0.4516   0.27393
51  −28.000  −0.4348   0.26241
52  −27.500  −0.4271   0.25774
53  −27.000  −0.4200   0.25327
```

54	−26.500	−0.4131	0.24882
55	−26.000	−0.4062	0.24434
56	−25.500	−0.3994	0.23983
57	−25.000	−0.3928	0.23528
58	−24.500	−0.6316	0.28434
59	−24.000	−0.6189	0.27910
60	−23.500	−0.6063	0.27363
61	−23.000	−0.5944	0.26800
62	−22.500	−0.5864	0.26316
63	−22.000	−0.5798	0.25856
64	−21.500	−0.5601	0.25012
65	−21.000	−0.5456	0.24493
66	−20.500	−0.5327	0.23959
67	−20.000	−0.5208	0.23378
68	−19.500	−0.5151	0.22784
69	−19.000	−0.5113	0.22207
70	−18.500	−0.5017	0.21407
71	−18.000	−0.4812	0.20800
72	−17.500	−0.4682	0.20249
73	−17.000	−0.4578	0.19649
74	−16.500	−0.4495	0.18992
75	−16.000	−0.4518	0.18212
76	−15.500	−0.4513	0.17414
77	−15.000	−0.4466	0.16514
78	−14.500	−0.4333	0.15976
79	−14.000	−0.4248	0.15366
80	−13.500	−0.4219	0.14629
81	−13.000	−0.4238	0.13774
82	−12.500	−0.4305	0.12786
83	−12.000	−0.5596	0.08561
84	−11.500	−0.6039	0.07487
85	−11.000	−0.6461	0.06579
86	−10.500	−0.6872	0.05789
87	−10.000	−0.7295	0.05097
88	−9.500	−0.7538	0.04704
89	−9.000	−0.7533	0.04317
90	−8.500	−0.6994	0.04004
91	−8.000	−0.6423	0.03826
92	−7.500	−0.5841	0.03717
93	−7.000	−0.5212	0.03518
94	−6.500	−0.4560	0.03146
95	−6.000	−0.3492	0.02241
96	−5.500	−0.2398	0.02031
97	−5.000	−0.1860	0.02371
98	−4.500	−0.1323	0.02644
99	−4.000	−0.0895	0.03074
100	−3.500	−0.0180	0.02909
101	−3.000	0.0563	0.02758
102	−2.500	0.1416	0.02384
103	−2.000	0.2354	0.02109
104	−1.500	0.3390	0.01912
105	−1.000	0.4313	0.01773
106	−0.500	0.5069	0.01685
107	0.000	0.5697	0.01647
108	0.500	0.6254	0.01640
109	1.000	0.6822	0.01642
110	1.500	0.7374	0.01645

111	2.000	0.7940	0.01650
112	2.500	0.8519	0.01659
113	3.000	0.9087	0.01671
114	3.500	0.9638	0.01698
115	4.000	1.0196	0.01732
116	4.500	1.0742	0.01761
117	5.000	1.1251	0.01780
118	5.500	1.1740	0.01806
119	6.000	1.2222	0.01836
120	6.500	1.2687	0.01867
121	7.000	1.3110	0.01895
122	7.500	1.3500	0.01937
123	8.000	1.3826	0.01987
124	8.500	1.4017	0.02066
125	9.000	1.4045	0.02280
126	9.500	1.4067	0.02564
127	10.000	1.4103	0.02867
128	10.500	1.4152	0.03195
129	11.000	1.4191	0.03563
130	11.500	1.4198	0.04005
131	12.000	1.4158	0.04543
132	12.500	1.4163	0.05099
133	13.000	1.4148	0.05726
134	13.500	1.4083	0.06460
135	14.000	1.4116	0.07114
136	14.500	1.4065	0.07906
137	15.000	1.4062	0.08659
138	15.500	1.4031	0.09479
139	16.500	1.3902	0.11101
140	17.000	1.3862	0.12017
141	17.500	1.3792	0.12962
142	18.000	1.3688	0.14064
143	18.500	1.3561	0.15246
144	19.000	1.3419	0.16500
145	19.500	1.3245	0.17891
146	20.000	1.2870	0.19975
147	20.500	1.1796	0.25614
148	21.000	1.1827	0.27118
149	22.500	1.2193	0.30716
150	23.000	1.2267	0.31554
151	23.500	1.2407	0.32234
152	24.000	1.2555	0.32836
153	24.500	1.2710	0.33380
154	25.000	1.2908	0.34245
155	25.500	1.3016	0.34853
156	26.000	1.3099	0.35323
157	26.500	1.3229	0.35916
158	27.000	1.3361	0.36435
159	27.500	1.3491	0.36906
160	28.000	1.3618	0.37335
161	28.500	1.3773	0.38052
162	29.000	1.3859	0.38409
163	29.500	1.3970	0.38883
164	30.000	1.4086	0.39364
165	30.500	1.4195	0.39803
166	31.000	1.4299	0.40207
167	31.500	1.4396	0.40587

168	32.000	1.4504	0.41239
169	32.500	1.4589	0.41609
170	33.000	1.4673	0.41939
171	33.500	1.4764	0.42368
172	34.000	1.4853	0.42808
173	34.500	1.4934	0.43213
174	35.000	1.5006	0.43594
175	35.500	1.5075	0.43964
176	36.000	1.5138	0.44315
177	36.500	1.5197	0.44653
178	37.000	1.5248	0.44970
179	37.500	1.5291	0.45282
180	38.000	1.5337	0.45847
181	39.000	1.5416	0.46383
182	39.500	1.5451	0.46674
183	40.000	1.5484	0.46971
184	40.500000	1.551400	0.472850
185	50.000000	1.197249	0.706468
186	60.000000	0.866537	0.940546
187	70.000000	0.553064	1.136236
188	80.000000	0.258531	1.271601
189	90.000000	0.000000	1.332094
190	100.000000	−0.180972	1.271601
191	110.000000	−0.387145	1.136236
192	120.000000	−0.606576	0.940546
193	130.000000	−0.838074	0.706468
194	140.000000	−1.072573	0.460725
195	150.000000	−0.804430	0.231657
196	160.000000	−0.536286	0.045836
197	170.000000	−0.268143	0.010000
198	180.000000	0.000000	0.010000

A.11 S826 12% re191

```
 1   Alpha       C_L        C_D
 2   −180.000000  0.000000   0.080142
 3   −170.000000  0.172038   0.119092
 4   −160.000000  0.344077   0.231134
 5   −150.000000  0.516115   0.402428
 6   −140.000000  0.663584   0.611781
 7   −130.000000  0.579930   0.833219
 8   −120.000000  0.468413   1.039141
 9   −110.000000  0.327565   1.203679
10   −100.000000  0.166318   1.305843
11    −90.000000 −0.000000   1.332094
12    −80.000000 −0.166318   1.305843
13    −70.000000 −0.327565   1.203679
14    −60.000000 −0.468413   1.039141
15    −50.000000 −0.579930   0.833219
16    −40.000000 −0.663584   0.611781
17    −30.000000 −0.425610   0.368219
18    −25.000000 −0.413300   0.245090
19    −24.000    −0.3929    0.23523
20    −23.000    −0.3735    0.22634
21    −22.000    −0.3539    0.21681
22    −21.000    −0.3307    0.20672
23    −20.000    −0.3093    0.19782
24    −19.000    −0.2884    0.18909
25    −18.000    −0.2706    0.18153
26    −17.000    −0.2616    0.17626
27    −16.000    −0.2329    0.16481
28    −15.000    −0.2158    0.15691
29    −14.000    −0.2042    0.14748
30    −13.000    −0.1906    0.13560
31    −12.000    −0.1722    0.12332
32    −11.000    −0.1585    0.11066
33    −10.000    −0.1455    0.09636
34     −9.000    −0.1547    0.07851
35     −8.000    −0.2061    0.06862
36     −7.000    −0.1857    0.05245
37     −6.000    −0.1124    0.03836
38     −5.000     0.0095    0.02388
39     −4.000     0.1216    0.01905
40     −2.000     0.3690    0.01583
41     −1.000     0.4801    0.01601
42      0.000     0.5895    0.01632
43      1.000     0.6974    0.01674
44      2.000     0.8033    0.01726
45      3.000     0.9074    0.01791
46      4.000     1.0085    0.01868
47      5.000     1.1064    0.01963
48      6.000     1.1998    0.02079
49      7.000     1.2850    0.02225
50      8.000     1.3486    0.02512
51      9.000     1.3727    0.03116
52     10.000     1.3879    0.03889
53     11.000     1.4005    0.04853
```

54	12.000	1.4205	0.06016
55	13.000	1.3991	0.07656
56	14.000	1.3335	0.10088
57	15.000	1.2565	0.13423
58	16.000	1.1969	0.17642
59	17.000	1.1704	0.22425
60	20.000	0.8948	0.26707
61	21.000	0.9023	0.28372
62	22.000	0.9126	0.30038
63	23.000	0.9148	0.31920
64	24.000	0.9242	0.33505
65	25.000	0.9310	0.35156
66	26.000	0.9406	0.37101
67	27.000	0.9479	0.38771
68	28.000	0.9539	0.40588
69	29.000	0.9606	0.42438
70	31.000	0.9663	0.45684
71	32.000	0.9703	0.47437
72	33.000	0.9721	0.49312
73	34.000	0.9719	0.50953
74	35.000	0.9717	0.52596
75	36.000	0.9689	0.54252
76	37.000	0.9661	0.55752
77	39.000000	0.958500	0.589850
78	40.000000	0.947978	0.611781
79	50.000000	0.828471	0.833219
80	60.000000	0.669161	1.039141
81	70.000000	0.467950	1.203679
82	80.000000	0.237596	1.305843
83	90.000000	0.000000	1.332094
84	100.000000	−0.166318	1.305843
85	110.000000	−0.327565	1.203679
86	120.000000	−0.468413	1.039141
87	130.000000	−0.579930	0.833219
88	140.000000	−0.663584	0.611781
89	150.000000	−0.516115	0.402428
90	160.000000	−0.344077	0.231134
91	170.000000	−0.172038	0.119092
92	180.000000	0.000000	0.080142

A.12 S826 14% re198

```
 1   Alpha        C_L        C_D
 2   −180.000000  0.000000   0.133157
 3   −170.000000  0.308200   0.171301
 4   −160.000000  0.616400   0.280952
 5   −150.000000  0.610538   0.448340
 6   −140.000000  0.584994   0.652393
 7   −130.000000  0.533499   0.867296
 8   −120.000000  0.443562   1.065649
 9   −110.000000  0.316848   1.221811
10   −100.000000  0.163682   1.315049
11   −90.000000  −0.000000   1.332094
12   −80.000000  −0.163682   1.315049
13   −70.000000  −0.316848   1.221811
14   −60.000000  −0.443562   1.065649
15   −50.000000  −0.533499   0.867296
16   −40.000000  −0.584994   0.652393
17   −30.000000  −0.610538   0.448340
18   −25.000000  −0.625070   0.358601
19   −24.000000  −0.629318   0.342019
20   −23.000000  −0.634309   0.325943
21   −22.000000  −0.640209   0.310394
22   −21.000000  −0.647220   0.295390
23   −20.000   −0.3233     0.19509
24   −19.000   −0.3014     0.18270
25   −18.000   −0.2853     0.17435
26   −17.000   −0.2723     0.16632
27   −16.000   −0.2622     0.15830
28   −15.000   −0.2663     0.15228
29   −13.000   −0.2493     0.13369
30   −12.000   −0.2545     0.12617
31   −11.000   −0.2773     0.11612
32   −10.000   −0.2410     0.09888
33    −8.000   −0.3632     0.07990
34    −5.000   −0.0814     0.02017
35    −4.000    0.0842     0.01439
36    −3.000    0.2374     0.01370
37    −2.000    0.3966     0.01351
38    −1.000    0.5305     0.01319
39     0.000    0.6487     0.01331
40     1.000    0.7620     0.01364
41     2.000    0.8764     0.01409
42     3.000    0.9856     0.01462
43     4.000    1.0930     0.01513
44     5.000    1.1934     0.01558
45     6.000    1.2875     0.01601
46     7.000    1.3665     0.01657
47     8.000    1.3901     0.01923
48     9.000    1.3930     0.02452
49    10.000    1.4007     0.03012
50    11.000    1.4104     0.03829
51    12.000    1.4150     0.04858
52    14.000    1.4101     0.07548
53    15.000    1.3940     0.09312
```

```
54    16.000    1.3764    0.11268
55    17.000    1.3408    0.13760
56    18.000    1.2866    0.17126
57    19.000    1.2054    0.22458
58    20.000    1.1907    0.26878
59    21.000    0.9246    0.29539
60    30.000000    0.872197    0.448340
61    40.000000    0.835706    0.652393
62    50.000000    0.762141    0.867296
63    60.000000    0.633660    1.065649
64    70.000000    0.452641    1.221811
65    80.000000    0.233831    1.315049
66    90.000000    0.000000    1.332094
67   100.000000   −0.163682    1.315049
68   110.000000   −0.316848    1.221811
69   120.000000   −0.443562    1.065649
70   130.000000   −0.533499    0.867296
71   140.000000   −0.584994    0.652393
72   150.000000   −0.610538    0.448340
73   160.000000   −0.616400    0.280952
74   170.000000   −0.308200    0.171301
75   180.000000    0.000000    0.133157
```

A.13 Tidal Turbine Blade Data

	r/R	r	Lc	Twist
1				
2	0.104500	1.047789	0.801712	6.450000
3	0.113500	1.138029	0.800000	6.450000
4	0.122500	1.228269	0.801515	6.450000
5	0.131500	1.318509	0.805665	6.450000
6	0.140500	1.408749	0.811859	6.450000
7	0.149500	1.498989	0.829465	6.450000
8	0.158500	1.589230	0.863243	6.450000
9	0.167500	1.679470	0.905688	6.450000
10	0.176500	1.769710	0.967965	6.450000
11	0.185500	1.859950	1.051239	6.450000
12	0.194500	1.950190	1.133005	6.450000
13	0.203500	2.040430	1.218836	6.450000
14	0.212500	2.130671	1.312101	6.450000
15	0.221500	2.220911	1.386989	6.450000
16	0.230500	2.311151	1.417688	6.450000
17	0.239500	2.401391	1.415969	6.432942
18	0.248500	2.491631	1.411020	6.383865
19	0.257500	2.581871	1.403155	6.305919
20	0.266500	2.672112	1.392686	6.202253
21	0.275500	2.762352	1.379929	6.076015
22	0.284500	2.852592	1.365195	5.930353
23	0.293500	2.942832	1.348798	5.768417
24	0.302500	3.033072	1.331051	5.593355
25	0.311500	3.123312	1.312268	5.408315
26	0.320500	3.213553	1.292762	5.216447
27	0.329500	3.303793	1.272847	5.020898
28	0.338500	3.394033	1.252836	4.824818
29	0.347500	3.484273	1.233042	4.631355
30	0.356500	3.574513	1.213778	4.443658
31	0.365500	3.664753	1.195358	4.264875
32	0.374500	3.754994	1.178096	4.098156
33	0.383500	3.845234	1.162304	3.946648
34	0.392500	3.935474	1.147202	3.801550
35	0.401500	4.025714	1.131823	3.652333
36	0.410500	4.115954	1.116202	3.499557
37	0.419500	4.206195	1.100376	3.343781
38	0.428500	4.296435	1.084380	3.185564
39	0.437500	4.386675	1.068247	3.025466
40	0.446500	4.476915	1.052015	2.864046
41	0.455500	4.567155	1.035719	2.701864
42	0.464500	4.657395	1.019393	2.539477
43	0.473500	4.747636	1.003073	2.377447
44	0.482500	4.837876	0.986794	2.216332
45	0.491500	4.928116	0.970592	2.056692
46	0.500500	5.018356	0.954502	1.899085
47	0.509500	5.108596	0.938559	1.744072
48	0.518500	5.198836	0.922799	1.592211
49	0.527500	5.289077	0.907257	1.444062
50	0.536500	5.379317	0.891968	1.300184
51	0.545500	5.469557	0.876968	1.161137
52	0.554500	5.559797	0.862292	1.027479
53	0.563500	5.650037	0.847975	0.899770

54	0.572500	5.740277	0.834053	0.778570
55	0.581500	5.830518	0.820560	0.664438
56	0.590500	5.920758	0.807533	0.557932
57	0.599500	6.010998	0.795006	0.459613
58	0.608500	6.101238	0.783016	0.370040
59	0.617500	6.191478	0.771596	0.289771
60	0.626500	6.281718	0.760783	0.219367
61	0.635500	6.371959	0.750364	0.155819
62	0.644500	6.462199	0.740106	0.095601
63	0.653500	6.552439	0.730016	0.038499
64	0.662500	6.642679	0.720098	−0.015703
65	0.671500	6.732919	0.710359	−0.067223
66	0.680500	6.823159	0.700804	−0.116275
67	0.689500	6.913400	0.691439	−0.163076
68	0.698500	7.003640	0.682268	−0.207841
69	0.707500	7.093880	0.673299	−0.250787
70	0.716500	7.184120	0.664536	−0.292129
71	0.725500	7.274360	0.655986	−0.332083
72	0.734500	7.364600	0.647653	−0.370866
73	0.743500	7.454841	0.639543	−0.408692
74	0.752500	7.545081	0.631662	−0.445778
75	0.761500	7.635321	0.624017	−0.482341
76	0.770500	7.725561	0.616611	−0.518595
77	0.779500	7.815801	0.609451	−0.554757
78	0.788500	7.906041	0.602543	−0.591042
79	0.797500	7.996282	0.595892	−0.627667
80	0.806500	8.086522	0.589503	−0.664848
81	0.815500	8.176762	0.583383	−0.702800
82	0.824500	8.267002	0.577537	−0.741739
83	0.833500	8.357242	0.571971	−0.781882
84	0.842500	8.447482	0.566982	−0.821894
85	0.851500	8.537723	0.562743	−0.860533
86	0.860500	8.627963	0.559068	−0.898147
87	0.869500	8.718203	0.555773	−0.935084
88	0.878500	8.808443	0.552673	−0.971693
89	0.887500	8.898683	0.549583	−1.008325
90	0.896500	8.988923	0.546319	−1.045326
91	0.905500	9.079164	0.542695	−1.083047
92	0.914500	9.169404	0.538527	−1.121836
93	0.923500	9.259644	0.533629	−1.162042
94	0.932500	9.349884	0.527818	−1.204014
95	0.941500	9.440124	0.520909	−1.248100
96	0.950500	9.530364	0.510807	−1.295964
97	0.959500	9.620605	0.496029	−1.347726
98	0.968500	9.710845	0.477302	−1.401424
99	0.977500	9.801085	0.455355	−1.455094
100	0.986500	9.891325	0.430917	−1.506773
101	0.995500	9.981565	0.396390	−1.555776
102	1.000000	10.026685	0.396390	−1.555776

XXVII

A.14 Input Variables

```
1  2.5    Vinput[m/s]
2  0      Tmin[s]
3  0.1    Deltat[s]
4  10     Tmax[s]
5  0.05   Steepness
6  10.0   Twave[s]
```